Correlations in Polymer Blends: Simulations, Perturbation Theory, and Coarse-Grained Theory

A THESIS
SUBMITTED TO THE FACULTY OF THE GRADUATE SCHOOL
OF THE UNIVERSITY OF MINNESOTA
BY

Jun Kyung Chung

IN PARTIAL FULFILLMENT OF THE REQUIREMENTS
FOR THE DEGREE OF
DOCTOR OF PHILOSOPHY

Adviser: David C. Morse

September, 2009

Acknowledgements

First of all, I would like to thank my adviser, Professor David Morse, for his guidance during the two years I spent in his research group. He was always willing to help all of his students and patient enough to explain his reasoning repeatedly. In addition, I want to express my sincere gratitude to him for helping me wrap up the life as a graduate student.

I also thank Professor Jiali Gao for his kind help while I was in his research group and even after I left the group.

Professor Yuichi Kubota was very helpful in solving many problems encountered as a graduate student.

I am also very grateful to the other members of my final examination committee: Professor Charles Campbell, Professor Tim Lodge, and Professor Oriol Valls.

Professor Marcus Müller at the University of Göttingen graciously helped me run his computer program to generate important data for this thesis.

Over the last six years I spent at the University of Minnesota, I met so many wonderful friends. Jian was almost like a second academic adviser to me. Raghu and Andrew kept me from feeling isolated from the rest of the world. Jorge was always willing to help me in any possible way. Kiniu gave me a lot of helpful advice about research. Seongho Wu was my collaborator and helped me refine my research skill. I also want to thank Dat, Sujeewa, and Yaroslav for being good friends for many years. It would not be possible to mention the names of all the friends I have met, but I can say this without any doubt: not a single day I spent in Minnesota was wasted because I met you.

Lastly, I thank my father, mother, and two sisters who have supported me unconditionally throughout my whole life.

Dedication

This thesis is dedicated to my grandmother who made my childhood full of wonderful memories.

ABSTRACT

A thermodynamic perturbation theory of symmetric polymer blends is developed that properly accounts for the correlation in the spatial arrangement of monomers. By expanding the free energy of mixing in powers of a small parameter α which controls the incompatibility of two monomer species, we show that the perturbation theory has the form of the original Flory-Huggins theory, to first order in α. However, the lattice coordination number in the original theory is replaced by an effective coordination number. A random walk model for the effective coordination number is found to describe Monte Carlo simulation data very well.

We also propose a way to estimate Flory-Huggins χ parameter by extrapolating the perturbation theory to the limit of a hypothetical system of infinitely long chains. The first order perturbation theory yields an accurate estimation of χ to first order in α. Going to second order, however, turns out to be more involved and an unambiguous determination of the coefficient of α^2 term is not possible at the moment.

Lastly, we test the predictions of a renormalized one-loop theory of fluctuations using two coarse-grained models of symmetric polymer blends at the critical composition. It is found that the theory accurately describes the correlation effect for relatively small values of χN. In addition, the universality assumption of coarse-grained models is examined and we find results that are supportive of it.

Contents

List of Tables

List of Figures

Chapter 1

Introduction

Polymers are a class of molecules that consist of many repeating chemical units called monomers. In particular, a homopolymer is made out of a single type of monomers, while a block copolymer can be thought of as homopolymers of different types connected together. Their spatial extent is usually much larger than the size of a monomer and this difference in length scales makes them amenable to coarse-grained modeling: relatively simple models could be used to describe the physics of polymers at the length scale larger than the size of a polymer. In coarse-grained models of polymers, a monomer (also called bead) represents a multiple of real chemical units, reducing the number of degrees of freedom significantly. At the same time, they retain essential features of real polymer systems such as connectivity of monomers in a polymer and the excluded volume interaction between monomers. In this thesis, thermodynamics of binary homopolymer blends will be studied using such coarse-grained models.

1.1 Flory-Huggins theory

Flory-Huggins (FH) theory [1,2,3,4,5,6] describes the statistical mechanics and thermodynamics of homogeneous polymer mixtures. In its most general form, the free energy of mixing per monomer is expressed as a sum of the form [7],

$$\Delta f = k_\mathrm{B} T \sum_i^{A,B} \frac{\phi_i}{N_i} \ln \phi_i + \Delta f_\mathrm{int}(\phi, T) \quad , \tag{1.1}$$

1

where N_i is the degree of polymerization of species i, for $i = A$ or B, $\phi_A = \phi$ and $\phi_B = 1 - \phi_A$ are volume fractions, $k_\mathrm{B}T$ is thermal energy, and $\Delta f_{\mathrm{int}}(\phi, T)$ is an interaction free energy per monomer. The first term on the right hand side of Eq. (1.1) is the ideal entropy upon mixing and it is obtained by assuming that the conformational entropy of individual molecule is the same when the two types of molecules are mixed as when they are separated. Note also that the notion of volume fraction here makes sense only in symmetric blends or in incompressible blends.

In order to capture the variety of behaviors observed in real polymer mixtures, it has long been understood [7, 8, 9, 10] that Δf_{int} should be allowed to exhibit an essentially arbitrary dependence on temperature and composition. In any case, the essential content of the theories is that the quantity $\Delta f_{\mathrm{int}}(\phi, T)$ is independent of chain length. In other words, $\Delta f_{\mathrm{int}}(\phi, T)$ is the part of free energy which is sensitive only to the local structure of a polymer liquid. In a corresponding generalized form of self consistent field theory (SCFT) for inhomogeneous liquids [11, 12], the key assumption is that the free energy density at any point in the liquid depends only on the temperature and average monomer concentration very near that point, independent of chain lengths, chain architecture, or compositions at distant points.

The original FH theory combined this assumption of locality with a random mixing approximation. It considered a lattice model in which there are N_L sites and monomers of type i and j on neighboring sites interact with a potential energy v_{ij}. The volume fraction of each species is thus given by $\phi_i = \frac{M_i N_i}{N_L}$ where M_i is the number of chains of type i. In the absence of vacancies, the random mixing approximation yields

$$\Delta f_{\mathrm{int}} = \alpha z_{\mathrm{latt}} \phi_A \phi_B \quad , \tag{1.2}$$

where $\alpha = v_{AB} - (v_{AA} + v_{BB})/2$ and z_{latt} is the number of lattice sites neighboring each site. The Flory-Huggins parameter χ is defined in the original theory by

$$\chi \equiv \frac{\alpha z_{\mathrm{latt}}}{k_\mathrm{B}T} \quad . \tag{1.3}$$

1.2 Perturbation theory

The random mixing approximation is known to substantially overestimate the actual energy of mixing for lattice models. In simulation studies of a lattice model blend,

Sariban and Binder [13, 14] found that the energy of mixing was much smaller (roughly half) than that predicted by FH theory slightly modified for a lattice with vacancies. More recently, Matsen and coworkers [15, 16] studied a lattice model of diblock copolymer melts and found that the random mixing approximation predicted a order-disorder transition temperature (a temperature at which the two blocks phase-separate into A-rich and B-rich domains) much larger than that observed in their simulations. These studies clearly showed the problem of the approximation in describing thermodynamics of polymer systems.

The inaccuracy of the random mixing approximation is in part a result of the fact that it neglects the existence of an inter-molecular correlation hole. The immediate neighborhood of any monomer in a dense polymer liquid is crowded with other monomers from the same chain. In a nearly incompressible liquid, this causes a compensating depression in the number of neighboring monomers from other chains, leading to a decrease in the inter-molecular interaction energy. In a lattice model, the simplest way to correct for this effect is to replace z_{latt} by $z_{\text{latt}} - 2$ to take into account the fact that two nearest neighboring sites of a monomer are always occupied by two monomers from the same chain.

To better account for the correlation effect, we develop a perturbation theory of symmetric blends ($N_A = N_B = N$) using both lattice and continuum models (Chapter 4). Taylor expansion of the free energy in powers of a small parameter α, which is a measure of incompatibility between an A monomer and a B monomer, will yield

$$\Delta f \simeq k_{\text{B}} T \sum_i^{A,B} \frac{\phi_i}{N_i} \ln \phi_i + \alpha z(N) \phi_A \phi_B + \mathcal{O}(\alpha^2) \quad . \tag{1.4}$$

In this expansion, $z(N)$ is an effective coordination number whose value is sensitive to local correlations in the one component reference state with $\alpha = 0$. The effective coordination number turns out to be directly proportional to the average number of inter-molecular neighbors of a test monomer for the case of a lattice model. The perturbation theory can accurately describe the thermodynamics of a mixture of long chains because $z(N)$ properly takes the effect into account.

The coefficients appearing in the expansion of Eq. (1.4) (e.g. $z(N)$) are defined in terms of the positions of monomers and how they interact with each other. Therefore, they can be measured directly from simulations of the models in the one-component

reference state. Also, they can be related to model specific parameters used in more coarse-grained theories, allowing the parameters to be estimated via computer simulations for a given model.

1.3   Coarse-grained loop expansion

The FH theory (and SCFT) has long been believed to be exact in the limit of infinitely long chains. The basis for this belief is, in part, the predictions of a variety of closely related one-loop theories of fluctuation effects. The one-loop theory [17, 18, 19, 20, 21, 22] is a coarse-grained theory, that, when properly interpreted [21, 22], predicts small corrections to the free energy of an underlying FH theory. The relative magnitude of the fluctuation correction to the free energy is found [18, 19, 21, 22] to scale as $\bar{N}^{-1/2}$, where $\bar{N} = c^2 b^6 N$ is an invariant degree of polymerization for the system of chains of length N with statistical segment length b at average monomer concentration c. This also implies that the FH theory becomes asymptotically exact as $N \to \infty$.

The result of the one-loop theory that the corrections to the FH theory are controlled by $\bar{N}$ is consistent with the coarse-grained nature of the theory. This is because $\sqrt{\bar{N}}$ is a measure of density at the scale of a size of a chain molecule: consider a size of volume occupied by a Gaussian chain with N segments and statistical segment length b. The root mean square of the end to end distance is $R = b\sqrt{N}$ and the volume the chain occupies is approximately $R^3 = b^3 N^{3/2}$. Now the number of chains in the same volume can be estimated by $cR^3/N = cb^3\sqrt{N}$. Therefore, one can see that $\sqrt{\bar{N}}$ measures the extent of overlap of chains and $\bar{N}$ is a proper measure of a degree of polymerization for coarse-grained models that are not supposed to have the same meaning about what constitute a monomer.

In relation to the perturbation theory, non-perturbative coarse-grained theories can predict the chain length dependence of the coefficients in the expansion of Eq. (1.4). Therefore one can test them by comparing these predictions to the results of simulations in which the coefficients are evaluated directly.

1.4 Outline

The works presented in this thesis are efforts to develop a perturbation theory of symmetric polymer blends and also test quantitatively the predictions of a coarse-grained theory (renormalized one-loop theory [22, 23]) that tries to account for the correlation effect. Along the way, an attempt to examine the universality assumption of coarse-grained models, taking two widely used models as representatives, is made.

In Chapter 2, a brief review of standard coarse-grained theories of correlation in polymer physics is given.

Chapter 3 will be devoted to explanation of the computational models and methods employed in the works presented here.

Chapter 4 is based on a published work by Morse and Chung [24]. We first construct a thermodynamic perturbation theory of a class of symmetric polymer blends in which the incompatibility of two monomer species is controlled by a small parameter α. We find that the theory is almost identical to the original FH theory except for the fact that the lattice coordination number in the original theory is replaced by a chain length dependent effective coordination number. Using the Gaussian random walk model for the chain, we develop an analytical theory on how the effective coordination number depends on the chain length N and present Monte Carlo simulations to test the predictions. The renormalized one-loop theory is also shown to give consistent results with the perturbation theory. We also argue that the *true* FH χ parameter can be obtained by taking the limit $N \to \infty$ of the perturbation theory.

In Chapter 5, the first order perturbation theory for symmetric blends of the previous chapter is extended to second order in an attempt to improve the accuracy of the FH χ parameter to second order in α.

Based on the developments, the simulation results of composition fluctuations in models of symmetric polymer blends will be reported and compared to the predictions of the one-loop theory in Chapter 6. Especially, we take advantage of the situation of having two microscopically different coarse-grained models at our disposal and try to see if they show consistent results at larger length scale than a polymer. We show that if a physical observable in polymer systems is a function only of χN and $\bar{N}$ (e.g. large scale composition fluctuations), one should be able to collapse data of the quantity from

one model onto those from the other model by a mapping procedure. We find evidence that supports the universality of the two models.

Chapter 2

Coarse-grained models of correlations in polymer liquids

In this chapter, two coarse-grained theories of polymer liquids will be reviewed in some detail. One is the random phase approximation that attempts to describe correlations in monomer concentrations and the other is a renormalized one-loop theory that describes the effect of the correlations upon polymer thermodynamics.

2.1 Model and notation

Throughout this thesis, we consider a coarse-grained model of blends where there are M_k molecules of type k with chain length N_k and statistical segment length b_k in a volume V. All the energy will be measured in units of $\beta^{-1} = k_{\mathrm{B}}T$ where k_{B} is the Boltzmann constant and T is temperature. The average volume per monomer is $v = V/(\sum_k M_k N_k)$ and the spatially averaged monomer concentration is $c = v^{-1}$.

In the model, a homopolymer is composed of monomers whose positions are specified by the position vector $\mathbf{R}_{mk}(s)$, where s is a monomer index along a molecule m and k denotes the type (A or B) of the monomer. The fluctuating number concentration of monomer of type k at position $\mathbf{r}$ is defined as

$$c_k(\mathbf{r}) = \sum_{m,s} \delta(\mathbf{r} - \mathbf{R}_{mk}(s)), \qquad (2.1)$$

in which m is taken over molecules of species k and s runs from 1 to N_k. The volume fraction of monomers of species k is defined as

$$\phi_k(\mathbf{r}) \equiv v c_k(\mathbf{r}) \quad , \tag{2.2}$$

while $\delta c_k(\mathbf{r})$ will denote the deviation of the concentration from its ensemble average, i.e.

$$\delta c_k(\mathbf{r}) \equiv c_k(\mathbf{r}) - \langle c_k(\mathbf{r}) \rangle \quad . \tag{2.3}$$

Spatial averages of these quantities will be written with the position dependence removed, e.g. $c_k \equiv M_k N_k / V$ and $\phi_k \equiv v c_k$.

The correlation in monomer concentrations is characterized by a static structure factor

$$S_{kk'}(\mathbf{r}, \mathbf{r}') = \langle \delta c_k(\mathbf{r}) \delta c_{k'}(\mathbf{r}') \rangle \tag{2.4}$$

or its Fourier transform

$$\tilde{S}_{kk'}(\mathbf{q}) \equiv \int d\mathbf{r} \, \langle \delta c_k(\mathbf{r}) \delta c_{k'}(0) \rangle e^{i\mathbf{q} \cdot \mathbf{r}} \quad . \tag{2.5}$$

The total potential energy of the model of polymer blends we consider has a form

$$U = U_{\text{chain}} + U_{\text{int}} \quad . \tag{2.6}$$

Here, U_{chain} is an intra-molecular potential energy and U_{int} is a pairwise additive potential energy given by

$$U_{\text{int}} = \frac{1}{2} \sum_{k,k'} \int d\mathbf{r} \int d\mathbf{r}' \, U_{kk'}(\mathbf{r} - \mathbf{r}') c_k(\mathbf{r}) \, c_{k'}(\mathbf{r}') \quad , \tag{2.7}$$

in which $U_{kk'}(\mathbf{r} - \mathbf{r}')$ is an interaction potential energy between two monomers of species k and k'.

In the idealized limit of an effectively incompressible mixture in which the average volume per monomer at constant pressure is independent of composition, the matrix $\tilde{S}_{kk'}(\mathbf{q})$ may be characterized by a scalar function $S(\mathbf{q}) = \tilde{S}_{AA}(\mathbf{q}) = \tilde{S}_{BB}(\mathbf{q}) = -\tilde{S}_{AB}(\mathbf{q})$. In the same limit, the Helmholtz free energy of mixing per monomer Δf for the model blend is related to the long wavelength limit $S(0) \equiv \lim_{\mathbf{q} \to 0} S(\mathbf{q})$ by the identity

$$S^{-1}(0) = v \frac{\partial^2 \beta \Delta f}{\partial \phi_A^2} \quad . \tag{2.8}$$

On the other hand, the free energy of mixing can be decomposed into an ideal part and an excess part as

$$\Delta f = f_{\text{id}} + f_{\text{ex}} \tag{2.9}$$

where f_{id} is the entropy upon mixing introduced in Eq. (1.1) and f_{ex} is defined by the above equation. Substituting Eq. (2.9) into Eq. (2.8) yields

$$S^{-1}(0) = v \left(\frac{1}{N_A \phi_A} + \frac{1}{N_B \phi_B} - 2\chi_a \right) \quad, \tag{2.10}$$

where we defined an *apparent* χ parameter

$$\chi_a \equiv -\frac{1}{2k_{\text{B}}T} \frac{\partial^2 f_{\text{ex}}}{\partial \phi_A^2} \quad. \tag{2.11}$$

2.2 Random phase approximation (RPA)

The random phase approximation is an analytical method to calculate a static structure factor $\tilde{S}(\mathbf{q})$ of homogeneous polymer liquids [3, 4, 5, 25]. This formalism originates from the theory of electronic structure of solids and was first introduced to the field of polymer physics by de Gennes [25]. The basic idea of the RPA is to use the linear response theory to calculate $\tilde{S}(\mathbf{q})$ together with the self-consistent field framework.

2.2.1 General formulation for polymer mixtures

Imagine applying a weak external perturbing potential $V_k(\mathbf{r})$ coupled to monomer concentration $c_k(\mathbf{r})$. Note that one can take any system as the reference system and we have not specified it yet. The linear response theory relates the ensemble averaged concentration deviation from the unperturbed value to the correlation function as,

$$\delta \langle c_k(\mathbf{r}) \rangle = -\beta \sum_{k'} \int d\mathbf{r}' \; S_{kk'}(\mathbf{r} - \mathbf{r}') \; V_{k'}(\mathbf{r}'), \tag{2.12}$$

where $S_{kk'}(\mathbf{r} - \mathbf{r}') = \langle \delta c_k(\mathbf{r}) \delta c_{k'}(\mathbf{r}') \rangle$ is the structure factor.

To apply the linear response theory to the polymer mixture at hand, we take a system of non-interacting polymer chains as the reference state. As a result, the structure factor matrix $\mathbf{S}$ has non-zero elements only along the diagonal, which are just intra-molecular correlation functions. The perturbing potential has two contributions, first of which is a

weak potential applied from the outside of the system. The other comes from interaction between polymers, which consists of local density fluctuations and compressibility. Let $V_k(\mathbf{r})$ be the external potential and $V_k^{RPA}(\mathbf{r})$ be the part caused by interaction between polymers. Eq. (2.12) can be written as

$$\delta\langle c_k(\mathbf{r})\rangle = -\beta \sum_{k'} \int d\mathbf{r}' \ S_{kk'}^{(0)}(\mathbf{r}-\mathbf{r}') \left[V_{k'}(\mathbf{r}') + V_{k'}^{RPA}(\mathbf{r}')\right], \tag{2.13}$$

in which $S_{kk'}^{(0)}$ is the structure factor of the non-interacting chain system. After Fourier transforming both sides,

$$\delta\langle \tilde{c}_k(\mathbf{q})\rangle = -\beta \sum_{k'} \ \tilde{S}_{kk'}^{(0)}(\mathbf{q}) \left[\tilde{V}_{k'}(\mathbf{q}) + \tilde{V}_{k'}^{RPA}(\mathbf{q})\right]. \tag{2.14}$$

Let $\chi_{kk'}$ be a dimensionless *phenomenological* interaction parameter between monomers of type k and k' and $\delta\langle \phi_{k'}(\mathbf{r})\rangle = v\delta\langle c_k(\mathbf{r})\rangle$, then $V_k^{RPA}(\mathbf{r})$ can be written explicitly as

$$V_k^{RPA}(\mathbf{r}) = \beta^{-1} \sum_{k'} \chi_{kk'} \ \delta\langle \phi_{k'}(\mathbf{r})\rangle + \frac{1}{\kappa} \sum_{k'} \delta\langle \phi_{k'}(\mathbf{r})\rangle, \tag{2.15}$$

where the first term represents the mean potential felt by a monomer of type k and the second term accounts for the weak compressibility. For the case of strictly incompressible liquids, we either introduce a Lagrange multiplier to impose the constraint or let $\kappa \to 0$ at the end of calculation. Taking Fourier transformation of both sides of Eq. (2.15) yields

$$\tilde{V}_k^{RPA}(\mathbf{q}) = \sum_{k'} \hat{\chi}_{kk'} \ \delta\langle \tilde{\phi}_{k'}(\mathbf{q})\rangle \quad , \tag{2.16}$$

where $\hat{\chi}_{kk'} \equiv \beta^{-1}\chi_{kk'} + \kappa^{-1}$ was defined for notational convenience. Substituting Eq. (2.16) into Eq. (2.14) and rearranging terms, one obtains

$$\sum_{k''} \left[\delta_{kk''} + v\beta \sum_{k'} \tilde{S}_{kk'}^{(0)}(\mathbf{q}) \ \hat{\chi}_{k'k''}\right] \delta\langle \tilde{c}_{k''}(\mathbf{q})\rangle = -\beta \sum_{k'} \tilde{S}_{kk'}^{(0)}(\mathbf{q}) \ \tilde{V}_{k'}(\mathbf{q}). \tag{2.17}$$

For further simplification, define a matrix $\tilde{\mathbf{A}}$ with elements

$$\tilde{A}_{kk''}(\mathbf{q}) = \delta_{kk''} + v\beta \sum_{k'} \tilde{S}_{kk'}^{(0)}(\mathbf{q}) \ \hat{\chi}_{k'k''} \quad , \tag{2.18}$$

in which $\delta_{kk''}$ is the Kronecker delta. Or, in matrix notation

$$\tilde{\mathbf{A}} = \mathbf{I} + v\beta\tilde{\mathbf{S}}^{(0)}\hat{\chi} \tag{2.19}$$

Similarly, Eq. (2.17) can be written compactly in matrix form as

$$\tilde{\mathbf{A}}\delta\langle\tilde{\mathbf{c}}\rangle = -\beta\tilde{\mathbf{S}}^{(0)}\tilde{\mathbf{V}}. \tag{2.20}$$

Solving for $\delta\langle\tilde{\mathbf{c}}\rangle$, we get

$$\delta\langle\tilde{\mathbf{c}}\rangle = -\beta\tilde{\mathbf{A}}^{-1}\tilde{\mathbf{S}}^{(0)}\tilde{\mathbf{V}}. \tag{2.21}$$

On the other hand, if we applied the linear response theory with the interacting polymer mixture as the reference state, we would have

$$\delta\langle\tilde{\mathbf{c}}\rangle = -\beta\tilde{\mathbf{S}}\tilde{\mathbf{V}}, \tag{2.22}$$

where $\tilde{\mathbf{S}}$ is the structure factor matrix of the interacting system. Therefore, we arrive at the RPA structure factor matrix for the mixture as

$$\tilde{\mathbf{S}} = \tilde{\mathbf{A}}^{-1}\tilde{\mathbf{S}}^{(0)} = (\mathbf{I} + v\beta\tilde{\mathbf{S}}^{(0)}\hat{\chi})^{-1}\tilde{\mathbf{S}}^{(0)} \quad . \tag{2.23}$$

For a more general case of a compressible liquid with an interaction energy of the form given in Eq. (2.7), the mean potential is given by

$$V_k^{RPA}(\mathbf{r}) = v^{-1}\beta^{-1}\sum_{k'}\int d\mathbf{r}'\ U_{kk'}(\mathbf{r}-\mathbf{r}')\delta\langle\phi_{k'}(\mathbf{r}')\rangle. \tag{2.24}$$

Or in Fourier space,

$$\tilde{V}_k^{RPA}(\mathbf{q}) = v^{-1}\beta^{-1}\sum_{k'}\tilde{U}_{kk'}(\mathbf{q})\delta\langle\tilde{\phi}_{k'}(\mathbf{q})\rangle. \tag{2.25}$$

Note that this version of the interpretation of the RPA is more *microscopic* than the previous one because the interaction parameter $\tilde{U}_{kk'}(\mathbf{q})$ is directly related to the bare interaction potential. By comparing Eq. (2.25) with Eq. (2.16), the RPA structure factor for the system [26] can be identified as

$$\tilde{\mathbf{S}} = \left[\mathbf{I} + \tilde{\mathbf{S}}^{(0)}\tilde{\mathbf{U}}\right]^{-1}\tilde{\mathbf{S}}^{(0)} \tag{2.26}$$

2.2.2 RPA structure factor for blends

Specializing Eq. (2.23) for the case of an incompressible binary blend, consider a AB polymer blend in which the lengths of the two types of chains are N_A and N_B. The radii

of gyration and the average number density will be denoted by $R_{g,i}$ and c_i for $i = A$ or B. The volume per monomer is given by $v = c^{-1} = (c_A + c_B)^{-1}$. The structure factor matrix $\tilde{\mathbf{S}}^{(0)}$ for the non interacting polymer blend has the form of a diagonal matrix given by

$$\tilde{\mathbf{S}}^{(0)} = \begin{bmatrix} \tilde{S}_{AA}^{(0)}(\mathbf{q}) & 0 \\ 0 & \tilde{S}_{BB}^{(0)}(\mathbf{q}) \end{bmatrix}. \tag{2.27}$$

In the case where the continuous random walk model is used to represent a single chain, $\tilde{S}_{ii}^{(0)}(\mathbf{q})$ becomes a single chain structure factor $\Omega_i(\mathbf{q}) \equiv c_i N_i f_D(q^2 R_{g,i}^2)$ in which $f_D(x) = \frac{2}{x^2}(e^{-x} - 1 + x)$ is the Debye function. In the following, $\mathbf{q}$ dependence of various quantities will be suppressed for simplicity. With this, we get

$$
\begin{aligned}
\tilde{\mathbf{A}}^{-1} &= (\mathbf{I} + v\beta\tilde{\mathbf{S}}^{(0)}\hat{\chi})^{-1} \\
&= \frac{1}{|\tilde{\mathbf{A}}|} \begin{bmatrix} 1 + v\beta\tilde{S}_{BB}^{(0)}\,\hat{\chi}_{BB} & -v\beta\tilde{S}_{AA}^{(0)}\,\hat{\chi}_{AB} \\ -v\beta\tilde{S}_{BB}^{(0)}\,\hat{\chi}_{AB} & 1 + v\beta\tilde{S}_{AA}^{(0)}\,\hat{\chi}_{AA} \end{bmatrix},
\end{aligned}
\tag{2.28}
$$

in which the determinant $|\tilde{\mathbf{A}}|$ is given by

$$
\begin{aligned}
|\tilde{\mathbf{A}}| &= 1 + v\tilde{S}_{AA}^{(0)}(\chi_{AA} + \kappa^{-1}\beta) + \tilde{S}_{BB}^{(0)}(\chi_{BB} + \kappa^{-1}\beta) \\
&+ v^2 S_{AA}^{(0)} S_{BB}^{(0)}\left[\kappa^{-1}\beta(\chi_{AA} + \chi_{BB} - 2\chi_{AB}) + \chi_{AA}\,\chi_{BB} - \chi_{AB}^2\right].
\end{aligned}
\tag{2.29}
$$

For the case of incompressible liquid, we take $\kappa \to 0$ limit and keep the terms linear in κ^{-1} to get

$$\tilde{\mathbf{A}}^{-1} \to \frac{1}{\tilde{S}_{AA}^{(0)} + \tilde{S}_{BB}^{(0)} - 2v\chi} \begin{bmatrix} S_{BB}^{(0)} & -S_{AA}^{(0)} \\ -S_{BB}^{(0)} & S_{AA}^{(0)} \end{bmatrix}, \tag{2.30}$$

in which we defined $\chi \equiv \chi_{AB} - \frac{1}{2}(\chi_{AA} + \chi_{BB})$. Finally, we obtain the RPA for incompressible binary blends as

$$\tilde{\mathbf{S}}(\mathbf{q}) = S(\mathbf{q}) \begin{bmatrix} 1 & -1 \\ -1 & 1 \end{bmatrix}. \tag{2.31}$$

The scalar structure factor $\tilde{S}(\mathbf{q})$ is given by

$$[S(\mathbf{q})]^{-1} = [\tilde{S}_{AA}^{(0)}(\mathbf{q})]^{-1} + [\tilde{S}_{BB}^{(0)}(\mathbf{q})]^{-1} - 2v\chi \tag{2.32}$$

2.3 Renormalized one-loop theory of fluctuations

A renormalized one-loop theory (ROLT) of fluctuations is a coarse-grained theory that tries to take into account the composition fluctuation effects ignored in FH theory (and SCFT) or mean field theories in general. Recent theoretical developments by Wang [21] and Grzywacz *et al.* [22] have successfully removed the so-called UV divergence which had plagued the theory previously. In this section, the model and main results of the theory when it is applied to polymer blends [23] are reviewed. ROLT will allow us to interpret SCFT and RPA as exact theories only for the hypothetical system of infinitely long chains.

We will consider the model of blends introduced in Sec. 2.1. Let B_0 be a dimensionless compression energy and χ_0 be a dimensionless bare interaction parameter between species A and B. For our model binary blends, we assume $U_{ij}(\mathbf{r} - \mathbf{r}')$ takes the form

$$\left(U_{ij}\right) = v \begin{pmatrix} B_0 & B_0 + \chi_0 \\ B_0 + \chi_0 & B_0 \end{pmatrix} \delta_\Lambda(\mathbf{r} - \mathbf{r}') \quad , \tag{2.33}$$

where δ_Λ is a function with a range Λ^{-1} and $\int d\mathbf{r} \delta_\Lambda = 1$. In the limit of $\Lambda \to \infty$, δ_Λ approaches the Dirac δ function. In that limit, the Helmholtz free energy per volume f, can be written as a sum,

$$\beta f = \frac{\beta F}{V} = f_{\mathrm{id}} + f_{\mathrm{mf}} + f_{\mathrm{corr}}, \tag{2.34}$$

in which f_{id} is the ideal Flory-Huggins entropy of mixing and f_{mf} is the mean field approximation for the free energy per volume. In a translationally invariant system, they are given by,

$$f_{\mathrm{id}} = \frac{\phi_A}{N_A v} \ln \phi_A + \frac{\phi_B}{N_B v} \ln \phi_B \tag{2.35}$$

$$\begin{aligned} f_{\mathrm{mf}} &= \frac{1}{2} \sum_{i,j} \int d\mathbf{r} \; U_{ij}(\mathbf{r}) \langle c_i(\mathbf{r}) \rangle \langle c_j(\mathbf{r}) \rangle \\ &= v^{-1} \chi_0 \phi_A \phi_B \quad . \end{aligned} \tag{2.36}$$

The last term in Eq. (2.34) is the free energy due to the correlations in the number densities of monomer species. The one-loop approximation f_{1L} for f_{corr} in the case of a compressible liquid is given by

$$f_{\mathrm{1L}} = \frac{1}{2} \int \frac{d\mathbf{q}}{(2\pi)^3} \ln\left[\det\left|\mathbf{I} + \tilde{\mathbf{\Omega}}(\mathbf{q}) \tilde{\mathbf{U}}(\mathbf{q})\right|\right] \quad . \tag{2.37}$$

The matrix elements of $\tilde{\boldsymbol{\Omega}}(\mathbf{q})$ and $\tilde{\mathbf{U}}(\mathbf{q})$ are

$$\tilde{\Omega}_{ij}(\mathbf{q}) = \delta_{ij}\Omega_i(\mathbf{q}) \tag{2.38}$$

$$\tilde{U}_{ij}(\mathbf{q}) = \int d\mathbf{r}\, U_{ij}(\mathbf{r})e^{i\mathbf{q}\cdot\mathbf{r}} \quad, \tag{2.39}$$

in which $\Omega_i(\mathbf{q}) = v^{-1}\phi_i N_i f_D(q^2 R_{g,i}^2)$ is the intra-molecular correlation function of a continuous random walk model with a radius of gyration $R_{g,i}$ and $f_D(x)$ is the Debye function. A derivation of Eq. (2.37) by a fictitious charging process is given in Appendix A.

In the limit of incompressible liquids, which is effected by taking the limit $B_0 \to \infty$, f_{1L} is reduced to

$$f_{1L} = \frac{1}{2}\int \frac{d^3q}{(2\pi)^3} \ln\left[(\Omega_A + \Omega_B - 2\chi_0 v\Omega_A\Omega_B)\, v\right] \quad. \tag{2.40}$$

The Fourier integral in Eq. (2.40) is known to diverge at high values of q, a behavior known as the UV divergence. However, in recent works, Wang [21] and Grzywacz *et al.* [22] analyzed the structure of the high q divergence of f_{1L} by introducing a cutoff Λ for the integral. Grzywacz *et al.* showed f_{1L} can be expressed as a sum

$$f_{1L} = f_{1L}^\Lambda + f_{1L}^* \tag{2.41}$$

of an UV divergent part f_{1L}^Λ which increases with increasing Λ plus a contribution f_{1L}^* that is independent of Λ. They interpreted $f_{1L}^\Lambda + f_{\mathrm{mf}}$ as the relevant form of SCFT that should be regarded as an input to the one-loop theory. The remaining cutoff independent f_{1L}^* was identified as a universal correction to the underlying SCFT.

After this renormalization, the total free energy density can be recast as a sum of the form,

$$f = f_{\mathrm{id}} + f_{\mathrm{int}} + f_{\mathrm{end}} + f_{1L}^* \quad, \tag{2.42}$$

where f_{end} is a non universal excess free energy associated with chain ends and has N^{-1} chain length dependence. The SCF interaction free energy is given by,

$$f_{\mathrm{int}} = v^{-1}\chi_e\phi_A\phi_B \quad, \tag{2.43}$$

where χ_e is an effective SCF interaction parameter that is independent of chain length. The UV convergent part of correlation free energy f_{1L}^* has a specific dependence on

parameters of SCFT, i.e.

$$
\begin{aligned}
f_{1\mathrm{L}}^* &= \frac{1}{R^3}\hat{f}_1^*(\chi N, \phi_A, N_B/N_A, R_B/R_A) \\
&= \frac{v^{-1}}{N\bar{N}^{1/2}}\hat{f}_1^*(\chi N, \phi_A, N_B/N_A, R_B/R_A)
\end{aligned}
\tag{2.44}
$$

where $R = R_A$ is a reference length that is taken to be the end-end distance of a A chain, $N = N_A$ is a reference degree of polymerization and $\hat{f}_1^*$ is a function obtained by non-dimensionalizing the renormalized form of the integral in Eq. (2.40). The above equation shows clearly that the universal correction is smaller than the SCF free energy $(f_{\mathrm{id}} + f_{\mathrm{int}} + f_{\mathrm{end}})$ by a factor of $\bar{N}^{-1/2}$. The χ parameter in Eq. (2.44) is left unspecified because different choices (χ_a or χ_e) result in different variants of the theory [23].

Chapter 3

Molecular simulations: models and methods

3.1 Models of polymers

For the study of polymer melts and blends, atomistic and chemically realistic models are too expensive in terms of computational cost. The reason is that for these systems, there exists a wide range of characteristic time and length scales and the cost is determined by the shortest scale [27]. Therefore, simulations of many chains in realistic representation is prohibitively time consuming.

In the study of meso-scale (length scale larger than a monomer but less than bulk material) correlation effects in melts and blends, however, the microscopic details of a given model should not matter as long as it reflects the essential features of real systems at the physical scale of interest [28]. This premise of coarse-grained modeling is also a topic we will investigate in this thesis. For this reason, computational studies of polymeric liquids have been done using so called coarse-grained models. An effective interaction unit, or bead in any coarse-grained model of polymer, represents a number of chemical monomers. They are connected via a bond and two monomers are not allowed to occupy the same position due to the excluded volume interaction.

Most coarse-grained models are constructed either on a lattice or in a continuum space. Lattice models are computationally efficient compared to continuum models. The main reasons are: (1) integer arithmetic, and (2) fast checking of excluded volume

[27, 29]. For our study we employ a bead-spring model as a continuum model, and the bond fluctuation model as a lattice model.

3.1.1 Bead-spring model (BSM)

We adopt a bead-spring model of a linear polymer chain where the interaction between two non-bonded beads is described in a variant of Lennard-Jones (LJ) form

$$F(r) = \begin{cases} 4[(\sigma/r)^{12} - (\sigma/r)^6] + 1 & \text{for } r < 2^{1/6}\sigma \\ 0 & \text{otherwise} \end{cases}$$

where r is the distance between two non-bonded beads. Monomers of the same type (A-A or B-B), then interact via a potential

$$v_{AA}(r) = v_{BB}(r) = \epsilon F(r) \quad . \tag{3.1}$$

The interaction between monomers of different type (A-B) is given by

$$v_{AB}(r) = \epsilon(1 + \xi)F(r) \quad , \tag{3.2}$$

where ξ is a small parameter that controls the incompatibility of the two types. In this model, ϵ and σ are the units of energy and length and all other quantities can be expressed as combinations of them. The temperature of the simulated system is in units of ϵ/k_{B} with k_{B} being the Boltzmann constant.

Two bonded monomers interact via a harmonic potential of the form

$$v_{bond}(r) = \frac{1}{2}\kappa(r - l)^2 \quad , \tag{3.3}$$

where r is the distance between two bonded beads and κ is a spring constant which is measured in units of ϵ/σ^2. l is a reference length. This interaction will be the same regardless of the types of beads in polymer blends. Another popular choice for a bond potential is the FENE (finite extensible nonlinear elastic) potential [30, 31] which allows only a finite extension of bond length to prevent two bonds from cutting through each other. With proper choice of constant κ, however, chain crossing can also be prevented without causing inefficiency in simulation.

3.1.2 Bond fluctuation model (BFM)

A lattice model which has been widely used for the study of many chain systems is the bond fluctuation model [32]. It is different from a simple self-avoiding walk (SAW) model in which there are 6 bond vectors possible in 3-dimensions for a simple cubic lattice and a bead occupies one lattice site. In the BFM constructed on a simple cubic lattice, each bead blocks 8 sites of the elementary cube of the lattice. Also the bond vector connecting two monomers takes one out of 108 choices, making the model closer to a continuum model than the SAW model. In the model we adopt [33, 34], a bond vector is taken from the allowed set

$$\mathbf{b} = P(2,0,0), P(2,1,0), P(2,1,1), P(2,2,1), P(3,0,0), P(3,1,0) \tag{3.4}$$

where P stands for all permutations and sign combinations of the components of vectors listed. The inter and intra molecular interaction are modeled via a square well potential of spatial range $\sqrt{6}$ in units of lattice spacing. This spatial range amounts to a bead having 54 interacting neighbors. More precisely, the interaction energy between same type (A-A or B-B) is given by

$$v_{AA}(r) = v_{BB}(r) = -\epsilon\xi \qquad \text{if } r \leq \sqrt{6} \tag{3.5}$$

while monomers of different types interact via

$$v_{AB}(r) = \epsilon\xi \qquad \text{if } r \leq \sqrt{6} \quad, \tag{3.6}$$

where r is the distance between centers of two beads. As in the bead spring model, ξ controls the incompatibility of the two species A and B.

3.2 Monte Carlo sampling

Two main simulation methods for systems described by classical statistical mechanics are molecular dynamics (MD) and Monte Carlo (MC) sampling [35, 36]. The term Monte Carlo is used for a class of probabilistic methods that use random numbers. One of the many problems where MC method becomes the tool of choice is the calculation of multi-dimensional integrals [37]. Also, only MC methods can be used to study models on lattices such as classical spin systems [38, 39]. The basic idea of the MC

method applied to molecular simulations is as follows: a trial change of system configuration is suggested and it is accepted or rejected by an appropriate criterion in such a way that system configurations are sampled according to its equilibrium distribution or Boltzmann distribution. This scheme, called importance sampling, will be explained in detail in Section 3.2.1.

Molecular dynamics is the other method used widely in the field of molecular simulation. It provides numerical solutions to Newton's equations of motion for classical many-body systems. As a result, the method generates both static and dynamic information about the simulated model. The reasons of choosing MC method over MD method for the study of polymer thermodynamics are two fold. First, thermodynamics can be studied without realistic dynamics for which MD is the necessary tool. Secondly, because of the first reason, one can implement various trial changes of the configuration of molecules which are unrealistic, but help the exploration of the configurational phase space tremendously. The latter point is also crucial for simulations of long chain molecules because by natural dynamic process, the diffusive motion of entire molecule is very slow.

3.2.1 Importance sampling

Importance sampling is a way to sample configurations of a model system according to its Boltzmann probability distribution. Although configurations vary continuously in molecular simulations, the following discussion will assume that configurations of the system of interest can be counted discretely and each distinct configuration will be labelled by an index l. Therefore, the canonical ensemble average and equilibrium probability distribution can be expressed as,

$$P_l^{eq} = \frac{\exp(-\beta U_l)}{\sum_m \exp(-\beta U_m)} \tag{3.7}$$

$$\langle A \rangle = \sum_l A_l P_l^{eq} \tag{3.8}$$

By importance sampling, we want the initial arbitrary probability distribution $P_l(t = 0)$ to approach to P_l^{eq} after some transient period. Even though there is only one simulation system at hand, it is conceptually helpful to imagine there are infinite number

of replicas of the system and the number of replicas in state l is proportional to $P_l(t)$. The way we make $P_l(t=0)$ converge to P_l^{eq} is by making transition from one state to another and accepting or rejecting the proposed transition. $w_{l \to m}$ will be used to denote the probability of a system in state l at time t to move to state m at time $t+1$.

To derive how $P_l(t)$ evolves in discrete time step, we denote with $N_l(t)$ the number of replicas in state l at time t. At time $t+1$,

$$N_l(t+1) = N_l(t) + \sum_{m \neq l} N_m(t) w_{m \to l} - \sum_{m \neq l} N_l(t) w_{l \to m}. \tag{3.9}$$

Dividing both sides of the above equation by the total number of replicas $\mathcal{N} = \sum_l N_l(t)$ and noting $\frac{N_l(t)}{\mathcal{N}} = P_l(t)$, we obtain the master equation,

$$P_l(t+1) = P_l(t) + \sum_{m \neq l} [P_m(t) w_{m \to l} - P_l(t) w_{l \to m}] \quad . \tag{3.10}$$

The summation in the above equation exclude the term with $m = l$, but the term does not contribute to the sum, so we can remove the restriction on it. Then,

$$
\begin{aligned}
P_l(t+1) &= P_l(t) + \sum_m [P_m(t) w_{m \to l} - P_l(t) w_{l \to m}] \\
&= P_l(t) + \sum_m P_m(t) w_{m \to l} - P_l(t) \sum_m w_{l \to m} \\
&= \sum_m P_m(t) w_{m \to l}.
\end{aligned}
\tag{3.11}
$$

The last line results from the fact that $\sum_m w_{l \to m} = 1$.

Once $P_l(t)$ reaches to P_l^{eq}, it should not change as time progresses. By setting $P_l(t) = P_l(t+1) = P_l^{eq}$ in Eq. (3.11), we obtain

$$\sum_m (P_m^{eq} w_{m \to l} - P_l^{eq} w_{l \to m}) = 0. \tag{3.12}$$

The above equation dictates the relation between P_l^{eq} and $w_{l \to m}$ when equilibrium has been reached. In practice, we require a more strict condition known as the detailed balance condition [36, 35, 38, 39]

$$P_m^{eq} w_{m \to l} = P_l^{eq} w_{l \to m}. \tag{3.13}$$

In appendix B, a short proof that the detailed balance condition will drive $P_l(t=0)$ to P_l^{eq} is given. Once equilibrium is established, the ensemble average (Eq. (3.8))

becomes the simple mean of the observed values of A, i.e. if L instances of A are measured during the course of a simulation,

$$\langle A \rangle \approx \frac{1}{L} \sum_{i=1}^{L} A_i \quad . \tag{3.14}$$

Because each measurement in the sum is not independent, care needs to be taken in the estimation of error of the obtained average (Appendix C).

3.2.2 Metropolis algorithm

In practice, a transition from one state (old state denoted by 'o') to another state (new state denoted by 'n') happens in two steps: a new state of the system is proposed and the proposed state is accepted or rejected according to certain probability. Let A be the event where a new state of the system is proposed and B be the event where the proposed state is accepted. Adopting notations of probability theory, the transition event can be denoted by $A \cap B$ and the rule for the conditional probability says $P(A \cap B) = P(B|A)P(A)$, where $P(B|A)$ is the conditional probability that event B happens given that event A happens. That is, if $G(o \rightarrow n)$ is the probability of suggesting or generating state n given the system is in state o and $A(o \rightarrow n)$ is the probability of accepting the proposed transition,

$$w_{o \rightarrow n} = G(o \rightarrow n)A(o \rightarrow n) \quad . \tag{3.15}$$

Assuming $G(o \rightarrow n)$ is known, there are many choices for the acceptance probability $A(o \rightarrow n)$ that satisfy Eq. (3.13). The most commonly used one is the Metropolis function [40]

$$A(o \rightarrow n) = min \left\{ 1, \frac{P_n^{eq} G(n \rightarrow o)}{P_o^{eq} G(o \rightarrow n)} \right\} \tag{3.16}$$

Using a property of the Metropolis function $(min\{1, x\} = x(min\{1, \frac{1}{x}\})$ for $x > 0)$,

it can be shown that Eq. (3.16) satisfies the detailed balance condition, i.e.

$$
\begin{aligned}
P_o^{eq} w_{o \to n} &= P_o^{eq} G(o \to n) A(o \to n) \\
&= P_o^{eq} G(o \to n) min \left\{ 1, \frac{P_n^{eq} G(n \to o)}{P_o^{eq} G(o \to n)} \right\} \\
&= P_o^{eq} G(o \to n) \frac{P_n^{eq} G(n \to o)}{P_o^{eq} G(o \to n)} min \left\{ 1, \frac{P_o^{eq} G(o \to n)}{P_n^{eq} G(n \to o)} \right\} \\
&= P_n^{eq} G(n \to o) min \left\{ 1, \frac{P_o^{eq} G(o \to n)}{P_n^{eq} G(n \to o)} \right\} \\
&= P_n^{eq} w_{n \to o} \quad\quad\quad\quad\quad\quad (3.17)
\end{aligned}
$$

As long as the equilibrium probability distribution is known and the probability of generating a trial configuration can be calculated, Eq. (3.16) can be used to ensure that the detailed balance condition is satisfied.

3.3 Semi grand canonical ensemble

Semi grand ensemble [13] for symmetric polymer blends (same chain length and statistical segment length) is a statical ensemble in which the total number of polymers in the system is conserved, but the type of a chain is allowed to change. This ensemble has the advantage over both canonical and grand canonical ensembles when one wants to simulate a phase separation of the model blend or composition fluctuations. In canonical ensemble, it occurs through diffusive motion of chains and it becomes very slow near the critical point. In grand canonical ensemble in which the numbers of both types of chains are fluctuating, a move creating a chain in a dense system has a very small chance to be accepted because it would violate the excluded volume constraint most of the time.

3.3.1 Derivation

The semi grand ensemble is derived from first considering grand canonical ensemble in which both the total number of chains and the number of chains of each type can change [41, 38]. Let M_A, M_B, and M_t be the numbers of A chains, B chains, and the total number of chains, i.e. $M_t = M_A + M_B$. Also let $N = N_A = N_B$ be the degree of polymerization for the chains. The configurational part of the grand canonical partition

function for the system is given by,

$$\mathcal{L}_G = \int dM_A \int dM_B \int dE e^{\beta N(M_A\mu_A + M_B\mu_B)} e^{-\beta E} \Gamma(M_A, M_B, E) \quad , \tag{3.18}$$

in which E is the total potential energy, μ_A, μ_B are monomer chemical potentials of the two species, and $\Gamma(M_A, M_B, E)$ is a density of states. The semi-grand ensemble is constructed by constraining the system in the part of configuration space where M_t is fixed. Let M be the difference in the numbers of chains, $M \equiv M_A - M_B$. Then,

$$M_A = \frac{M_t + M}{2} \tag{3.19}$$

$$M_B = \frac{M_t - M}{2} \tag{3.20}$$

$$M_A\mu_A + M_B\mu_B = \frac{M_t}{2}(\mu_A + \mu_B) + \frac{M}{2}(\mu_A - \mu_B) \tag{3.21}$$

In this constrained space, the grand canonical partition function is reduced to a semi grand partition function defined as,

$$\mathcal{L}_{SG} \equiv \int_{-M_t}^{M_t} dM e^{\beta \frac{NM\Delta\mu}{2}} \int dE e^{-\beta E} \tilde{\Gamma}(M, E) \quad . \tag{3.22}$$

In Eq. (3.22) we defined

$$\Delta\mu \equiv \mu_A - \mu_B \quad , \tag{3.23}$$

$$\tilde{\Gamma}(M, E) \equiv \int dM_A \int dM_B \delta(M_t - M_A - M_B)\delta(M - (M_A - M_B))\Gamma(M_A, M_B, E) \quad , \tag{3.24}$$

where $\delta(x)$ is the Dirac delta function. A formal relation between $\mathcal{L}_G$ and $\mathcal{L}_{SG}$ is

$$\mathcal{L}_G = \int dM_t e^{\beta N \frac{NM_t(\mu_A+\mu_B)}{2}} \mathcal{L}_{SG} \quad . \tag{3.25}$$

An alternative way of defining the semi grand canonical ensemble is to use the number of A chains M_A as an argument (instead of M) of the density of states. In this case, the ensemble is defined as a sum of canonical ensembles with M_A ranging from 0 to M_t, i.e.

$$\begin{aligned}
\mathcal{L}_{SG} &\equiv \int_0^{M_t} dM_A \, e^{\beta N M_A \Delta\mu} \int dE e^{-\beta E} \tilde{\Gamma}(2M_A - M_t, E) \\
&= \sum_{M_A=0}^{M_t} e^{\beta\mu M_A} Z(M_A, \beta)
\end{aligned} \tag{3.26}$$
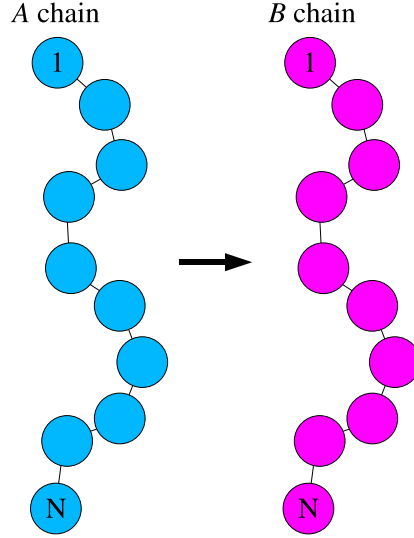
Figure 3.1: In a semi grand canonical move, a chain molecule switches its type from A to B or vice versa, depending on its original type

where $Z(M_A, \beta)$ is the canonical partition function with a fixed number of A chains and $\mu \equiv N\Delta\mu$ is the chemical potential difference between an A chain and a B chain.

3.3.2 Type switching MC move

For a MC simulation in the semi grand ensemble, there is a move where a chain is picked up randomly and tried for its type change, in addition to usual trial moves for configurational change (Fig. 3.1). One can derive the acceptance probability for such a move by recalling the probability of the system being in a microstate with M_A chains of type A and M_B chains of type B is

$$P^{eq} \propto \frac{1}{M_A! M_B!} e^{\beta \frac{NM\Delta\mu}{2}} e^{-\beta U} \quad , \tag{3.27}$$

where U instead of E was used to emphasize that it is configurational energy. Consider a trial move to change a randomly picked A chain to a B chain. In the new state of the system, the numbers of A and B chains will be $M_A - 1$ and $M_B + 1$, respectively.

Therefore,

$$G(o \to n) \;=\; \frac{M_A}{M_t} \tag{3.28}$$

$$G(n \to o) \;=\; \frac{M_B + 1}{M_t} \tag{3.29}$$

To obtain the acceptance probability for this transition, the factors appearing in the Metropolis function (Eq. (3.16)) need to be calculated:

$$P_n^{eq} G(n \to o) \;=\; \frac{1}{(M_A - 1)!(M_B + 1)!} e^{\frac{\beta N (M_A - M_B - 2)\Delta\mu}{2}} e^{-\beta U_n} \frac{M_B + 1}{M_t} \quad, \tag{3.30}$$

$$P_o^{eq} G(o \to n) \;=\; \frac{1}{M_A! M_B!} e^{\frac{\beta N (M_A - M_B)\Delta\mu}{2}} e^{-\beta U_o} \frac{M_A}{M_t} \quad, \tag{3.31}$$

in which U_o and U_n denote old and new values of U. Substituting above equations into Eq. (3.16), the acceptance probability for the $A \to B$ identity switch is obtained as,

$$A(o \to n) = min\left\{1, e^{-\beta[(U_n - U_o) + N\Delta\mu]}\right\}. \tag{3.32}$$

Similar considerations for the $B \to A$ identity switch move yields

$$A(o \to n) = min\left\{1, e^{-\beta[(U_n - U_o) - N\Delta\mu]}\right\}. \tag{3.33}$$

Eqs. (3.32) and (3.33) can be combined in the following form, which is also applicable to the usual canonical moves,

$$A(o \to n) = min\left\{1, e^{-\beta[(U_n - U_o) - N\Delta\mu(M_n - M_o)/2]}\right\} \quad, \tag{3.34}$$

in which M_n and M_o are new and old values of M, respectively.

3.3.3 $S(\mathbf{q} \to 0)$ measurement

Assuming effective incompressibility of a blend, $S(\mathbf{q})$ (Eq. (2.5)) can be expressed as,

$$S(\mathbf{q}) \;=\; \frac{1}{4}[\tilde{S}_{AA}(\mathbf{q}) + \tilde{S}_{BB}(\mathbf{q}) - \tilde{S}_{AB}(\mathbf{q}) - \tilde{S}_{BA}(\mathbf{q})]$$

$$\;=\; \frac{1}{4V}\langle |\delta\tilde{c}_A(\mathbf{q}) - \delta\tilde{c}_B(\mathbf{q})|^2 \rangle, \tag{3.35}$$

where $\delta c_i(\mathbf{r}) \equiv c_i(\mathbf{r}) - \langle c_i(\mathbf{r}) \rangle$ and $\delta\tilde{c}_i(\mathbf{q}) = \int d\mathbf{r}\, e^{i\mathbf{q}\cdot\mathbf{r}} \delta c_i(\mathbf{r})$. To evaluate $S(0)$, one needs $\delta\tilde{c}_i(\mathbf{q} = 0)$ which can be expressed as,

$$\delta\tilde{c}_i(\mathbf{q} = 0) \;=\; \int d\mathbf{r}\, \delta c_i(\mathbf{r})$$

$$\;=\; N M_i - N\langle M_i \rangle \tag{3.36}$$

Using Eqs. (3.35) and (3.36), $S(0)$ can be expressed in terms of the variance in the number of chains of type A as

$$
\begin{aligned}
S(0) &= \frac{N^2}{4V}\langle |M_A - M_B - (\langle M_A\rangle - \langle M_B\rangle)|^2\rangle \\
&= \frac{N^2}{V}\langle (M_A - \langle M_A\rangle)^2\rangle \quad .
\end{aligned}
\tag{3.37}
$$

The second line of Eq. (3.37) follows from the fact that in this ensemble $M_t = M_A + M_B$ is constant.

3.4 Hybrid Monte Carlo

In hybrid Monte Carlo (HMC) method [40, 42], a trial configuration is constructed by numerically solving equations of motions of the system, just as in a regular molecular dynamics (MD) simulation. The most attractive feature about this method is that the trial configuration of the system is one which is energetically favorable: it is the most natural configuration of the system which follows realistic dynamics.

Consider a system of N particles described by a classical Hamiltonian,

$$
H(\mathbf{r}, \mathbf{p}) = \sum_{i=1}^{N} \frac{\mathbf{p}_i^2}{2m} + U(\mathbf{r}) \quad ,
\tag{3.38}
$$

where $U(\mathbf{r})$ is the total potential energy of the system and $\mathbf{r}$ and $\mathbf{p}$ denote the positions and momenta of the N particles collectively. To generate a trial configuration in a HMC move, Hamilton's equations are integrated using some discretization scheme $\hat{g}(\delta t)$ where δt is a size of time step. That is, the equations of motion

$$
\frac{d\mathbf{r}_i}{dt} = \frac{\partial H}{\partial \mathbf{p}_i}
\tag{3.39}
$$

$$
\frac{d\mathbf{p}_i}{dt} = -\frac{\partial H}{\partial \mathbf{r}_i}
\tag{3.40}
$$

are solved numerically for $i = 1, \cdots, N$. Denoting the new positions and momenta by $\mathbf{r}'$ and $\mathbf{p}'$ respectively, we can write symbolically

$$
(\mathbf{r}', \mathbf{p}') = \hat{g}(\delta t)(\mathbf{r}, \mathbf{p}).
\tag{3.41}
$$

Because $\mathbf{r}'$ is determined by current values of $\mathbf{r}$ and $\mathbf{p}$, the probability $G(\mathbf{r} \to \mathbf{r}')$ is equal to $G(\mathbf{p})$ of generating momenta of particles in the system. At the beginning of the HMC move, momenta are drawn from Gaussian probability distribution

$$
\begin{aligned}
G(\mathbf{p}) &= \mathcal{N} \exp(-\beta \sum_{i=1}^{N} \frac{\mathbf{p}_i^2}{2m}) \\
&= \mathcal{N} \exp(-\beta K(\mathbf{p})) \quad\quad (3.42)
\end{aligned}
$$

where $\mathcal{N}$ is a normalization constant and we defined K to denote kinetic energy. Substituting this probability into the Metropolis function (Eq. 3.16), we obtain the following acceptance criterion for a suggested move

$$
\begin{aligned}
A(\mathbf{r} \to \mathbf{r}') &= min\left\{1, \frac{P_n^{eq} G(n \to o)}{P_o^{eq} G(o \to n)}\right\} \\
&= min\left\{1, \frac{Q^{-1} \exp(-\beta U(\mathbf{r}')) \mathcal{N} \exp(-\beta K(\mathbf{p}'))}{Q^{-1} \exp(-\beta U(\mathbf{r})) \mathcal{N} \exp(-\beta K(\mathbf{p}))}\right\} \\
&= min\left\{1, \exp(-\beta[H(\mathbf{r}', \mathbf{p}') - H(\mathbf{r}, \mathbf{p})])\right\} \quad , \quad\quad (3.43)
\end{aligned}
$$

where Q is the partition function $\frac{1}{N! h^{3N}} \int d\mathbf{r} \, d\mathbf{p} e^{-\beta H(\mathbf{r}, \mathbf{p})}$ and h is the Planck constant. If the numerical integration scheme $\hat{g}(\delta t)$ conserves the total energy H, all trial moves will be accepted. In practice, however, it is not the case and some will be rejected. The acceptance rate of a trial of HMC tends to decrease as the number of particles in the system increases. This is because of the numerical inaccuracy introduced by solving equations of motion gets large with the number of particles in the system. Similarly, a large number of integration steps tends to decrease the acceptance rate as well. Two important constraints about the integration scheme $\hat{g}(\delta t)$ is that it has to be time reversible and preserve phase space area [40]. A simple integration method that satisfies the conditions is the velocity Verlet algorithm [35].

3.5 Configurational-bias Monte Carlo (CBMC)

The basic idea of CBMC was first introduced by Rosenbluth and Rosenbluth to sample equilibrium polymer chain conformations [43]. The goal was to grow a new chain molecule in a dense environment where there already exist many other chains. A conformation generated randomly would almost always violate the excluded volume constraint.

To get around the problem, they devised an algorithm that generates energetically favorable trial conformations, therefore applying a bias in the generation of configurations. This bias would have to be corrected in a later stage. Generating a biased configuration that has some sort of advantage whose benefits exceed the complexity introduced in the algorithm is the spirit behind any type of configuration-biased MC sampling scheme.

This class of algorithms takes advantage of the freedom in the way a trial configuration is generated. Because the number of possible ways is virtually unlimited, one can devise a clever way to create a trial move that either has a high probability of being accepted or accelerates the exploration of the configuration space by the system. This type of moves is especially useful in simulations of long polymer chains because their equilibration times scale as N^3 for $N > N_e$ where N_e is an entanglement length [4]. There are many such moves proposed for simulations of polymers. For the simulations presented in this thesis, three types of CBMC moves were implemented, namely slithering snake type move, single rebridging, and double rebridging move.

3.5.1 Slithering snake move (Reptation)

In the reptation move [44], a new configuration of a linear chain along its own path is generated by removing a randomly chosen end monomer and attaching it to the other end. Implementation of the move consists of the following steps.

1. Pick a chain at random.

2. Choose one of the two ends at random. The monomer of the chosen end will be removed and attached to the other end.

3. At the end where the monomer from the other end will be attached, generate a number of trial bond vectors according to a probability proportional to the Boltzmann factor associated with the bond potential energy.

4. Choose one of trial bonds according to a probability proportional to the Boltzmann factor associated with external (or non-bonded) potential energy of the attached monomer if it were to be positioned at proposed trial positions.

5. Repeat previous steps for the reverse move using the old configuration as the chosen one.
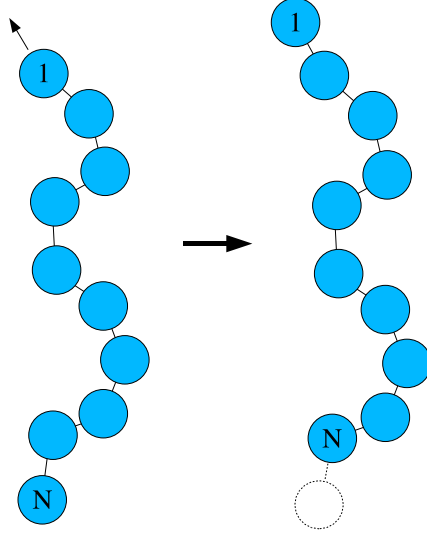
Figure 3.2: In reptation move, a chain molecule moves along its own path

6. Accept the new configuration of the chain according to Metropolis rule.

To calculate the acceptance probability of this move, we first calculate the probability of generating the new configuration chosen at the end of step 4. The probabilities associated with step 1 and 2 are $\frac{1}{M_t}$ and $\frac{1}{2}$, respectively, and M_t is the total number of chains in the system. In step 3, assume k trial bonds are generated according to the Boltzmann weight associated with bond potential energy $v_{bond}(\mathbf{b})$. Then, the probability density of generating a particular bond is given by

$$P_{bond}(\mathbf{b}) = \frac{e^{-\beta v_{bond}(\mathbf{b})}}{\int d\mathbf{b}' e^{-\beta v_{bond}(\mathbf{b}')}} = C_{bond} \; e^{-\beta v_{bond}(\mathbf{b})} \tag{3.44}$$

At step 4, one of the k candidates for the bond $(\mathbf{b}_1, \cdots \mathbf{b}_k)$ will be chosen according to the probability proportional to the Boltzmann factor associated with non-bonded potential energy of them. If candidate i $(1 \leq i \leq k)$ is chosen, the probability of the event is,

$$P_{ext}(\mathbf{b}_i) = \frac{e^{-\beta v_{ext}(\mathbf{b}_i)}}{W(o \rightarrow n)} \quad, \tag{3.45}$$

where $v_{ext}(\mathbf{b}_i)$ is the non-bonded potential energy associated with the new position of the regrown end monomer and we defined a quantity called 'Rosenbluth weight' as,

$$W(o \to n) \equiv \sum_{j=1}^{k} e^{-\beta v_{ext}(\mathbf{b}_j)}. \tag{3.46}$$

Combining all the probabilities in the above steps, the generation probability $G(o \to n)$ is determined to be

$$G(o \to n) = \left(\frac{1}{M_t}\right) \left(\frac{1}{2}\right) C_{bond} \ e^{-\beta v_{bond}(\mathbf{b}_i)} \frac{e^{-\beta v_{ext}(\mathbf{b}_i)}}{W(o \to n)} \tag{3.47}$$

To compute the generation probability of the reverse move $G(n \to o)$, one pretends that the new configuration has been accepted and repeat the steps used in the calculation of $G(o \to n)$. However, for this case, only $k-1$ trial bonds $(\mathbf{b}'_1, \cdots \mathbf{b}'_{k-1})$ need to be generated and there is no decision making because the old configuration is already known. Denoting the original bond vector by $\mathbf{b}_o$,

$$G(n \to o) = \left(\frac{1}{M_t}\right) \left(\frac{1}{2}\right) C_{bond} \ e^{-\beta v_{bond}(\mathbf{b}_o)} \frac{e^{-\beta v_{ext}(\mathbf{b}_o)}}{W(n \to o)} \quad, \tag{3.48}$$

where

$$W(n \to o) \equiv e^{-\beta v_{ext}(\mathbf{b}_o)} + \sum_{j=1}^{k-1} e^{-\beta v_{ext}(\mathbf{b}'_j)}. \tag{3.49}$$

The change in the total potential energy is caused only by this monomer being removed from one end and attached to the other end. Therefore,

$$U_n - U_o = (v_{bond}(\mathbf{b}_i) + v_{ext}(\mathbf{b}_i)) - (v_{bond}(\mathbf{b}_o) + v_{ext}(\mathbf{b}_o)) \tag{3.50}$$

Assuming the simulation is done in canonical or semi grand canonical ensemble,

$$\frac{P_n^{eq} G(n \to o)}{P_o^{eq} G(o \to n)} = e^{-\beta(U_n - U_o)} \frac{e^{-\beta v_{bond}(\mathbf{b}_o)} \frac{e^{-\beta v_{ext}(\mathbf{b}_o)}}{W(n \to o)}}{e^{-\beta v_{bond}(\mathbf{b}_i)} \frac{e^{-\beta v_{ext}(\mathbf{b}_i)}}{W(o \to n)}}$$

$$= \frac{W(o \to n)}{W(n \to o)} \tag{3.51}$$

Finally, the acceptance probability for this move is

$$A(o \to n) = min \left\{ 1, \frac{W(o \to n)}{W(n \to o)} \right\}. \tag{3.52}$$

3.5.2 Rebridging Monte Carlo

In this type of move, a part of a chain is erased and regrown within itself (single rebridging) [45, 46] or parts of two chains are erased and regrown to form a new pair of chains in which the connectivity of the original chains are altered (double rebridging) [47, 48, 49]. In fact, a single rebridging algorithm is an important part of a corresponding double rebridging algorithm. Although there is no limit for the number of segments or monomers to be regrown in principle, we implemented a move that involves erasing only one monomer and regrowing it in both types of moves because of its simplicity.

For single rebridging, we implement a continuum version of the crank-shaft move [50] where an erased monomer is put back near a circle formed by the loci of points which are equidistant from two adjacent monomers. The distance was chosen to be one that minimize the bare bond potential energy.

For double rebridging, we adopt the scheme proposed by Banaszak and de Pablo [49] and implement it with our version of the single rebridging move. In our implementation of the scheme, a chain is chosen at random and the rest of the chains of the same type are scanned for a potential bridging sites. One can bias these processes in any possible way that will enhance the chance for the move to be accepted.

Trimer single rebridging

During a trimer single rebridging move, a chain is picked randomly and a monomer, which is not one of two end monomers, is chosen. The monomer is erased from the chain and regrown at a new position. A *bridge* in the following will refer to the three monomers involved in this type of move (those labelled 0, 1, and 2 in Fig. 3.3). Implementation steps of the move are as follows:

1. Pick a chain at random and decide which end to call the head of the chain also randomly.

2. Pick a non-end monomer from the chosen chain (labeled as 1 in Fig. 3.3) at random and remove it.

3. Generate trial positions according to a probability proportional to $e^{-\beta v_{bond}}$. To enhance the chance of success, apply a bias to restrict the new positions around
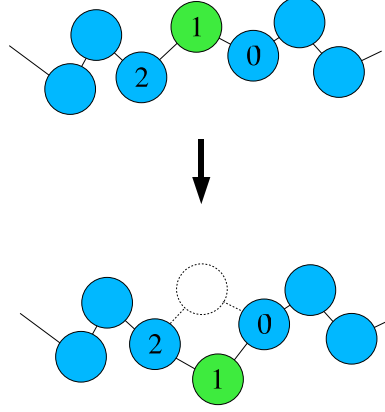
Figure 3.3: In a single rebridging move, two bonds connected to a monomer marked as 1 are erased and regrown.

a circle formed by rotation of two joined bond vectors from the adjacent two monomers (similar to a crank-shaft move).

4. Choose one of the trial positions according to a probability proportional to the Boltzmann factor associated with external interaction energy.

5. Accept the proposed new position of the monomer according to the Metropolis rule.

Calculation of the acceptance probability would be similar to the one for the reptation move, which showed all the essential features in CBMC moves. The probabilities associated with the first two steps are $\frac{1}{M_t}$, $\frac{1}{2}$, and $\frac{1}{N-2}$. As before, k trial positions are generated with probabilities proportional to $e^{-\beta v_{bond}}$. For this move, however, we apply a bias additionally. The probability of generating a particular bond $\mathbf{b}$ directed from monomer 2 to monomer 1 is

$$P_{bond}(\mathbf{b}) = C_{norm} \ e^{-\beta v_{bond}(\mathbf{b})} \ e^{-\beta \frac{\kappa_\theta}{2}(\theta-\theta_0)^2}, \tag{3.53}$$
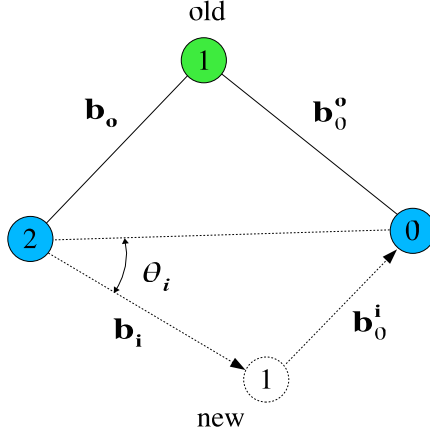
Figure 3.4: Monomer 1 is erased and regrown from monomer 2. The new bond vector from monomer 2 to new position of monomer 1 is denoted by $\mathbf{b}_i$ and the new bond vector from monomer 1 to monomer 0 is denoted by $\mathbf{b}_0^i$

where a normalization constant C_{norm} is given by

$$C_{norm}^{-1} = \int d\mathbf{b}' e^{-\beta v_{bond}(\mathbf{b}')} e^{-\beta \frac{\kappa_\theta}{2}(\theta' - \theta_0)^2} \quad . \tag{3.54}$$

κ_θ is an elastic constant obtained by Taylor expanding the bare potential energy associated the bond between monomer 1 and 0 about the energy minimum for which $\theta = \theta_0$ [51]. At step 4, one of k trial bonds $(\mathbf{b}_1, \cdots \mathbf{b}_k)$ is chosen with a probability for choosing bond i $(1 \leq i \leq k)$ being,

$$P_{closure}(\mathbf{b}_i) = \frac{e^{-\beta[v_{ext}(\mathbf{b}_i) + v_{bond}(\mathbf{b}_0^i)]}}{W(o \rightarrow n)} \quad , \tag{3.55}$$

where $\mathbf{b}_0^i$ is the bond vector from trial position i to monomer 0. The Rosenbluth weight $W(o \rightarrow n)$ for the move is given by

$$W(o \rightarrow n) = \sum_{j=1}^{k} e^{-\beta[v_{ext}(\mathbf{b}_j) + v_{bond}(\mathbf{b}_0^j)]} \quad . \tag{3.56}$$

Combining all the probabilities so far, the probability of generating new configuration (say, $\mathbf{b}_i$ was chosen) is

$$
\begin{aligned}
G(o \to n) \;=\; & \frac{1}{2}\left(\frac{1}{M_t}\right)\left(\frac{1}{N-2}\right) C_{norm}\; e^{-\beta v_{bond}(\mathbf{b}_i)} e^{-\beta\frac{\kappa_\theta}{2}(\theta_i-\theta_0)^2} \\
& \times\; \frac{e^{-\beta[v_{ext}(\mathbf{b}_i)+v_{bond}(\mathbf{b}_0^i)]}}{W(o \to n)} \quad .
\end{aligned} \tag{3.57}
$$

$G(n \to o)$ is calculated the same way as $G(o \to n)$ except that $k-1$ trial positions $(\mathbf{b}_1', \cdots \mathbf{b}_{k-1}')$ are generated and there is no decision making. Again, denoting the original bond vector from 2 to 1 by $\mathbf{b}_o$,

$$
\begin{aligned}
G(n \to o) \;=\; & \frac{1}{2}\left(\frac{1}{M_t}\right)\left(\frac{1}{N-2}\right) C_{norm}\; e^{-\beta v_{bond}(\mathbf{b}_o)} e^{-\beta\frac{\kappa_\theta}{2}(\theta_o-\theta_0)^2} \\
& \times\; \frac{e^{-\beta[v_{ext}(\mathbf{b}_o)+v_{bond}(\mathbf{b}_0^o)]}}{W(n \to o)} \quad ,
\end{aligned} \tag{3.58}
$$

in which

$$
W(n \to o) = e^{-\beta[v_{ext}(\mathbf{b}_o)+v_{bond}(\mathbf{b}_0^o)]} + \sum_{j=1}^{k-1} e^{-\beta[v_{ext}(\mathbf{b}_j')+v_{bond}(\mathbf{b}_0^{'j})]} \quad . \tag{3.59}
$$

Assuming canonical or semi grand canonical probability distributions,

$$
A(o \to n) = min\left\{1, \frac{W(o \to n)e^{\beta\frac{\kappa_\theta}{2}(\theta_i-\theta_0)^2}}{W(n \to o)e^{\beta\frac{\kappa_\theta}{2}(\theta_o-\theta_0)^2}}\right\}. \tag{3.60}
$$

A point worth mentioning about Eq. (3.60) is that the normalization constants C_{norm} for both forward $(o \to n)$ and reverse $(n \to o)$ moves were the same, therefore they cancel out in the acceptance probability. This is because C_{norm} depends on the positions of two monomers 0 and 2 by construction. When this bridging scheme is applied to trimer double rebridging in the next section, there is no such cancellation and normalization constants associated with each bridge will show up explicitly in the acceptance probability.

Trimer double rebridging

For this move, a chain is picked randomly and a non-end monomer is chosen at random. Next, all the chains of the same type as the chosen one are scanned to find a potential
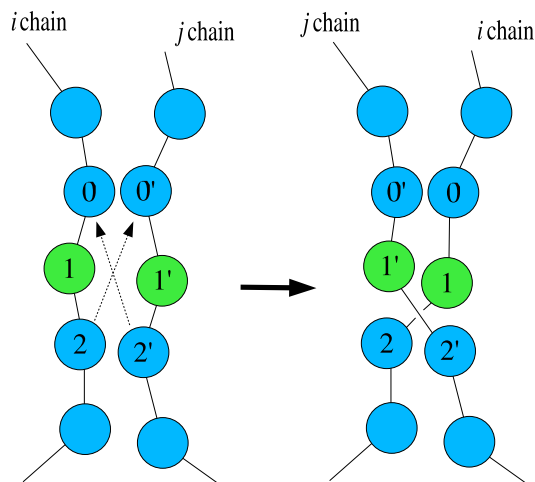
Figure 3.5: In a double rebridging move, a monomer from each is erased and regrown to be connected to the other chain, resulting in a dramatic change of chain configurations.

bridging partner based on a distance criterion. The rest of steps are similar to those of a single rebridging move, except that a bridge is now constructed from one chain to the other.

The implementation steps are,

1. Pick a chain at random and decide which end to call the head of the chain with equal probabilities.

2. Pick a non-end monomer from the chosen chain (labeled as 1 in Fig. 3.5).

3. Examine the chains of the same type for a potential bridging partner. For each chain examined, also pick a head monomer at random. To preserve chain architecture, monomers at the same position as the one in the chosen chain at step 1 are considered.

4. After scanning all the chains of the same type to identify a potential bridging site, pick one at random and construct two bridges: one from monomer 2 of i chain to

monomer 0 of j chain and the other from monomer 2 of j chain to monomer 0 of i chain.

5. Accept the proposed new configuration according to the Metropolis rule.

Calculation of the acceptance probability for this move needs some care because the normalization constants of the probability distributions of choosing a bond with bias are distinct for each bridge.

As for the single trimer move, the probability associated with the first two steps is $\frac{1}{M_t} \times \frac{1}{2} \times \frac{1}{N-2}$. During the next step, all monomers of the same type located at the same position as the picked one are examined and a chain is selected as a potential bridging pair with a weighting factor which will bias the choice in a way that increases the chance of success. Let us assume the label of the chosen chain is i. While scanning all the chains of the same type, a weighting factor W_j for a specific chain j and a normalization constant Z are recorded where

$$W_j(o \rightarrow n) \equiv P_{sep}(\mathbf{r}_{i2,j0})P_{sep}(\mathbf{r}_{j2,i0}) \quad , \tag{3.61}$$

$$Z(o \rightarrow n) \equiv \sum_{k \neq i} P_{sep}(\mathbf{r}_{i2,k0})P_{sep}(\mathbf{r}_{k2,i0}). \tag{3.62}$$

$P_{sep}(r)$ is a probability density that might reflect the equilibrium distribution of distance between two monomers bonded to a common monomer and $\mathbf{r}_{i2,j0}$ denotes the distance between monomer 2 of i chain and monomer 0 of j chain, for example. When scanning is completed, chain j is chosen with the probability

$$P_j(o \rightarrow n) = \frac{W_j(o \rightarrow n)}{Z(o \rightarrow n)} \tag{3.63}$$

Once a chain (labeled j) is chosen, a single bridge from monomer 2 of chain i to monomer 0 of chain j is constructed as described in the previous section, producing the associated Rosenbluth factor $W_A(o \rightarrow n)$. The other bridge from monomer 2 of chain j to monomer 0 of chain i will give another Rosenbluth factor $W_B(o \rightarrow n)$. To calculate the acceptance probability, let $\mathbf{b}_A$ and $\mathbf{b}_B$ be chosen trial bond vectors connecting monomer 2 and monomer 1 in each bridge. $\mathbf{b}_0^A$ and $\mathbf{b}_0^B$ are vectors from monomer 1 to
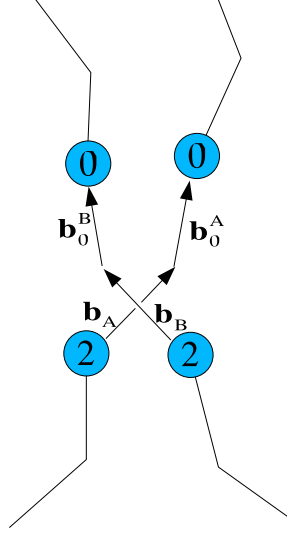
Figure 3.6: In a trimer double rebridging move, two single bridges are constructed: one from monomer 2 of i chain to monomer 0 of j chain (indicated by A), the other from monomer 2 of j chain to monomer 0 of i chain (indicated by B)

monomer 0 in each bridge. The probability of generating the new configuration is given by

$$
\begin{aligned}
G(o \rightarrow n) \;=\;& \left(\frac{1}{M_t}\right)\left(\frac{1}{2}\right)\left(\frac{1}{N-2}\right) P_j(o \rightarrow n) \\
\times\;& C_{bond} e^{-\beta v_{bond}(\mathbf{b}_A)} C_{\theta_A} e^{-\beta \frac{\kappa_{\theta_A}}{2}(\theta_A - \theta_{A0})^2} \frac{e^{-\beta[v_{ext}(\mathbf{b}_A)+v_{bond}(\mathbf{b}_0^A)]}}{W_A(o \rightarrow n)} \\
\times\;& C_{bond} e^{-\beta v_{bond}(\mathbf{b}_B)} C_{\theta_B} e^{-\beta \frac{\kappa_{\theta_B}}{2}(\theta_B - \theta_{B0})^2} \frac{e^{-\beta[v_{ext}(\mathbf{b}_B)+v_{bond}(\mathbf{b}_0^B)]}}{W_B(o \rightarrow n)} \quad .
\end{aligned}
\tag{3.64}
$$

The normalization constants C_{bond}, C_{θ_A}, and C_{θ_B} are

$$
C_{bond}^{-1} \;=\; \int e^{-\beta v_{bond}(b)} b^2 db
\tag{3.65}
$$

$$
C_{\theta_A}^{-1} \;=\; \int_0^\pi e^{-\beta \frac{\kappa_{\theta_A}}{2}(\theta - \theta_{A0})^2} \sin\theta d\theta
\tag{3.66}
$$

$$
C_{\theta_B}^{-1} \;=\; \int_0^\pi e^{-\beta \frac{\kappa_{\theta_B}}{2}(\theta - \theta_{B0})^2} \sin\theta d\theta \quad .
\tag{3.67}
$$

While C_{bond} is constant once the bond potential is given, $C_{\theta_A} \neq C_{\theta_B}$ in general because configurations of bridge ends (monomers 0 and 2) will be different. Substituting Eq. (3.64) and similar expression for the reverse move into the Metropolis function, the acceptance probability is found to be

$$A(o \to n) = min\left\{1, \frac{P_i(n \to o)\tilde{W}_A(o \to n)\tilde{W}_B(o \to n)}{P_j(o \to n)\tilde{W}_{A'}(n \to o)\tilde{W}_{B'}(n \to o)}\right\}, \qquad (3.68)$$

where A' and B' denote the original chain configurations of i chain and j chain, respectively. $\tilde{W}_A(o \to n)$ is defined as,

$$\tilde{W}_A(o \to n) \equiv \frac{W_A(o \to n)}{C_{\theta_A}\ e^{-\beta\frac{\kappa_{\theta_A}}{2}(\theta_A - \theta_{A0})^2}} \qquad (3.69)$$

and similar definitions of $\tilde{W}$'s are given for other bridges B, A', and B'.

Chapter 4

Perturbation theory and local correlations in polymer liquids

4.1 Introduction

In dense polymer liquids, the immediate neighborhood of a monomer along a chain is partly occupied by monomers from the same chain rather than monomers from other chains. This local correlation in the spatial arrangement of monomers was not taken into account properly in the original Flory-Huggins (FH) lattice theory of polymer mixtures [1,2]. That is, in the original theory of binary AB blends, it was assumed that a neighboring site of a monomer is occupied by a monomer of type i with a probability ϕ_i, where ϕ_i is the volume fraction of monomers of type i (=A,B). This assumption is called the random mixing approximation and it neglects the fact that a monomer in a polymer molecule is connected to other monomers from the same chain, therefore likely to be surrounded by them.

The random mixing approximation is known to overestimate the energy of mixing. In simulations of a simple cubic lattice diluted with a modest density of vacancies, Sariban and Binder [13, 14] found that the energy of mixing was roughly half that predicted by an analogous approximation for a lattice with vacancies. In more recent lattice Monte Carlo simulations of diblock copolymer melts on a diluted fcc lattice, Matsen and coworkers [15, 16] also considered a lattice mean-field (i.e., random mixing) approximation for the order-disorder transition of symmetric diblocks, and found that

it predicts a transition temperature more than twice that observed in their simulations, again indicating a large overestimation of the energy arising from AB pair interactions. These studies indicate that a proper description of the correlation effect is needed for a theory to describe correct thermodynamics of mixtures.

In this chapter, we develop a first order perturbation theory of a class of models of structurally symmetric blends. The goal is to obtain a perturbative expansion of free energy in powers of a small parameter α that is proportional to the difference between A-B and A-A (or B-B) interaction energy. We find that the free energy of mixing per monomer is given, to first order in α, by

$$\Delta f \simeq \frac{k_{\mathrm{B}}T}{N} \sum_{i}^{A,B} \phi_i \ln \phi_i + \alpha z(N)\phi_A \phi_B + \mathcal{O}(\alpha^2) \quad , \tag{4.1}$$

where N is the degree of polymerization of a polymer of type A or B and $k_{\mathrm{B}}T$ is thermal energy. For the case of a lattice model, $z(N)$ in the above equation is found to be proportional to the average number of *inter-molecular* neighbors, implying it takes proper account of the correlation in the arrangement of monomers.

Several authors have previously proposed approximations that are either equivalent or very closely related to the first order perturbation theory. Müller and Binder [52] proposed a "modified Flory-Huggins" approximation for the free energy of mixing Δf of a simple lattice model where the lattice coordination number was replaced by an average number of inter-molecular neighbors. In discussions of the results of continuum bead-spring simulations of symmetric blends, Grest *et al.* [53] discussed a one fluid approximation that is equivalent to the first order perturbation theory for a continuum model. Escobedo and de Pablo [54] considered closely related approximation that differs from the perturbation theory in the way that the first order coefficient of the free energy expansion is calculated. Both Müller and Binder and Escobedo and de Pablo showed that their proposed approximation can provide accurate predictions for the critical temperature in simulations of symmetric binary blends. This appears to be a natural consequence of the identification of their modified FH theories as a first order perturbation theory.

In Sec. 4.3 of this chapter, we analyze the chain length dependence of the short distance behavior of the inter-molecular radial distribution function (RDF), and of related quantities such as $z(N)$. Our analysis starts from the (verifiable) assumption that, in a

nearly incompressible liquid, the total RDF, including both intra- and inter-molecular contributions, changes extremely little with changes in chain length N. The intra-molecular correlation function must, however, change slightly with N, due to changes in the number of chemically distant monomers from the same chain in the neighborhood of any test monomer. This causes a systematic decrease in the depth of the inter-molecular correlation function with decreasing N, and thus an increase in $z(N)$, as chemically distant intra-molecular neighbors are simply replaced by inter-molecular neighbors in the immediate environment of any test monomer. The relevant concentration of chemically distant intra-molecular neighbors of any test monomer can be calculated using a simple random walk model. Combining the model with the stated assumption, we find that $z(N)$ can be expressed as

$$z(N) = z^\infty[1 + \beta \bar{N}^{-1/2}] \quad , \tag{4.2}$$

where z^∞ is a model dependent constant, $\bar{N} \equiv Nb^6/v^2$, b is the statistical segment length, v is the volume per monomer, and β is a universal constant given by

$$\beta = \left(\frac{6}{\pi}\right)^{3/2} = 2.64 \tag{4.3}$$

for any structurally symmetric model. Previously, Müller and Binder [52] found that the above functional form fits their $z(N)$ values in bond fluctuation model simulations very well but determined β empirically due to lack of a theoretical prediction.

Another question we address in this chapter is how to identify the FH interaction parameter χ such that a meaningful comparison between coarse grained theories and simulations can be made. Simulations of dense polymer liquids are providing increasingly precise tests of the assumptions underlying self consistent field theory (SCFT). Lattice Monte Carlo and continuum simulations of simple coarse-grained models have been used to quantify slight deviations from the random walk model for polymer statistics in melts and deviations from the RPA description of composition fluctuations in both polymer blends [13, 55, 52, 53] and block copolymer melts [56, 57, 58, 59, 15].

In order to compare either simulation or experimental data to SCFT predictions for multicomponent systems, however, one must somehow choose values for the SCF interaction free energy $\Delta f_{int}(\phi, T)$ and/or the FH interaction parameter χ relevant to the RPA analysis of long-wavelength scattering [7]. Because the relationship between

$\Delta f_{\text{int}}(\phi, T)$ and the underlying microscopic parameters is never known *a priori*, the temperature and (sometimes) composition dependence of Δf_{int} or χ have thus far been determined by fitting RPA predictions to the available measurements of composition fluctuations, in the analysis of either experiment or simulations. The uncertainty introduced by this fitting procedure becomes a potentially serious problem, however, when one's goal is to precisely quantify small deviations from RPA predictions, which is necessary in order to test theories that predict corrections to SCFT. For this purpose, it would be useful to have an independent way of unambiguously defining and accurately calculating Δf_{int} for a simulation model using the microscopic information that is available in a simulation. Here, we propose a way of doing this for symmetric models, which is based on an extrapolation of the perturbation theory to the limit of infinitely long polymers.

4.2 Perturbation theory

In this section, we will consider a general class of structurally symmetric binary polymer blends using a similar languages for lattice and continuum models. We consider a system containing a total of M_t structurally identical chains, each containing N monomers, in which $\phi_A M_t$ are of type A and $\phi_B M_t$ are of type B. Let α be a small parameter that controls the magnitude of the difference between AB and AA interactions. The state $\alpha = 0$ is thus a ideal mixture of M_t physically indistinguishable chains, in which a fraction ϕ_A can be chosen to be A chains at random.

We consider a class of lattice models in which double occupancy of lattice sites is forbidden and monomers on neighboring sites of types i and j interact via a pair potential $v_{ij}(\alpha)$ of the form

$$v_{ij}(\alpha) = u + \alpha b_{ij} \quad . \tag{4.4}$$

Here, u is the interaction between all neighboring monomers, α is a small parameter, and b_{ij} is a symmetric matrix of dimensionless coefficients, with $b_{AB} = b_{BA}$. To maintain the symmetry between the two species, we require that $b_{AA} = b_{BB}$. The value of the parameter u is relevant if and only if the system contains vacancies, because changes in u can then effect correlations in the one-component reference liquid.

We also consider a class of structurally symmetric continuum models. Consider a

system of M_t chains of length N in a volume V, giving an overall monomer concentration $c = M_t N/V$ or an average monomer volume $v = 1/c$. The total potential energy is the sum of intra-molecular bonding potentials, which are assumed to be the same for A and B chains, plus a sum of non-bonded pair potentials. The pair potential for monomers of type i and j separated by a distance r is assumed to be of the form

$$v_{ij}(r) = u(r) + \alpha b_{ij}(r) \quad , \tag{4.5}$$

with $b_{AA}(r) = b_{BB}(r)$, where α has units of energy.

Let $H(\alpha)$ be the total potential energy of either model. The configurational part of the partition function is given by

$$Z = \text{Tr } e^{-H(\alpha)/k_\text{B}T}, \tag{4.6}$$

where Tr denotes an integral over monomer positions for the continuum models or a sum over all distinguishable micro-states in a lattice model. We will formulate a perturbation theory for the free energy per monomer

$$f \equiv -\frac{k_\text{B}T}{M_t N} \ln Z. \tag{4.7}$$

We define a quantity θ to be

$$\theta(\phi, \alpha) \equiv \frac{\partial f}{\partial \alpha} = \frac{1}{M_t N} \left\langle \frac{\partial H(\alpha)}{\partial \alpha} \right\rangle \tag{4.8}$$

To first order in α, the free energy per monomer is thus given by

$$f(\phi, \alpha) \simeq f_0 + \frac{k_\text{B}T}{N} \sum_i \phi_i \ln \phi_i + \alpha \theta(\phi, 0) + \mathcal{O}(\alpha^2), \tag{4.9}$$

in which f_0 is the free energy per monomer of a corresponding one-component reference state, with $\alpha = 0$, when all of the chains are treated as indistinguishable in the calculation of entropy. The ideal free energy of mixing term accounts for the combinatorial entropy associated with the random labelling of chains as A or B. The quantity $\theta(\phi, \alpha = 0)$ is evaluated in the resulting ideal mixture.

In the simple case of a lattice model with $v_{AA} = u$ and $v_{AB} = u + \alpha$, θ is simply equal to the total number of AB neighbor pairs in the system, divided by the total number $M_t N$ of monomers.

In a continuum model with $b_{AA} = b_{BB} = 0$, θ is given by the sum of values of $b_{AB}(r)$ for all interacting AB monomer pairs, divided by $M_t N$.

The composition dependence of θ within the ideal mixture can be determined by simple combinatorical arguments. To show this, we consider lattice and continuum models separately.

4.2.1 θ for lattice models

Let $z_c(N)$ be the average number of sites neighboring each monomer that are occupied by monomers from a different chain, evaluated in the reference state $\alpha = 0$ (i.e., the average number of inter-molecular neighbors per monomer). Let $w_c(N)$ be the average number of neighboring sites that are occupied by monomers from the same chain (the average number of intra-molecular neighbors). Then, the average total number of occupied neighbors $y_c(N)$ is given by

$$y_c(N) = z_c(N) + w_c(N). \tag{4.10}$$

In the absence of vacancies, $y_c(N)$ must equal the lattice coordination number. For the case of lattice models, $\frac{\partial H}{\partial \alpha}$ can be written as

$$\frac{\partial H}{\partial \alpha} = \frac{1}{2} \sum_{s=1}^{M_t N} \sum_{<s'>} b_{t(s)t(s')}, \tag{4.11}$$

where $t(s)$ denotes the type of monomer occupying site s and $\sum_{<s'>}$ extends over the sites around s that are within the interaction range. θ can be expressed as

$$
\begin{aligned}
\theta(\phi, 0) &= \left\langle \frac{1}{M_t N} \frac{1}{2} \sum_{s=1}^{M_t N} \sum_{<s'>} b_{t(s)t(s')} \right\rangle \\
&= \frac{1}{2} \left\langle \sum_{<s'>} b_{t(s=1)t(s')} \right\rangle \\
&= \frac{1}{2} w_c(N) \sum_i^{A,B} \phi_i b_{ii} + \frac{1}{2} z_c(N) \sum_{i,j}^{A,B} \phi_i \phi_j b_{ij} \\
&= \frac{1}{2} y_c(N) \left(\phi_A b_{AA} + \phi_B b_{BB} \right) + z_c(N) \left(b_{AB} - \frac{b_{AA} + b_{BB}}{2} \right) \phi_A \phi_B
\end{aligned}
\tag{4.12}
$$

In Eq. (4.12), the average is calculated in the $\alpha = 0$ state. As can be seen from the functional form, the first term corresponds to the intra-molecular contribution and the

second term comes from the inter- molecular interaction. The last line can be obtained by using incompressibility condition $\phi_A + \phi_B = 1$. For symmetric blends, $b_{AA} = b_{BB}$ and

$$\theta(\phi, 0) = \frac{1}{2}y(N) + z(N)\phi_A\phi_B, \tag{4.13}$$

where we defined

$$y(N) \equiv y_c(N)b_{AA} \tag{4.14}$$

$$z(N) \equiv z_c(N)(b_{AB} - b_{AA}). \tag{4.15}$$

Now, Eq. (4.9) can be written as

$$
\begin{aligned}
f(\phi, \alpha) &\simeq f_0 + \frac{1}{2}\alpha y(N) + \frac{k_{\mathrm{B}}T}{N}\sum_i \phi_i \ln \phi_i + \alpha z(N)\phi_A\phi_B + \mathcal{O}(\alpha^2) \\
&= f_0 + \frac{1}{2}\alpha y(N) + \Delta f,
\end{aligned}
\tag{4.16}
$$

where we defined the free energy of mixing per monomer as

$$\Delta f \equiv \frac{k_{\mathrm{B}}T}{N}\sum_i \phi_i \ln \phi_i + \alpha z(N)\phi_A\phi_B + \mathcal{O}(\alpha^2) \tag{4.17}$$

To first order in α, Δf is identical to the modified Flory-Huggins theory of Müller and Binder. [52]

4.2.2 θ for continuum models

In a continuum model with a pair potential given by Eq. (4.5),

$$\frac{\partial H}{\partial \alpha} = \frac{1}{2}\sum_{i,j}^{A,B} \int d\mathbf{r} \int d\mathbf{r}' \, b_{ij}(\mathbf{r} - \mathbf{r}')c_i(\mathbf{r})c_j(\mathbf{r}') \quad, \tag{4.18}$$

in which $c_i(\mathbf{r})$ is a monomer density defined in Eq. (2.1). Therefore $\theta(\phi, 0)$ can be written as

$$
\begin{aligned}
\theta(\phi, 0) &= \frac{1}{M_t N}\frac{1}{2}\sum_{i,j}^{A,B} \int d\mathbf{r} \int d\mathbf{r}' \, b_{ij}(\mathbf{r} - \mathbf{r}')\langle c_i(\mathbf{r})c_j(\mathbf{r}')\rangle \\
&= \frac{v}{2}\sum_{i,j}^{A,B} \int d\mathbf{r}\langle c_i(\mathbf{r})c_j(0)\rangle b_{ij}(\mathbf{r})
\end{aligned}
\tag{4.19}
$$

where $v = c^{-1} = V/M_t N$ is the volume per monomer.

To discuss a perturbation theory for continuum models, it is useful to introduce some notation for inter and intra-molecular correlations in the one component reference liquid, with $\alpha = 0$. Let $g_{\text{inter}}(\mathbf{r}, s, N)$ denote the inter-molecular radial distribution function (RDF) for a test monomer with monomer index s in a reference liquid containing chains of length N, defined such that $g_{\text{inter}}(\mathbf{r}, s, N) \to 1$ as $\mathbf{r} \to \infty$. The product $c g_{\text{inter}}(\mathbf{r}, s, N)$ is thus the probability density (probability per volume) of finding any monomer from a different chain separated by a vector $\mathbf{r}$ from such a test monomer. Let $\omega(\mathbf{r}, s, N)$ be an intra-molecular correlation function in this reference liquid, defined as the probability density for finding any other monomer from the same chain separated by a vector $\mathbf{r}$ from a test monomer with monomer index s. Let $g_{\text{tot}}(\mathbf{r}, s, N)$ be the total RDF for a test monomer with a specific monomer index s, defined so that

$$c g_{\text{tot}}(\mathbf{r}, s, N) = \omega(\mathbf{r}, s, N) + c g_{\text{inter}}(\mathbf{r}, s, N) \quad , \tag{4.20}$$

and so that $g_{\text{tot}}(\mathbf{r}, s, N) \to 1$ as $\mathbf{r} \to \infty$. In addition, $\bar{g}_{\text{inter}}(\mathbf{r}, N)$, $\bar{g}_{\text{tot}}(\mathbf{r}, N)$, and $\bar{\omega}(\mathbf{r}, N)$ will be used to denote the averages of $g_{\text{inter}}(\mathbf{r}, s, N)$, $g_{\text{tot}}(\mathbf{r}, s, N)$, and $\omega(\mathbf{r}, s, N)$, respectively, with respect to s.

In an ideal mixture with $\alpha = 0$, random labelling of a fraction ϕ_A of the chains as A and the remainder as B yields

$$\langle c_i(\mathbf{r}) c_j(0) \rangle = \delta_{ij} c \bar{\omega}(\mathbf{r}, N) \phi_j + c^2 \bar{g}_{\text{inter}}(\mathbf{r}, N) \phi_i \phi_j \quad . \tag{4.21}$$

Eq. (4.21) is obtained by noting that $\langle c_i(\mathbf{r}) c_j(0) \rangle$ is the probability of finding a monomer of type i at a position $\mathbf{r}$, given there is a monomer of type j at $\mathbf{r} = 0$. A monomer at $\mathbf{r}$ can be only be inter-molecular neighbor if $i \neq j$. If $i = j$, it could be either intra or inter-molecular neighbors. Because c is the probability of finding a monomer at $\mathbf{r} = 0$ and $c \bar{g}_{\text{inter}}(\mathbf{r}, N)$ is the probability of finding an inter-molecular monomer in a melt or $\alpha = 0$ state given there is one at $\mathbf{r} = 0$, the contribution to $\langle c_i(\mathbf{r}) c_j(0) \rangle$ by inter-molecular pair is $c \phi_i \bar{g}_{\text{inter}}(\mathbf{r}, N) c \phi_j$ (the second term in Eq. (4.21)). By a similar reasoning, the contribution from intra-monomer for $i \neq j$ is $\bar{\omega}(\mathbf{r}, N) c \phi_j$, which is the first term of Eq. (4.21).

Substituting Eq. (4.21) into Eq. (4.19) and after a little algebra using the relations

$\phi_A + \phi_B = 1$ and $c\bar{g}_{\text{tot}}(\mathbf{r}, N) = \bar{\omega}(\mathbf{r}, N) + c\bar{g}_{\text{inter}}(\mathbf{r}, N)$, one gets

$$
\begin{aligned}
\theta(\phi, 0) \;=\; & \frac{c}{2} \int d\mathbf{r}\, \bar{g}_{\text{tot}}(\mathbf{r}, N)\big(b_{AA}(\mathbf{r})\phi_A + b_{BB}(\mathbf{r})\phi_B\big) \\
& + \; c \int d\mathbf{r}\, \bar{g}_{\text{inter}}(\mathbf{r}, N)\Big(b_{AB}(\mathbf{r}) - \frac{b_{AA}(\mathbf{r}) + b_{BB}(\mathbf{r})}{2}\Big)\phi_A\phi_B.
\end{aligned}
\tag{4.22}
$$

For the case of $b_{AA}(\mathbf{r}) = b_{BB}(\mathbf{r})$, it reduces to Eq. (4.13) where $y(N)$ and $z(N)$ are defined by

$$
\begin{aligned}
y(N) \;\equiv\; & c \int d\mathbf{r}\, \bar{g}_{\text{tot}}(\mathbf{r}, N) b_{AA}(\mathbf{r}) \\
z(N) \;\equiv\; & c \int d\mathbf{r}\, \bar{g}_{\text{inter}}(\mathbf{r}, N)(b_{AB}(\mathbf{r}) - b_{AA}(\mathbf{r})) \quad .
\end{aligned}
\tag{4.23}
$$

In what follows, we will also consider the analogous quantities

$$
\begin{aligned}
y(s, N) \;\equiv\; & c \int d\mathbf{r}\, g_{\text{tot}}(\mathbf{r}, s, N) b_{AA}(\mathbf{r}) \\
z(s, N) \;\equiv\; & c \int d\mathbf{r}\, g_{\text{inter}}(\mathbf{r}, s, N)(b_{AB}(\mathbf{r}) - b_{AA}(\mathbf{r})) \quad ,
\end{aligned}
\tag{4.24}
$$

for a test monomer with a specific monomer index s, with $1 \leq s \leq N$.

4.3 Dependence of local liquid structure on chain length

In this section, we consider how properties of a one-component melt that are sensitive to short range correlations depend upon overall chain length N. Our reasoning applies equally well to lattice and continuum models, but we will hereafter adopt a notation appropriate to a continuum model. To proceed, we first consider how the intra-molecular correlation function $\omega(\mathbf{r}, s, N)$ depends upon s and N, and then consider how this translates into a corresponding s- and N-dependence of $g_{\text{inter}}(\mathbf{r}, s, N)$.

4.3.1 Intra-molecular distribution

Each monomer in a melt with $\alpha = 0$ is surrounded by a concentration $\omega(\mathbf{r}, s, N)$ of other monomers from the same chain, in addition to a concentration $cg_{\text{inter}}(\mathbf{r}, s, N)$ of monomers from other chains. If $P(\mathbf{r}, s', s, N)$ denotes a probability density of finding a monomer with index s' separated by a vector $\mathbf{r}$ from a monomer s,

$$
\omega(\mathbf{r}, s, N) \equiv \sum_{s'} P(\mathbf{r}, s', s, N).
\tag{4.25}
$$
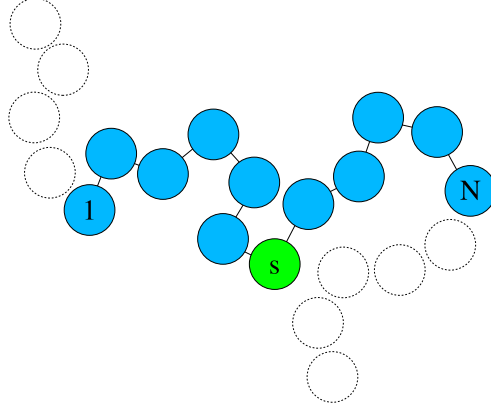
Figure 4.1: Schematic view for the difference $\delta\omega(\mathbf{r}, s, N)$ between the intra-molecular function $\omega^\infty(\mathbf{r})$ for an infinite chain and the corresponding correlation function $\omega(\mathbf{r}, s, N)$ for monomer s on a chain of length N. This difference is attributed to the contributions to $\omega^\infty(\mathbf{r})$ of the monomers $s \leq 0$ and $s > N$ that are "missing" from the finite chain. The concentration of these missing monomers near the test monomer (i.e., near $\mathbf{r} = 0$) can be estimated using a random walk model, if s is not too near either chain end. As the chain length is decreased from ∞, chemically distant monomers from the same chain are simply replaced by monomers from other chains, while leaving the total RDF $g_{\text{tot}}(\mathbf{r}, s, N)$ almost unchanged.

For small r, the concentration $\omega(\mathbf{r}, s, N)$ is dominated by monomers for which $|s' - s|$ is small. As a result, for monomers that are far from either chain end, $\omega(\mathbf{r}, s, N)$ depends only weakly on chain length N and index s.

In the limit $N \to \infty$, $P(\mathbf{r}, s, s', N)$ approaches a function

$$P^\infty(\mathbf{r}, s, s') \equiv \lim_{N\to\infty} P(\mathbf{r}, s, s', N) \tag{4.26}$$

that depends only on $|s - s'|$. For a monomer s which is not to close either chain end, $\omega(\mathbf{r}, s, N)$ also approaches a function

$$\omega^\infty(\mathbf{r}) \equiv \lim_{N\to\infty} \omega(\mathbf{r}, s = N/2, N) \tag{4.27}$$

that is independent of s. The limiting process in Eq. (4.27) is such that two ends of a chain grow simultaneously at the same temperature and density.

For chains with a finite length, the difference $\delta\omega(\mathbf{r}, s, N) = \omega^\infty(\mathbf{r}) - \omega(\mathbf{r}, s, N)$ can be estimated as follows. First we assume that for a sufficiently large N, a infinitely long chain and a chain of length N have very similar conformational statistics, i.e.

$$P(\mathbf{r}, s, s', N) \approx P^\infty(\mathbf{r}, s, s') \qquad (4.28)$$

for a sufficiently large N. This implies (Fig. 4.1)

$$
\begin{aligned}
\delta\omega(\mathbf{r}, s, N) &= \sum_{s'=-\infty}^{\infty} P^\infty(\mathbf{r}, s, s') - \sum_{s'=1}^{N} P(\mathbf{r}, s, s', N) \\
&\approx \sum_{s'=-\infty}^{0} P^\infty(\mathbf{r}, s, s') + \sum_{s'=N+1}^{\infty} P^\infty(\mathbf{r}, s, s'). \qquad (4.29)
\end{aligned}
$$

Because $\Delta s = |s' - s| \gg 1$ for the monomer s of interest to us, we may approximate $P^\infty(\mathbf{r}, s, s')$ by a Gaussian distribution for a continuous random walk

$$P_{\mathrm{id}}(\mathbf{r}, \Delta s) = \left(\frac{3}{2\pi\Delta s b^2} \right)^{3/2} \exp\left(-\frac{3r^2}{2\Delta s b^2} \right) \qquad . \qquad (4.30)$$

In the same limit, we may also approximate sums over s' by integrals to obtain an analytic approximation for $\delta\omega_{\mathrm{id}}(\mathbf{r}, s, N)$. Here and hereafter, a subscript id (for "ideal") is used to indicate approximations obtained using this idealized continuous random-walk chain model.

The effective coordination number $z(s, N)$ is sensitive only to the distribution of monomers that lie within the range of the pair potential from a test monomer. To characterize how the self-concentration $\omega(\mathbf{r}, s, N)$ within this small region depends upon s and N, we consider the s- and N-dependence of the distribution $\delta\omega_{\mathrm{id}}(\mathbf{r} = 0, s, N)$ for a random walk, evaluated at the position $\mathbf{r} = 0$ of the test monomer. The random-walk model yields a deviation

$$
\begin{aligned}
\delta\omega_{\mathrm{id}}(\mathbf{r} = 0, s, N) &= \sum_{s'=-\infty}^{0} P_{\mathrm{id}}(\mathbf{r} = 0, \Delta s) + \sum_{s'=N+1}^{\infty} P_{\mathrm{id}}(\mathbf{r} = 0, \Delta s) \\
&\approx \left(\frac{3}{2\pi b^2} \right)^{3/2} \left[\int_{s-1}^{\infty} \frac{dt}{(t+\frac{1}{2})^{3/2}} + \int_{N-s}^{\infty} \frac{dt}{(t+\frac{1}{2})^{3/2}} \right] \\
&= \left(\frac{3}{2\pi} \right)^{3/2} \frac{2}{b^3} \left[\frac{1}{\sqrt{s-\frac{1}{2}}} + \frac{1}{\sqrt{N-s+\frac{1}{2}}} \right]. \qquad (4.31)
\end{aligned}
$$

In approximating the discrete sums by integrals, we used

$$\sum_{s'=s}^{N} f(s') \approx \int_{s-1}^{N} ds' f(s' + \frac{1}{2}) \tag{4.32}$$

to minimize the error.

The random walk approximation clearly breaks down for s near the chain ends, as expected on physical grounds, since Eq. (4.31) predicts a $1/\sqrt{s}$ divergence at either chain end.

In the next section, $z(N)$ will be shown to depend upon on the average value

$$\delta\bar{\omega}(\mathbf{r}, N) \equiv \frac{1}{N} \sum_{s} \delta\omega(\mathbf{r}, s, N) \quad . \tag{4.33}$$

Using the above random walk model for $\delta\omega(\mathbf{r} = 0, s, N)$ yields

$$\delta\bar{\omega}_{\mathrm{id}}(\mathbf{r} = 0, N) = \frac{1}{v} \left(\frac{6}{\pi}\right)^{3/2} \frac{1}{\bar{N}^{1/2}} \tag{4.34}$$

in which $\bar{N} \equiv Nb^6/v^2$. The quantity $v\delta\bar{\omega}_{\mathrm{id}}(\mathbf{r} = 0, N) = (6/\pi)^{3/2}\bar{N}^{-1/2}$ is the corresponding volume fraction of the "missing" monomers in the vicinity of a randomly chosen test monomer.

Note that the integral with respect to s required to calculate $\bar{\omega}_{\mathrm{id}}(\mathbf{r} = 0, N)$ converges, despite the divergence of Eq. (4.31) for the integrand at both chain ends. This reflects the fact that the average with respect to s is dominated not by the contributions of a few monomers near the chain ends, but by those of many interior monomers. As a result, our use of a random walk model is sufficiently accurate to correctly calculate the prefactor of the dominant $\mathcal{O}(N^{-1/2})$ contribution to $\delta\omega(\mathbf{r} = 0, s, N)$. Further corrections that arise from the breakdown of the random walk model near both chain ends are expected to yield subdominant contributions of $\mathcal{O}(N^{-1})$.

4.3.2 Inter-molecular distribution

The value of $z(N)$ depends mostly on the behavior of the inter-molecular distribution $g_{\mathrm{inter}}(\mathbf{r}, s, N)$ for small r, which is less than the range of the pair potential (see Eq. (4.24)). Let us define the following limits of distribution functions:

$$\begin{aligned}
g_{\mathrm{tot}}^{\infty}(\mathbf{r}) &\equiv \lim_{N \to \infty} g_{\mathrm{tot}}(\mathbf{r}, s, N) \\
g_{\mathrm{inter}}^{\infty}(\mathbf{r}) &\equiv \lim_{N \to \infty} g_{\mathrm{inter}}(\mathbf{r}, s, N).
\end{aligned} \tag{4.35}$$

We make the following assumptions about how the small r behavior of distribution functions depends on chain length in a dense melt where the polymer coil size $\sqrt{N}b$ is much larger than the range of the pair potential:

1. In an almost incompressible liquid, $g_{\text{tot}}(\mathbf{r}, s, N)$ is almost independent of both s and N, except for monomers very close to one of the chain ends. This is what is meant when we say that the melt is effectively "incompressible". This implies that

$$g_{\text{tot}}(\mathbf{r}, s, N) \simeq g_{\text{tot}}^{\infty}(\mathbf{r}) \quad , \tag{4.36}$$

for all monomers except a few near the chain ends. For this to be true for all N, however, the decrease in the intra-molecular self-concentration $\omega(\mathbf{r}, s, N)$ with decreasing N must be exactly compensated by an increase in $cg_{\text{inter}}(\mathbf{r}, s, N)$. This implies

$$cg_{\text{inter}}(\mathbf{r}, s, N) \simeq cg_{\text{inter}}^{\infty}(\mathbf{r}) + \delta\omega(\mathbf{r}, s, N) \quad , \tag{4.37}$$

where $\delta\omega(\mathbf{r}, s, N) = \omega^{\infty}(\mathbf{r}) - \omega(\mathbf{r}, s, N)$.

Corrections to assumption (4.36) can arise, even for values of s that are far from either chain end, from contributions to $g_{\text{tot}}^{\infty}(\mathbf{r}, s, N)$ due to correlations between an interior test monomer and an end monomer. The resulting end-effect corrections (discussed in more detail in Sec. 4.3.3) are of order $1/N$.

2. The spatial distribution around a test monomer of chemically distant monomers from the same chain closely mimic the local distribution g_{inter} of monomers from other chains. We approximate it by the $g_{\text{inter}}^{\infty}(r)$ for a system of infinite chains. This implies that $\delta\omega(\mathbf{r}, s, N)$ of the chemically distant "missing" monomers is of the form

$$\delta\omega(\mathbf{r}, s, N) \propto g_{\text{inter}}^{\infty}(\mathbf{r}) \tag{4.38}$$

for large N, values of s far from either chain end, and values r less than the range of the potential.

3. The constant of proportionality in Eq. (4.38) depends on an overall concentration of "missing" monomers over a region larger than the range of the potential. We assume that an average concentration of missing monomers near a test monomer

can be obtained by using the random-walk model for the return probability $\delta\omega(\mathbf{r} = 0, s, N)$. More precisely,

$$\delta\omega(\mathbf{r}, s, N) \simeq \delta\omega_{\mathrm{id}}(0, s, N) g_{\mathrm{inter}}^{\infty}(\mathbf{r}) \tag{4.39}$$

under the same conditions that Eq. (4.38) applies.

Substituting Eq. (4.39) into Eq. (4.37), one obtains

$$g_{\mathrm{inter}}(\mathbf{r}, s, N) \simeq g_{\mathrm{inter}}^{\infty}(\mathbf{r}) \left[1 + v\delta\omega_{\mathrm{id}}(0, s, N) \right] \tag{4.40}$$

Using this approximation in Eq. (4.24) yields

$$z(s, N) \simeq z^{\infty} \left[1 + v\delta\omega_{\mathrm{id}}(0, s, N) \right] \quad , \tag{4.41}$$

where $\omega_{\mathrm{id}}(0, s, N)$ is given by Eq. (4.31) and we defined

$$z^{\infty} \equiv c \int d\mathbf{r}\, g_{\mathrm{inter}}^{\infty}(\mathbf{r})(b_{AB}(\mathbf{r}) - b_{AA}(\mathbf{r})) \quad . \tag{4.42}$$

Averaging with respect to s yields

$$
\begin{aligned}
z(N) &\simeq z^{\infty} \left[1 + v\delta\bar{\omega}_{\mathrm{id}}(0, N) \right] \\
&= z^{\infty} \left[1 + \left(\frac{6}{\pi} \right)^{3/2} \frac{1}{\bar{N}^{1/2}} \right] \quad ,
\end{aligned}
\tag{4.43}
$$

4.3.3 End effects

In addition to the dominant $\mathcal{O}(N^{-1/2})$ corrections to $z(N)$ predicted above, we also expect to find subdominant $\mathcal{O}(1/N)$ corrections to both $y(N)$ and $z(N)$ that arise from the perturbation of the liquid structure near chain ends.

Consider the contribution of end effects to the total correlation function $g_{\mathrm{tot}}(\mathbf{r}, s, N)$, and to the corresponding integral $y(s, N)$. Let $g_{\mathrm{tot}}(\mathbf{r}, s, s', N)$ be a distribution function for pairs of monomers with specified monomer indices s and s', defined so that $(c/N)g_{\mathrm{tot}}(\mathbf{r}, s, s', N)$ is the probability per unit volume of finding any monomer with index s' separated by $\mathbf{r}$ from a test monomer with index s, and so that

$$cg_{\mathrm{tot}}(\mathbf{r}, s, N) = \frac{c}{N} \sum_{s'} g_{\mathrm{tot}}(\mathbf{r}, s, s', N) \quad . \tag{4.44}$$

We assume that the deviation of $g_{\text{tot}}(\mathbf{r}, s, s', N)$ from $g_{\text{tot}}^{\infty}(\mathbf{r})$ (Eq.(4.35)) is dominated by pairs of (s, s') where one of them is near one end of the chains and the other is somewhere in the interior of the chain. Reflecting this assumption, we express $g_{\text{tot}}(\mathbf{r}, s, s', N)$ as

$$g_{\text{tot}}(\mathbf{r}, s, s', N) = g_{\text{tot}}^{\infty}(\mathbf{r}) + \delta g_{\text{end}}(\mathbf{r}, s) + \delta g_{\text{end}}(\mathbf{r}, s') \tag{4.45}$$

where $\delta g_{\text{end}}(\mathbf{r}, s)$ is a deviation that is large only for s near 1 or N, and vanishes for interior monomers. This functional form assumes that the correction $\delta g_{\text{end}}(\mathbf{r}, s)$ that arises from s near one of the chain ends is independent of s' when s' is an interior monomer, and similarly for the correction $\delta g_{\text{end}}(\mathbf{r}, s')$. This approximation captures the dominant $\mathcal{O}(N^{-1})$ corrections to $\bar{g}_{\text{tot}}(\mathbf{r}, N)$, but ignores smaller $\mathcal{O}(N^{-2})$ corrections arising from contributions in which both s and s' are near chain ends. Substituting Eq. (4.45) for $g_{\text{tot}}(\mathbf{r}, s, s', N)$ in Eq. (4.44) yields

$$g_{\text{tot}}(\mathbf{r}, s, N) = g_{\text{tot}}^{\infty}(\mathbf{r}) + \delta g_{\text{end}}(\mathbf{r}, s) + \frac{1}{N} d_{\text{end}}(\mathbf{r}) \tag{4.46}$$

where

$$d_{\text{end}}(\mathbf{r}) \equiv \sum_{s'} \delta g_{\text{end}}(\mathbf{r}, s') \quad . \tag{4.47}$$

The above approximation implies that for interior monomers, $g_{\text{tot}}(\mathbf{r}, s)$ deviates from $g_{\text{tot}}^{\infty}(\mathbf{r})$ by an amount that is proportional to $1/N$ but independent of s. As a result, $y(s, N)$ is expected to be of the form

$$y(s, N) \simeq y^{\infty} + \frac{\delta}{N} \quad , \tag{4.48}$$

for interior monomers for which $\delta g_{\text{end}}(\mathbf{r}, s) \approx 0$. We also defined

$$y^{\infty} \equiv c \int d\mathbf{r} g_{\text{tot}}^{\infty}(\mathbf{r}) b_{AA}(\mathbf{r}) \tag{4.49}$$

$$\delta \equiv c \int d\mathbf{r} d_{\text{end}}(\mathbf{r}) b_{AA}(\mathbf{r}) \tag{4.50}$$

The $1/N$ correction to $y(s, N)$ for interior monomers is the result of occasional close contact between an interior test monomers and end monomers. It is further assumed to be independent of the monomer index s of the interior test monomer. In addition, we expect to see a much larger deviation ($\mathcal{O}(1)$) from y^{∞} for the last few monomers at either chain end.

Similar reasoning suggests that the quantity $z(s, N)$ for s far from either chain end should also exhibit an $\mathcal{O}(1/N)$ contribution due to close contacts between the interior test monomer and end monomers of other chains, in addition to the $\mathcal{O}(N^{-1/2})$ correction described in Sec. 4.3.2. The same reasoning suggests that this $\mathcal{O}(1/N)$ correction for interior monomers should be independent of s, implying a functional form

$$z(s, N) \simeq z^\infty \left[\, 1 + v\delta\omega_{\mathrm{id}}(0, s, N) \,\right] + \frac{\gamma}{N} \tag{4.51}$$

in which z^∞ and γ are model-dependent parameters.

Finally, combining Eqs (4.43) and (4.48) yields

$$
\begin{aligned}
\left.\frac{\partial f}{\partial \alpha}\right|_{\alpha=0} &= \frac{1}{2}y(N) + z(N)\phi_A\phi_B \\
&\simeq \frac{1}{2}y^\infty + z^\infty \phi_A\phi_B \left[1 + v\delta\bar{\omega}_{\mathrm{id}}(0, N)\right] + \mathcal{O}(N^{-1}).
\end{aligned} \tag{4.52}
$$

4.4 Comparison to simulations

In this section, comparison of the theoretical predictions to both lattice and continuum simulations are presented. The lattice model data were obtained from the published results by Müller and Binder [52]. For continuum model, we conducted Monte Carlo simulations using the model and methods described in Chapter 3.

4.4.1 Lattice simulation

Fig. 4.2 shows a comparison of theoretical predictions to the lattice Monte Carlo results of Müller and Binder [52] for $z(N)$ for two different variants of the bond fluctuation model. In both variants of the model, a monomer occupies 8 sites within a cubic lattice, from which other monomers are excluded. The volume fraction of occupied sites is 50%. The top panel of Fig. 4.2 shows results for $z(N)$ for chains of length $N = 20, 40, 80$, and 160 for a model in which each monomer interacts with monomers that are located at any of 54 neighbors. The bottom panel shows results for a model where the number of interacting neighbors is 6, instead. We have compared both sets of data to a prediction

$$z(N) \simeq z^\infty \left[1 + \beta\bar{N}^{-1/2}\right] + \gamma'/N \quad, \tag{4.53}$$
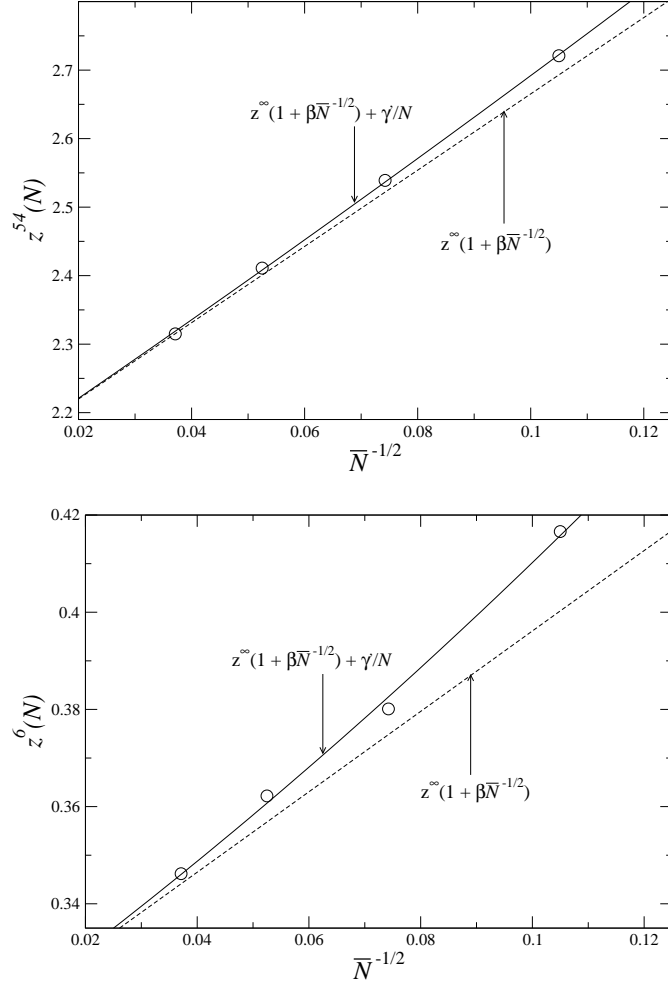
Figure 4.2: Lattice MC results of Müller and Binder [52] for $z(N)$ (symbols) vs. $\bar{N}^{-1/2}$ for two different variants of the bond fluctuation model. The top panel shows results for a model in which each site interacts with monomers located on any of 54 nearby sites, while the bottom shows results for a model in which each site can interact with only 6 neighboring sites. In each panel, the solid line is a best fit to Eq. (4.53), using the predicted value of $\beta = (6/\pi)^{3/2}$. This fit yields $z^{\infty} = 2.109$ and $\gamma' = 0.588$ for the model with 54 neighbors and $z^{\infty} = 0.3134$ and $\gamma' = 0.310$ for the model with 6 neighbors. Dashed lines show the estimated asymptote $z^{\infty}[1 + \beta \bar{N}^{-1/2}]$, with the same value for z^{∞}, in order to show the predicted asymptotic slope.

in which β is equal to $\left(\frac{6}{\pi}\right)^{3/2}$ but z and γ' are treated as adjustable parameters. The γ'/N term is included to account both for the $1/N$ contribution to Eq. (4.51) for interior monomers, and for contributions to the average over s arising from $\mathcal{O}(1)$ deviations from z^∞ for monomers near either chain end.

In the absence of a prediction for the coefficient β, Müller and Binder fit each of these data sets to a function $z(N) = z^\infty[1 + \beta_{fit}\bar{N}^{-1/2}]$, while treating both z^∞ and β_{fit} as adjustable parameters. This yields best fit parameters $\beta_{fit} = 2.846$ for z^{54} and $\beta_{fit} = 3.330$ for z^6 slightly higher than the predicted value of 2.64. The quality of the fit is approximately the same with either functional form.

Our predictions of a universal value for the asymptotic slope in these plots is consistent with this data. Inclusion of the $1/N$ end correction is necessary to adequately fit this data for modest values of N, however, particularly for the model with very short range interactions.

4.4.2 Continuum simulation

In this section, the results of the Monte Carlo simulation of the bead-spring model is presented. The simulation parameters of Eqs. (3.1) and (3.3) were $\epsilon = k_\mathrm{B}T$, $l = \sigma$, and $\kappa = 400\epsilon\sigma^{-2}$ The simulated chains are of length $N = 16$, 32, 64, 128, and 256 at a fixed monomer concentration of $c = 0.7\sigma^{-3}$. For these parameters, we obtain an asymptotic statistical segment length $b = 1.404\sigma$ (Fig. 4.3). The value was obtained by fitting R_g^2/N data to a renormalized one-loop theory predictions for the corrections for Gaussian chain scaling [23].

All simulations use a cubic $L \times L \times L$ simulation cell with periodic boundary conditions (Table 4.1). The methods used to facilitate the sampling of configuration space were hybrid Monte Carlo / molecular dynamics (MC/MD) [40], reptation [44], and double-rebridging [60] moves.

Fig. 4.4 shows the distribution functions $\bar{g}_\mathrm{tot}(\mathbf{r}, N)$ and $\bar{g}_\mathrm{inter}(\mathbf{r}, N)$ in the one-component liquid for the simulated systems. Results for $\bar{g}_\mathrm{tot}(\mathbf{r}, N)$ for chains of different length are indistinguishable at the scale of the main plot, but the correlation hole in $\bar{g}_\mathrm{inter}(\mathbf{r}, N)$ becomes visibly deeper with increasing N. The slight dependence of $\bar{g}_\mathrm{tot}(\mathbf{r}, N)$ on N is visible in the inset.
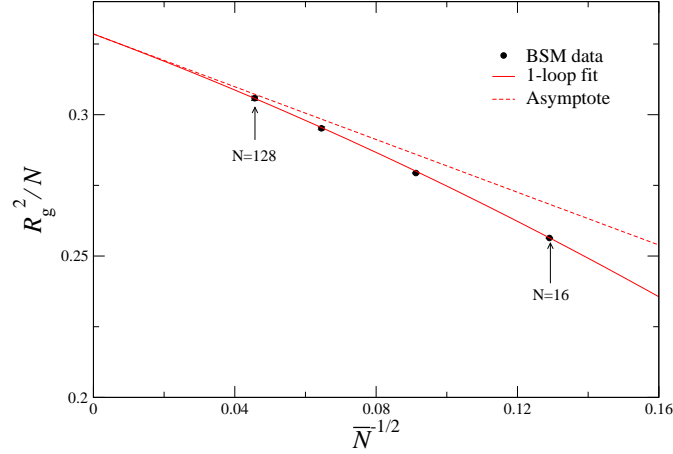
Figure 4.3: Data of $\frac{R_g^2}{N}$ vs. $\bar{N}^{-1/2}$. The renormalized one-loop theory predicts the corrections to Gaussian chain scaling as $\frac{R_g^2}{N} = \frac{b^2}{6}(1 - \frac{1.42}{\sqrt{\bar{N}}}) + \mathcal{O}(N^{-1})$. In fitting the data, b and the coefficient of the unknown term of order N^{-1} were treated as free parameters to yield $b \approx 1.404$. The asymptote is just $\frac{R_g^2}{N} = \frac{b^2}{6}(1 - \frac{1.42}{\sqrt{\bar{N}}})$
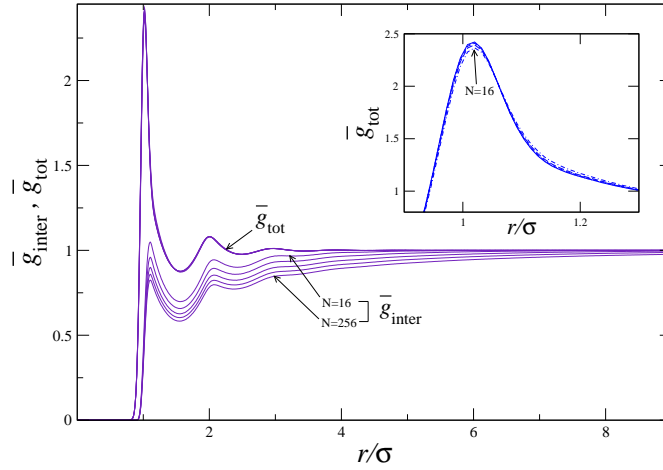
Figure 4.4: Intermolecular and total radial distribution functions $\bar{g}_{\text{inter}}(\mathbf{r}, N)$ and $\bar{g}_{\text{tot}}(\mathbf{r}, N)$ for the simulated systems. Results for $\bar{g}_{\text{tot}}(\mathbf{r}, N)$ for chains of different length are indistinguishable in the main plot. Inset: $\bar{g}_{\text{tot}}(\mathbf{r}, N)$ in an expanded scale, in which the slight dependence on N is visible.

Inter-molecular coordination number: $z(s, N)$ and $z(N)$

Our continuum model for blends was presented in Sec. 3.1.1. In terms of the language of Sec. 4.2.2, $b_{AA}(r) = b_{BB}(r) = 0$, $u(r) = \epsilon F(r)$, and $b_{AB}(r) = F(r)$. Also, the small parameter α can be identified with $\epsilon \xi$. Instead of calculating the integrals, $z(s, N)$ and $z(N)$ were measured on the fly by calculating corresponding discrete sums.

Fig. 4.5 shows our results for $z(N)$. To compare this data to theoretical predictions, we have fit values of $z(N)$ to Eq. (4.53). The fit for all chains agrees with the data to within our statistical errors.

Fig. 4.6 shows a corresponding comparison of theoretical predictions to simulation results for the quantity

$$z^{mid}(N) \equiv \frac{2}{N} \sum_{s=N/4+1}^{3N/4} z(s, N) \quad . \tag{4.54}$$

This is the average of $z(s, N)$ over the middle half of each chain. This quantity, unlike the average $z(N)$ over all monomers, excludes contributions from monomers very near the chain ends. By using Eq. (4.51) for $z(s, N)$, and approximating the sum over s in Eq. (4.54) by an integral over $N/4 < s < 3N/4$, we obtain a predicted N-dependence

$$z^{mid}(N) = z^\infty \left[1 + \beta^{mid} \bar{N}^{-1/2} \right] + \frac{\gamma}{N} \quad , \tag{4.55}$$

in which

$$\beta^{mid} \equiv (\sqrt{3} - 1) \left(\frac{6}{\pi} \right)^{3/2} \approx 1.932 \quad . \tag{4.56}$$

The approximation of a sum over s by an integral gives rise to errors of $\mathcal{O}(N^{-3/2})$, which lie beyond the $\mathcal{O}(1/N)$ accuracy of Eq. (4.51) for the summand $z(s, N)$. Because the

Table 4.1: Simulated models of melts

N	M_t	L	$\frac{R_g}{L}$
16	1176	29.955490	0.088
32	588	29.955490	0.108
64	294	29.955490	0.153
128	146	29.887407	0.217
256	144	37.483041	0.245

Figure 4.5: Simulation results for $z(N)$ (symbols) vs. $\bar{N}^{-1/2}$, compared to the prediction of Eq. (4.53), using the predicted value of $\beta = (6/\pi)^{3/2}$. A best fit to the data, shown by the solid line, yields parameters $z^\infty = 0.2957$ and $\gamma' = 0.3004$. The dashed line is the asymptotic line $z^\infty[1 + \beta\bar{N}^{-1/2}]$, with the same values for z^∞ and β. Error bars are shown, but are very small on this scale.
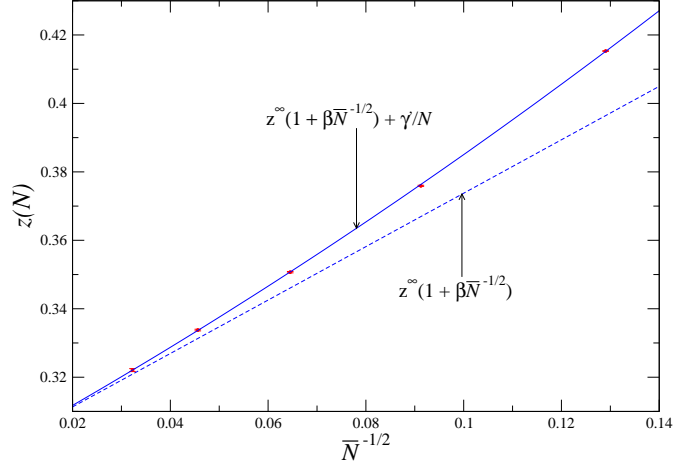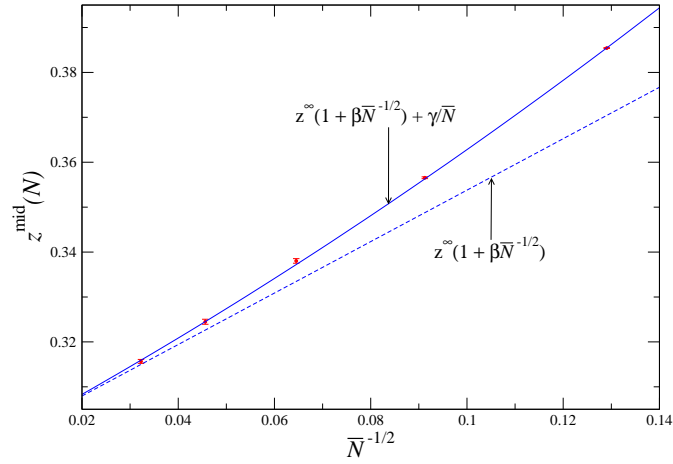

Figure 4.6: Simulation results for $z^{mid}(N)$ (symbols) vs. $\bar{N}^{-1/2}$, compared to the prediction of Eq. (4.55), using Eq. (4.56) for β^{mid}. A best fit, shown by the solid line, yields parameters $z^\infty = 0.2965$ and $\gamma = 0.2405$. The dashed line is the asymptote $z^\infty[1 + \beta\bar{N}^{-1/2}]$.

Figure 4.7: Simulation results for $z(s, N)$ (symbols) vs. s, for $s = 1, \ldots, N/2$ and chains of length $N = 16, \ldots, 256$, compared to the prediction of Eq. (4.51) shown by dashed lines. Values for the two parameters z^∞ and γ were taken from the fit of $z^{mid}(N)$ shown in Fig. 4.6.

sum over s that defines $z^{mid}(N)$ only includes interior monomers, for which we expect Eq. (4.51) for $z(s, N)$ to be valid, we may identify the constant γ in this fit with the constant γ in Eq. (4.51). The prediction fits the data for all $N = 16, \ldots, 256$ to within the statistical errors. A fit of the same data to $z^\infty[1 + \beta_{fit}^{mid} \bar{N}^{-1/2}]$, in which β_{fit}^{mid} is treated as an adjustable parameter, yields a slightly worse fit, and a value $\beta_{fit}^{mid} = 2.4698$ which is higher than the predicted value of β^{mid}.

Fig. 4.7 shows our simulation results for $z(s, N)$ for monomers $s = 1, \ldots, N/2$. Results for each chain length are compared to the predictions of Eq. (4.51), shown by dashed lines. Values for the two parameters z^∞ and γ have been taken from the fit of $z^{mid}(N)$ shown in Fig. 4.6. Agreement between this data for $z(s, N)$ and Eq. (4.51) is excellent for all N, and for all s except values near the chain ends, for which all analytic approximations are expected to fail.

Total coordination number: $y(s, N)$ and $y(N)$

We have also considered a quantity

$$y(s, N) = c \int d\mathbf{r} \; g_{\text{tot}}(\mathbf{r}, s, N) F(r) \tag{4.57}$$

that depends on the total RDF g_{tot}. For the blend model considered here, for which $b_{AA}(\mathbf{r})$, the quantity $y(N)$ that appears in the perturbation theory actually vanishes. We have nonetheless considered the quantity defined above as a way to test our assumptions about the chain length dependence of $g_{inter}(\mathbf{r}, s, N)$.

Fig. 4.8 shows our results for the average

$$y^{mid}(N) \equiv \frac{2}{N} \sum_{s=N/4+1}^{3N/4} y(s, N) \qquad (4.58)$$

of the total coordination number $y(s, N)$ over the middle half of each chain, and for $y(s, N)$ itself, respectively. Results for $y^{mid}(N)$ have been fit to a predicted form $y^{mid}(N) = y^\infty + \delta/N$, which follows immediately from Eq. (4.48) for $y(s, N)$ for interior monomers. Note that the fractional deviations of $y^{mid}(N)$ from y^∞ are much smaller than those found for $z^{mid}(N)$: For the shortest chains, with $N = 16$, $y^{mid}(N)$ deviates from y^∞ by about 1%, whereas $z^{mid}(N)$ deviates from z^∞ by roughly 30%.

In Fig. 4.9, we compare data for $y(s, N)$ for all s and N to the functional form predicted in Eq. (4.48) for interior monomers. Here, we have used the values of y^∞ and δ obtained from the fit shown in Fig. 4.8. This data clearly confirms that the small deviations $y(s, N)$ from y^∞ for interior monomers are independent of s and proportional to $1/N$, as expected if the dominant corrections to y^∞ arise from occasional contact of interior monomers with end monomers. The inset to Fig. 4.9 shows the much larger $\mathcal{O}(1)$ deviation of $y(s, N)$ from y^∞ for the last bead at each chain end.

4.5 SCFT and renormalized one-loop theory

There are good reasons to believe that a generalized form of SCFT becomes increasingly accurate with increasing chain length, and is exact in the limit of infinitely long chains. The strongest theoretical evidence for this hypothesis comes from investigation of corrections to SCFT within the context of the renormalized one-loop theory (ROLT) [22], as discussed below. The hypothesis that SCFT is asymptotically exact in the limit of infinitely long chains is also consistent with the striking success of the Flory-Huggins and (particularly) RPA theories in describing experimental data from mixtures of long finite polymers.
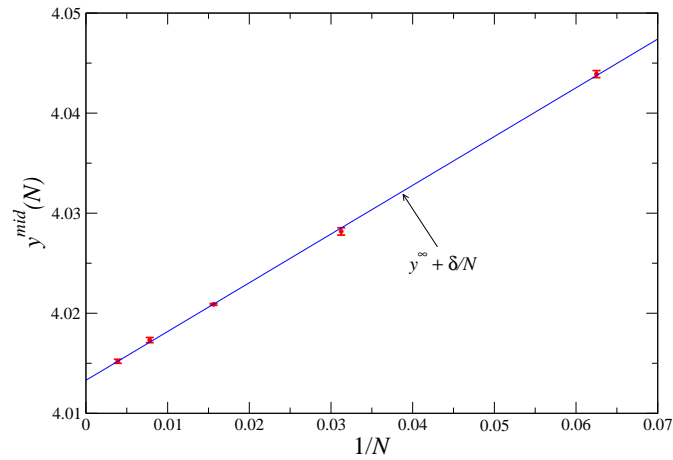
Figure 4.8: Simulation results for $y^{mid}(N)$ (symbols) vs. $1/N$. A best fit to $y^{mid}(N) = y^\infty + \delta/N$, shown by the solid line, yields parameters $y^\infty = 4.0133$ and $\delta = 0.4872$.
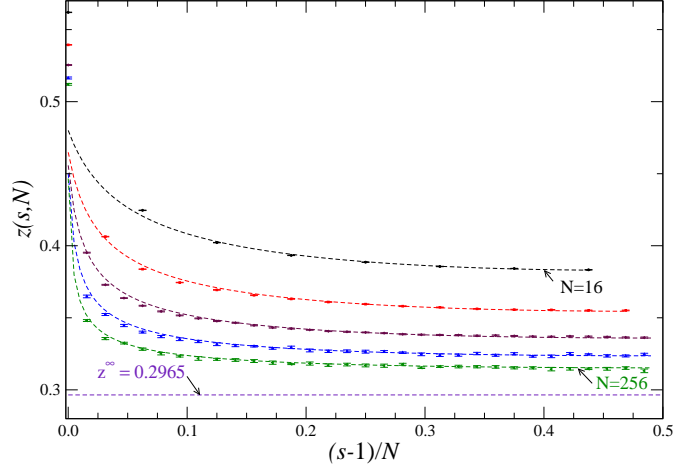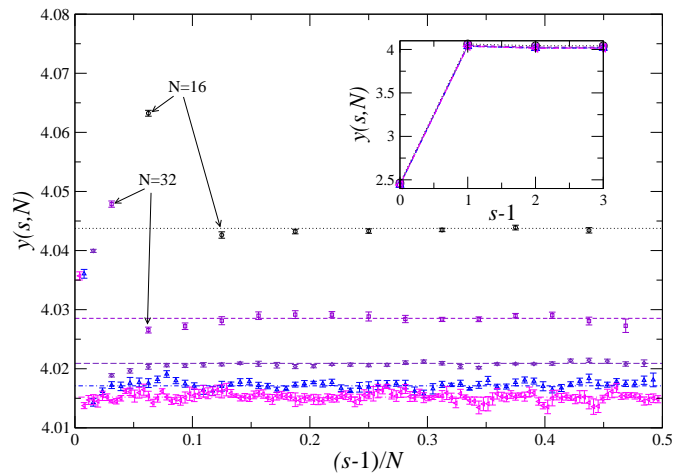

Figure 4.9: Simulation results for $y(s, N)$ (symbols) vs. s for $s = 1, \ldots, N/2$ and $N = 16, \ldots, 256$, compared to the prediction $y(s, N) = y^\infty + \delta/N$ (dashed lines). Values for the parameters y^∞ and δ were taken from the fit shown in Fig. 4.8.

The ROLT yields a prediction for the free energy per monomer of the form

$$f = k_{\mathrm{B}}T \sum_i \frac{\phi_i}{N_i} \ln \phi_i + f_{\mathrm{int}}(\phi, T) + f_{1\mathrm{L}}^* \quad , \tag{4.59}$$

in which $f_{1\mathrm{L}}^*$ is a one-loop correction to generalized Flory-Huggins theory (Note that $f_{1\mathrm{L}}^*$ was used to denote a contribution to the free energy per volume in Sec. 2.3). For symmetric models of the type considered here, the predicted correction $f_{1\mathrm{L}}^*$ is a function of the form

$$f_{1\mathrm{L}}^*(\phi, \chi_e N, N) = \frac{k_{\mathrm{B}}T}{N\bar{N}^{1/2}} \hat{f}_1^*(\phi, \chi_e N) \tag{4.60}$$

where $\hat{f}_1^*$ is a dimensionless function of ϕ and $\chi_e N$. Here, χ_e is an effective interaction parameter that is related to $\Delta f_{\mathrm{int}}(\phi, T)$ by

$$\chi_e \equiv -\frac{1}{2k_{\mathrm{B}}T} \frac{\partial^2 \Delta f_{\mathrm{int}}}{\partial \phi^2} \tag{4.61}$$

The SCF interaction free energy f_{int}, which is required as an input to the theory, can have an arbitrary composition dependence. To compare one-loop predictions to our perturbation theory of symmetric mixtures, we must also allow f_{int} to depend upon the parameter α of the underlying microscopic model.

4.5.1 SCFT

Because the one-loop contribution $f_{1\mathrm{L}}^*$ is smaller than the entropy of mixing by a factor of $N^{-1/2}$, the SCF contribution f_{int} may be identified by considering the limit $N \to \infty$ of the true free energy f. Therefore, an expansion of f_{int} to first order in α may be obtained by simply taking the limit $N \to \infty$ of the corresponding first order expansion of f, which is given in Eq.(4.16). This yields

$$f_{\mathrm{int}} = f_0 + \frac{1}{2}\alpha y^\infty + \alpha z^\infty \phi_A \phi_B \quad . \tag{4.62}$$

An expression for the corresponding contribution Δf_{int} to the free energy of mixing is given by

$$\Delta f_{\mathrm{int}} = \alpha z^\infty \phi_A \phi_B \quad . \tag{4.63}$$

This result yields an expansion of effective SCF interaction parameter χ_e, to first order in α, as

$$\chi_e = \frac{\alpha z^\infty}{k_{\mathrm{B}}T} \quad . \tag{4.64}$$

The fact that this expansion for χ_e is independent of composition is a special feature of the expansion of this class of symmetric models to first order in α: we do not expect it to survive any generalization to structurally asymmetric models or to higher order in α. Nothing rigorous can be said about the temperature dependence, even in this first order expansion, because the expansion with respect to α has been carried out at constant T, and z^∞ thus has an unknown dependence on T. The coefficient z^∞ would be independent of T only in an athermal reference system, such as a lattice model with no vacancies or a model of tangent hard spheres.

4.5.2 Renormalized one-loop theory

Both the ROLT for f and the simple perturbative expansion of f predict corrections to the SCF free energy, as defined above, that are of order $\bar{N}^{-1/2}$. The ROLT is not equivalent to first order perturbation theory because it predicts a correction $f^*_{1L}(\phi, \chi_e N, N)$ that is a nonlinear function of $\chi_e N$ and that exhibits singular behavior near the spinodal. We can test the consistency of the ROLT with the microscopic perturbation theory, however, by considering the predictions of the one-loop theory for the derivative $\theta = \partial f / \partial \alpha$ at $\alpha = 0$, and comparing expressions for the $\mathcal{O}(\bar{N}^{-1/2})$ contribution to this coefficient.

The one-loop expression for $\theta \equiv \partial f / \partial \alpha$ at $\alpha = 0$ can be expressed as a sum

$$\left.\frac{\partial f}{\partial \alpha}\right|_{\alpha=0} = \left.\frac{\partial f_{\text{int}}}{\partial \alpha}\right|_{\alpha=0} + \left.\frac{\partial f^*_{1L}}{\partial \alpha}\right|_{\alpha=0} \quad . \tag{4.65}$$

The SCF contribution is simply given by

$$\left.\frac{\partial f_{\text{int}}}{\partial \alpha}\right|_{\alpha=0} = \frac{1}{2}y^\infty + z^\infty \phi_A \phi_B \quad . \tag{4.66}$$

The one-loop correction is of the form

$$\left.\frac{\partial f^*_{1L}}{\partial \alpha}\right|_{\alpha=0} = \left.\frac{\partial \chi_e(\phi, \alpha)}{\partial \alpha}\right|_{\alpha=0} \left.\frac{\partial f^*_{1L}(\phi, \chi_e N, N)}{\partial \chi_e}\right|_{\chi_e=0} \quad . \tag{4.67}$$

It is straightforward to show, by using the functional form given in Eq. (4.60), that this correction is proportional to $\bar{N}^{-1/2}$.

In the work by Qin and Morse [23], the first derivative of the one-loop correction f^*_{1L} was calculated and given by

$$\left.\frac{\partial f^*_{1L}}{\partial \chi_e}\right|_{\chi_e=0} = k_{\text{B}}Tv\delta\bar{\omega}_{\text{id}}(\mathbf{r}=0, N)\phi_A \phi_B \quad . \tag{4.68}$$

Combining this with Eqs. (4.65-4.67) and Eq. (4.64) for χ_e yields

$$\left.\frac{\partial f}{\partial \alpha}\right|_{\alpha=0} = \frac{1}{2}y^{\infty} + z^{\infty}\phi_A\phi_B\left[1 + v\delta\bar{\omega}_{\mathrm{id}}(\mathbf{r}=0, N)\right] \quad . \tag{4.69}$$

This is identical to the expression obtained in Sec.4.3 (Eq. (4.52)).

We thus conclude that the ROLT implicitly contains a correct description of the N dependence of the correlation hole. This is enough to guarantee that the theory will yield a very accurate description of corrections to SCFT in weakly non-ideal symmetric blends, with $\chi_e N \ll 1$. This is confirmed by the work by Qin and Morse [23] where they compared published data of bond fluctuation model to the ROLT prediction. In Chapter 6 of this thesis, more extensive simulations of both a lattice and the continuum model are conducted to test the theory.

4.6 Conclusions

A simple physical picture has been given for how intra and inter-molecular correlation functions vary with chain length in a polymer melt. A theory based on this picture is in excellent agreement with computer simulation results. The structure of a one-component melt is related by perturbation theory to the free energy of mixing in corresponding structurally symmetric blends. The $\mathcal{O}(N^{-1/2})$ contribution to the depth of the intra-molecular correlation hole in the melt of finite chains leads to a slightly higher free energy of mixing in mixtures of shorter chains. This simply reflects the fact that monomers on shorter chains are less strongly screened from contact with other chains. Perturbation theory may be used to estimate the SCF interaction free energy appropriate for comparison of SCF theory to simulations, by identifying SCF theory with the $N \to \infty$ limit of the perturbation theory. If this prescription is used to identify SCF free energy, the predictions of the one-loop theory for corrections to SCF theory is found to be consistent with the perturbation theory presented here, insofar as both theories give identical results for a $\mathcal{O}(N^{-1/2})$ correction to the apparent interaction parameter in weakly non-ideal symmetric mixtures, with $\chi N \ll 1$.

Chapter 5

Second order perturbation theory of symmetric blends

5.1 Introduction

In this chapter, we construct a second order perturbation theory for the free energy of structurally symmetric polymer blends. This builds directly upon the analysis of first order perturbation theory given in Chapter 4. In both chapters, we consider a class of models for mixtures containing two types of structurally identical polymers, labelled 1 and 2, each containing N monomers, in which the Hamiltonian contains a small parameter α that controls the degree of thermodynamic incompatibility. In this chapter, we consider a class of models with a non-bonded pair interaction $v_{12}(r)$ between monomers of types 1 and 2 of the form

$$v_{12}(r, \alpha) = u(r) + \alpha b(r) \tag{5.1}$$

in which $u(r) = v_{11}(r) = v_{22}(r)$ is the interaction between chemically similar monomers. In the limit $\alpha = 0$, the liquid structure reduces to that of a dense one-component melt. The use of perturbation theory is motivated in part by the observation that the critical value of α beyond which a blend will phase separate is expected to decrease with increasing chain length as $1/N$, implying that this perturbation theory should provide a description of the one-phase region that becomes more accurate as N increases.

The free energy of mixing per monomer Δf in such a mixture can be expressed as

a sum

$$\Delta f = \frac{k_{\mathrm{B}}T}{N} \sum_i \phi_i \ln \phi_i + f_{\mathrm{ex}} \tag{5.2}$$

in which $f_{\mathrm{ex}} \to 0$ as $\alpha \to 0$. Expanding $f_{\mathrm{ex}}(\phi_1, \alpha, N)$ to second order in α yields a sum

$$f_{\mathrm{ex}}(\phi_1, \alpha, N) \simeq \left.\frac{\partial f_{\mathrm{ex}}}{\partial \alpha}\right|_{\alpha=0} \alpha \; + \; \frac{1}{2} \left.\frac{\partial^2 f_{\mathrm{ex}}}{\partial \alpha^2}\right|_{\alpha=0} \alpha^2 \tag{5.3}$$

in which the coefficients $\frac{\partial f_{\mathrm{ex}}}{\partial \alpha}$ and $\frac{\partial^2 f_{\mathrm{ex}}}{\partial \alpha^2}$ are functions of composition ϕ_1 and degree of polymerization N. The usefulness of this perturbation theory arises from the fact that these coefficients can be related to structural properties of the one-component state with $\alpha = 0$, which can be "measured" in simulations of this state.

In Chapter 4, we showed that the first order contribution has a composition dependence of the form

$$\left.\frac{\partial f_{\mathrm{ex}}}{\partial \alpha}\right|_{\alpha=0} = z(N)\phi_1\phi_2 \quad . \tag{5.4}$$

The coefficient $z(N)$ is an "effective coordination number" given by

$$z(N) = v^{-1} \int d\mathbf{r} \; \bar{g}_{\mathrm{inter}}(\mathbf{r}, N) b(\mathbf{r}) \tag{5.5}$$

where $\bar{g}_{\mathrm{inter}}(\mathbf{r}, N)$ is the intermolecular radial distribution function in a one-component ($\alpha = 0$) reference liquid of chains of length N, and v is the volume per monomer. The simple composition dependence given in Eq. (5.4) was obtained by a combinatorial argument that takes advantage of the fact that the relevant expectation value is evaluated in a state in which identical chains are assigned to species 1 and 2 at random.

The first goal of the present chapter is to derive an analogous expression for the second derivative $\partial^2 f_{\mathrm{ex}}/\partial \alpha^2$. This is accomplished in Sec. 5.2. There, we show that this quantity has a composition dependence of the form

$$\left.\frac{\partial^2 f_{\mathrm{ex}}}{\partial \alpha^2}\right|_{\alpha=0} = \frac{-1}{k_{\mathrm{B}}T}[\, g(N)\phi_1^2\phi_2^2 + h(N)\phi_1\phi_2 \,] \quad , \tag{5.6}$$

and we give expressions for the coefficients $h(N)$ and $g(N)$ in a form suitable for evaluation in a simulation of a one-component melt.

The second goal of this chapter is to clarify the relationship between the N-dependence of the coefficients $g(N)$ and $h(N)$ and the predictions of the renormalized loop expansion.

The renormalized loop expansion is a coarse-grained theory that predicts an expression for the excess free energy f_{ex} as an expansion in powers of $\bar{N}^{-1/2}$. Here,

$$\bar{N} \equiv Nb^6/v^2 \tag{5.7}$$

where b is the statistical segment length of a hypothetical infinite chain and v is the volume per monomer. The loop expansion of f_{ex} reduces in the limit $N \to \infty$ to a form consistent with self-consistent field (SCF) theory, which requires that f_{ex} depends only upon ϕ_1 and α. Let $f_{\text{int}}(\phi_1, \alpha)$ denote this long chain, SCF limit of f_{ex}.

The loop expansion cannot predict the SCF excess free energy $f_{\text{int}}(\phi_1, \alpha)$, but instead requires an expression for this function as an input. We assume here that f_{int} can be approximated for specific simulation models by an expansion in powers of α analogous to that given above for the true f_{ex}, of the form

$$f_{\text{int}}(\phi_1, \alpha) \simeq z^\infty \phi_1 \phi_2 \alpha - \frac{1}{2k_{\text{B}}T}[g_{\text{int}}\phi_1^2\phi_2^2 + h_{\text{int}}\phi_1\phi_2]\alpha^2 \quad , \tag{5.8}$$

where z^∞, g_{int}, and h_{int} are model-dependent SCF parameters. Starting from this representation of f_{int}, one can use the loop expansion to make testable predictions regarding the N dependence of the coefficients $z(N)$, $g(N)$, and $h(N)$, in which the corresponding SCF parameters appear as parameters. By comparing simulation results for $z(N)$, $g(N)$, and $h(N)$ to these predictions, we hope to both test these such predictions and (if they can be validated) determine values for the SCF parameters for specific models.

The relationship between the first order coefficients $z(N)$ and z^∞ was established in Chapter 4. We found there that the one-loop theory predicts an N-dependence

$$z(N) = z^\infty[1 + \beta_1\bar{N}^{-1/2}] + \mathcal{O}(N^{-1}) \quad , \tag{5.9}$$

with a universal coefficient $\beta_1 = (6/\pi)^{3/2}$. We also verified that simulation results for $z(N)$ for two different simulation models were consistent with this prediction.

These results of Chapter 4 yield a simple prescription for estimating f_{int} for any structurally symmetric model as an expansion to first order in α: one must measure $z(N)$ in simulations of melts with several chain lengths, and fit the results to Eq. (5.9) to obtain a value of z^∞. The resulting estimate of $f_{\text{ex}}(\phi, \alpha)$ can then be used as an input to the theory when comparing one-loop predictions to simulation results in systems with $\alpha \neq 0$. simulations of both blends and diblock copolymer melts. For simulations of

sufficiently long chains in the one-phase region, we expect this first order estimate of f_{int} to eventually become adequate, because the critical values of α falls as $1/N$. For chain lengths that we can easily simulate with a continuum bead-spring model, however, it appears that this approximation is not quite sufficient to describe data near the critical point of a blend or (particularly) the order-disorder transition of a diblock copolymer melt.

The present analysis was thus motivated primarily by our desire for an analogous prescription for calculating f_{int} and the corresponding Flory-Huggins interaction parameter to second order in α. We have been only partially successful in this regard: Unfortunately, we find that it is necessary to analytically calculate two-loop contribution to f_{ex}, which has not yet been attempted, in order to extract values for the second order SCF coefficients g_{int} and h_{int} from such an analysis.

5.2 Second derivative of free energy

We consider a liquid of M_t structurally identical chain molecules of length N, labelled $a = 1, \cdots, M_t$ in a box of fixed volume V. Among these are M_1 homopolymers of type 1 and M_2 of type 2, giving fractions $\phi_1 = \frac{M_1}{M_t}$ and $\phi_2 = \frac{M_2}{M_t}$, respectively.

The potential energy is a sum of intra-molecular bonding energies, which are the same for all chains, and a non-bonded pair interaction that contains a perturbation of the form defined in Eq. (5.1). Note that we have chosen to use a slightly less general form for the perturbation than that considered in Chapter 4, where we also allowed a perturbation proportional to α to be added to the $v_{11}(r)$ and $v_{22}(r)$ components. This restriction was made to simplify the analysis. The linear perturbation in the Hamiltonian used here may be written as a product $\delta H = \alpha \Theta$, where

$$\Theta = \sum_{a\epsilon 1} \sum_{b\epsilon 2} \sum_{s,s'} b(\mathbf{R}_a(s) - \mathbf{R}_b(s')) \quad . \tag{5.10}$$

Here and hereafter, $\sum_{a\epsilon i}$ denotes a sum over the molecule indices of molecules that have been assigned to type i, and $\mathbf{R}_a(s)$ is the position of monomer s of molecule a.

The first and second derivatives of free energy $F = -k_B T \ln Z$ with respect to α are

given by

$$\left.\frac{\partial F}{\partial \alpha}\right|_{\alpha=0} = \langle\Theta\rangle \tag{5.11}$$

$$\left.\frac{\partial^2 F}{\partial \alpha^2}\right|_{\alpha=0} = \frac{-1}{k_{\mathrm{B}}T}\left(\langle\Theta^2\rangle - \langle\Theta\rangle^2\right) \quad . \tag{5.12}$$

The required values of the average and variance of the extensive property Θ could, of course, be obtained from a simulation of a mixture with $\alpha = 0$ and a fixed composition, in which the chains are arbitrarily divided into two species, by a procedure similar to that used to measure, e.g., the average energy and heat capacity. The virtue of the more elaborate analysis given below is that it allows one to predict values for these quantities as functions of composition ϕ_1 by analyzing the results of a single simulation of a one-component melt.

5.2.1 Composition dependence

The reference state with $\alpha = 0$ is an ideal mixture, in which the identification of particular chains as members of species 1 or 2 is entirely random. In this state, the composition dependence of both $\langle\Theta\rangle$ and $\langle\Theta^2\rangle$ can be predicted by the combinatorial reasoning. We proceed here by first obtaining exact expressions for these quantities in a finite system, as functions of M_1 and M_2, and then evaluating the thermodynamic limit.

For this purpose, it is convenient to express Θ as a sum

$$\Theta = \sum_{a \epsilon 1} \sum_{b \epsilon 2} I_{ab} \quad , \tag{5.13}$$

where

$$I_{ab} \equiv \sum_{s} \sum_{s'} b(\mathbf{R}_a(s) - \mathbf{R}_b(s')) \tag{5.14}$$

is the contribution arising from interactions between molecules a and b, for $a \neq b$.

The average value $\langle\Theta\rangle$ in a mixture with $\alpha = 0$ is given by

$$\langle\Theta\rangle = \frac{M_1 M_2}{M_t(M_t - 1)}\langle I\rangle \quad , \tag{5.15}$$

where we have defined

$$I \equiv \sum_{a,b}' I_{ab} \quad . \tag{5.16}$$

Here and hereafter, a $\sum'_{a,b}$ denotes a double sum over all values of $a, b = 1, \ldots, M_t$ in a liquid of unlabelled chains, excluding terms with $a = b$. Our reasoning is as follows: the sum $\langle I \rangle = \sum'_{a,b} \langle I_{ab} \rangle$ contains $M_t(M_t - 1)$ statistically equivalent terms, each representing the interaction of a particular pair of molecules. Of these, only the $M_1 M_2$ terms in which a belongs to species 1 and b to species 2 contribute to $\langle \Theta \rangle$.

The quantity $\langle \Theta^2 \rangle$ can be expressed as a sum

$$\langle \Theta^2 \rangle = \sum_{a \epsilon 1} \sum_{b \epsilon 2} \sum_{c \epsilon 1} \sum_{d \epsilon 2} \langle I_{ab} I_{cd} \rangle \quad . \tag{5.17}$$

It is convenient to divide this into contributions

$$\langle \Theta^2 \rangle = \langle \Theta^2 \rangle_4 + \langle \Theta^2 \rangle_3 + \langle \Theta^2 \rangle_2 \tag{5.18}$$

in which $\langle \Theta^2 \rangle_n$ is the contribution to the sum in Eq. (5.17) in which the indices a, b, c, and d refer to n distinct molecules, with $n = 2, 3,$ or 4. The four molecule contribution $\langle \Theta^2 \rangle_4$ is thus the sum of terms in the sum in Eq. (5.17) in which $a \neq c$, and $b \neq d$, so that the molecules a, b, c and d are all distinct, with molecules a and c of type 1 and molecules b and d of type 2. The three chain contribution $\langle \Theta^2 \rangle_3$ is given by the set of terms with $a = c$ and $b \neq d$ or with $b = d$ and $a \neq c$. These all involve three distinct molecules, one of one type and two of the other. The two chain contribution $\langle \Theta^2 \rangle_2$ is given by the sum of terms in which $a = c$ and $b = d$, which involve only two molecules, one of each type.

To calculate the composition dependence of each of these contributions to $\langle \Theta^2 \rangle$ at $\alpha = 0$, it is useful to introduce the quantities

$$K_4 = \sum_{a,b,c,d}' \langle I_{ab} I_{cd} \rangle \tag{5.19}$$

$$K_3 = \sum_{a,b,d}' \langle I_{ab} I_{ad} \rangle \tag{5.20}$$

$$K_2 = \sum_{a,b}' \langle I_{ab}^2 \rangle \quad . \tag{5.21}$$

Here, we use a prime over a sum of several molecule indices, such as $\sum'_{a,b,c,d}$ to indicate a sum over all values $1, \ldots, M_t$ of all indicated indices, while keeping only terms in which

all of these index values (or molecules) are distinct. Straightforward combinatorial reasoning yields

$$\langle \Theta^2 \rangle_4 = \frac{M_1(M_1-1)M_2(M_2-1)}{M_t(M_t-1)(M_t-2)(M_t-3)}K_4 \tag{5.22}$$

$$\langle \Theta^2 \rangle_3 = \frac{M_1 M_2(M_2-1) + M_2 M_1(M_1-1)}{M_t(M_t-1)(M_t-2)}K_3 \tag{5.23}$$

$$\langle \Theta^2 \rangle_2 = \frac{M_1 M_2}{M_t(M_t-1)}K_2 \tag{5.24}$$

The above expression for $\langle \Theta^2 \rangle_4$ can be obtained by noting that K_4 is a sum over $M_t(M_t-1)(M_t-2)(M_t-3)$ statistically equivalent choices of values for a, b, c, and d, of which $M_1(M_1-1)M_2(M_2-1)$ contribute to the expression for $\langle \Theta^2 \rangle_4$, since we may make M_1 choices for a among molecules of type 1, M_1-1 choices for c, M_2 choices for b, and M_2-1 choices for d. Similarly, K_2 is a sum of $M_t(M_t-1)$ equivalent terms, of which $M_1 M_2$ contribute to $\langle \Theta^2 \rangle_2$. In the expression for $\langle \Theta^2 \rangle_3$, the first term in the numerator represents the contribution of terms in which a is of type 1 and b and c are type 2, while the second represents contributions in which a is of type 2. The above results can be rewritten as functions of ϕ_1 and ϕ_2, by writing M_i as $\phi_i M_t$. After a bit of algebra, we obtain:

$$\langle \Theta^2 \rangle_4 = \frac{M_t^4(M_t-4)!}{M_t!}\left[\phi_1^2\phi_2^2 - \frac{M_t-1}{M_t^2}\phi_1\phi_2\right]K_4 \tag{5.25}$$

$$\langle \Theta^2 \rangle_3 + \langle \Theta^2 \rangle_2 = \phi_1\phi_2\frac{M_t}{M_t-1}[K_3+K_2] \tag{5.26}$$

$$\langle \Theta \rangle = \phi_1\phi_2\frac{M_t}{M_t-1}\langle I \rangle \tag{5.27}$$

Combining all of these results, the variance in Θ can be written as a function of the form

$$\langle \Theta^2 \rangle - \langle \Theta \rangle^2 = G\phi_1^2\phi_2^2 + H\phi_1\phi_2 \quad , \tag{5.28}$$

in which

$$G = \frac{M_t^4(M_t-4)!}{M_t!}\left[K_4 - \frac{(M_t-2)(M_t-3)}{M_t(M_t-1)}\langle I \rangle^2\right] \tag{5.29}$$

$$H = \frac{M_t}{M_t-1}\left[K_3+K_2 - \frac{(M_t-1)}{(M_t-2)(M_t-3)}K_4\right] \quad . \tag{5.30}$$

These are exact relationships among quantities that are all defined for a system with a finite number of chains.

5.2.2 Thermodynamic limit

We are ultimately interested only in the thermodynamic limit, in which $M_t \to \infty$ while M_t/V is held fixed. To evaluate the behavior of the above expressions in this limit, we must first understand how the quantities K_2, K_3, K_4, $\langle I \rangle$ scale with M_t in this limit. Note that I_{ab} contains non-negligible contributions only from pairs of molecules a and b that are near enough to one another to interact via the short range perturbation $b(r)$. This guarantees that molecules a and b in the definitions of K_2 and $\langle I \rangle$, and molecules a, b and d in the definition of K_3, must all remain near one another as $M_t \to \infty$. This, in turn, guarantees that K_2, K_3, and $\langle I \rangle$ are all proportional to M_t, i.e., are all extensive. The quantity K_4, however, contains contribution from terms in which a remains near b and c remains near d, but the pairs ab and cd are arbitrarily far from one another. These distant pairs yield a dominant contribution $K_4 \sim \langle I \rangle^2$. In order for the variance of Θ to be extensive, as it must, the difference $K_4 - \langle I \rangle^2$ must be extensive. Our simulations confirm that this is the case.

By considering the limit $M_t \to \infty$, while assuming the M_t dependence for K_2, K_3, K_4 and $\langle I \rangle$ described above, we obtain limiting values

$$G \;=\; K_4 - \langle I \rangle^2 + \frac{4}{M_t} \langle I \rangle^2 \tag{5.31}$$

$$H \;=\; K_3 + K_2 - \frac{1}{M_t} \langle I \rangle^2 \quad . \tag{5.32}$$

The quantities G and H are both extensive. Note that the terms proportional to $\langle I \rangle^2/M_t$ are extensive because $\langle I \rangle \propto M_t$.

The excess free energy per monomer can thus be expanded to second order in α as a sum

$$f_{\text{ex}} \;\simeq\; z(N)\phi_1\phi_2\alpha - \frac{1}{2k_{\text{B}}T} \left[\, g(N)\phi_1^2\phi_2^2 + h(N)\phi_1\phi_2 \,\right] \alpha^2 \quad , \tag{5.33}$$

in which we have defined intensive quantities

$$g(N) \;=\; G(N)/(M_t N) \tag{5.34}$$

$$h(N) \;=\; H(N)/(M_t N) \quad . \tag{5.35}$$

The corresponding apparent interaction parameter

$$\chi_a \equiv -\frac{1}{2k_{\text{B}}T} \frac{\partial^2 f_{\text{ex}}}{\partial \phi_1^2} \quad , \tag{5.36}$$

which controls the magnitude of long wavelength composition fluctuations, is given by an expression

$$\chi_a(\phi_1, \alpha) \simeq \frac{z(N)\alpha}{k_{\mathrm{B}}T} - \frac{1}{2}[\, g(N)(6\phi_1\phi_2 - 1) + h(N)\,]\left(\frac{\alpha}{k_{\mathrm{B}}T}\right)^2 \qquad (5.37)$$

to the same order.

5.2.3 Alternative formulation

Eqs. (5.31) and (5.32) are not a convenient starting point for the design of an analysis algorithm, because straightforward algorithms to calculate the 3 and (particularly) 4 chain cluster contributions K_3 and K_4 can become awkward. We now put these expressions in a more computationally convenient form. Let

$$I_a \equiv \sum_{b \neq a} I_{ab} \quad , \qquad (5.38)$$

so that $I = \sum_a I_a$. The following identities relate the cluster functions K_2, K_3, and K_4 to the quantities $\sum'_{a,b}\langle I_{ab}^2\rangle$, $\sum_a\langle I_a^2\rangle$ and $\langle I^2\rangle$:

$$
\begin{aligned}
\sideset{}{'}\sum_{a,b}\langle I_{ab}^2\rangle &= K_2 \\
\sum_a\langle I_a^2\rangle &= \sum_a\sum_{b\neq a}\sum_{d\neq a}\langle I_{ab}I_{ad}\rangle \\
&= K_3 + K_2 \qquad (5.39) \\
\langle I^2\rangle &= \sum_a\sum_c\sum_{b\neq a}\sum_{d\neq c}\langle I_{ab}I_{cd}\rangle \\
&= K_4 + 4K_3 + 2K_2 \quad . \qquad (5.40)
\end{aligned}
$$

Solving for K_4 yields

$$K_4 = \langle I^2\rangle - 4\sum_a\langle I_a^2\rangle + 2\sideset{}{'}\sum_{a,b}\langle I_{ab}^2\rangle \quad . \qquad (5.41)$$

Using these identities, we obtain

$$
\begin{aligned}
G &= \langle I^2 \rangle - 4 \sum_a \langle I_a^2 \rangle + 2 \sum_{a,b}{}' \langle I_{ab}^2 \rangle - \langle I \rangle^2 \\
&\quad + 4 \langle I \rangle^2 / M_t \tag{5.42} \\
H &= \sum_a \langle I_a^2 \rangle - \langle I \rangle^2 / M_t \quad . \tag{5.43}
\end{aligned}
$$

This is the form we use to evaluate G and H in simulations.

The analysis algorithm that we use to calculate the quantities $\sum_{a,b}'\langle I_{ab}^2 \rangle$, $\sum_a \langle I_a^2 \rangle$, $\langle I \rangle$, and $\langle I^2 \rangle$ works as follows. For each microstate in a time sequence, loop over the molecule index a, over all monomers within a, and over all inter-molecular neighbors of these monomers. Within the code for processing one molecule, identify the molecule b to which each neighboring monomer belongs, and accumulate an instantaneous value of I_{ab} for each molecule $b \neq a$ that interacts with a via the perturbation $b(r)$. Also accumulate an instantaneous value for I_a. At the end of the code for one molecule a, increment variables that accumulate ensemble averages of $\sum_{a,b}' I_{ab}^2$ and $\sum_a I_a^2$, as well as accumulators for the ensemble average and instantaneous value of I. Increment the ensemble average of I^2 outside the loop over molecules.

5.3   Relationship to renormalized loop expansion

In this section, we derive expressions for the quantities $g(N)$ and $h(N)$ as functions of the parameters required as inputs to the renormalized loop expansion [26, 22]. The form of the renormalized loop expansion suggests that, for the class of symmetric models considered here, f_{ex} is given by a function of the form

$$
f_{\mathrm{ex}} = f_{\mathrm{int}}(\phi_1, \alpha) + \frac{1}{N} f_{\mathrm{end}}(\phi_1, \alpha) + \frac{k_{\mathrm{B}} T}{N} f^*(\phi_1, \chi_e N, \bar{N}) \tag{5.44}
$$

Here, f_{int} is a model-specific SCF free energy per monomer, and f_{end} is an additional excess free energy per chain due to end-group contributions. The effective interaction parameter χ_e is defined by a derivative

$$
\chi_e \equiv -\frac{1}{2k_{\mathrm{B}} T} \frac{\partial^2 f_{\mathrm{int}}}{\partial \phi_1^2} \quad . \tag{5.45}
$$

The quantity f^* is a universal correction to the free energy per chain that can in principle be predicted by the loop expansion, and that vanishes in the limit of very long chains. The loop expansion yields an expression for f^* as a sum

$$f^*(\phi_1, \chi_e N, \bar{N}) = \sum_{n=1}^{\infty} \frac{1}{\bar{N}^{n/2}} \hat{f}_n^*(\phi_1, \chi_e N) \tag{5.46}$$

in which n is an index for the number of loops. Thus far, only the one-loop contribution $\hat{f}_1^*$ has been calculated explicitly.

The first and second derivatives of f_{ex} with respect to α are

$$\frac{\partial f_{\text{ex}}}{\partial \alpha} = \frac{\partial f_{\text{int}}}{\partial \alpha} + \frac{1}{N} \frac{\partial f_{\text{end}}}{\partial \alpha} + \frac{\partial \chi_e}{\partial \alpha} k_{\text{B}} T \frac{\partial f^*}{\partial(\chi_e N)} \quad , \tag{5.47}$$

$$\frac{\partial^2 f_{\text{ex}}}{\partial \alpha^2} = \frac{\partial^2 f_{\text{int}}}{\partial \alpha^2} + \frac{1}{N} \frac{\partial^2 f_{\text{end}}}{\partial \alpha^2}$$
$$+ k_{\text{B}} T \frac{\partial^2 \chi_e}{\partial \alpha^2} \frac{\partial f^*}{\partial(\chi_e N)} + k_{\text{B}} T N \left(\frac{\partial \chi_e}{\partial \alpha}\right)^2 \frac{\partial^2 f^*}{\partial(\chi_e N)^2} \tag{5.48}$$

The first and second derivatives f_{int} are independent of N, as are the derivatives of f_{end}. The dominant N-dependence of the contributions arising from f^* can be determined by noting that the dominant contribution to f^*, the one-loop contribution, is order $\bar{N}^{-1/2}$. This implies that the last term in Eq. (5.47) for $\partial f_{\text{ex}}/\partial \alpha$ is of order $\bar{N}^{-1/2}$, as found in Chapter 4. It also implies that the dominant contribution to $\partial^2 f_{\text{ex}}/\partial \alpha^2$, which arises from the last term in Eq. (5.48), will diverge as

$$\frac{\partial^2 f_{\text{ex}}}{\partial \alpha^2} \sim \frac{N}{\bar{N}^{1/2}} \sim N^{1/2} \tag{5.49}$$

with increasing chain length.

In order for the composition dependence obtained from the loop expansion to match that obtained by our exact analysis of first and second order perturbation theory, we must assume that the expansion of each term in Eq. (5.44) yields a composition dependence of the same functional form. In particular, we must require that f_{int} has a Taylor expansion of the form shown in Eq. (5.8). This yields a SCF interaction parameter

$$\chi_e(\phi_1, \alpha) \simeq \frac{z^{\infty}\alpha}{k_{\text{B}}T} - \frac{1}{2}[g_{\text{int}}(6\phi_1\phi_2 - 1) + h_{\text{int}}]\left(\frac{\alpha}{k_{\text{B}}T}\right)^2 \tag{5.50}$$

with a composition dependence analogous to that found in Eq. (5.37) for χ_a.

For the same reason, we require that the end-group free energy f_{end} must have the analogous form

$$f_{\text{end}}(\phi_1, \alpha) \simeq z_{\text{end}}\phi_1\phi_2\alpha - \frac{1}{2k_{\text{B}}T}[g_{\text{end}}\phi_1^2\phi_2^2 + h_{\text{end}}\phi_1\phi_2]\alpha^2 \qquad (5.51)$$

in which z_{end}, g_{end}, and h_{end} are another set of model dependent parameters.

5.3.1 One-loop theory

The leading order contribution to f^* in powers of $\bar{N}^{-1/2}$ is given by the one loop contribution, which yields a contribution of order $1/N\bar{N}^{1/2}$ to f_{ex}. The contribution arising from f_{end} is of order $1/N^2$ for α less than a critical value of order $1/N$, and so is expected to be negligible by comparison. Here, we consider a one-loop approximation for the free energy per monomer in which we neglect f_{end}, giving

$$f_{\text{ex}} \simeq f_{\text{int}} + \frac{k_{\text{B}}T}{N}f^* \qquad (5.52)$$

and approximate f^* by the one-loop approximation $f^* \simeq \bar{N}^{-1/2}\hat{f}_1^*(\phi_1, \chi_e N)$

The one-loop contribution to the free energy per chain is given by an integral [23]

$$f^* \simeq \frac{vN}{2}\int^* \frac{d\mathbf{q}}{(2\pi)^3}\ln\left(\Omega_1 + \Omega_2 - 2\chi_e v\Omega_1\Omega_2\right) \qquad (5.53)$$

where the symbol $\int^*$ denotes the UV convergent part of a Fourier integral, and $v = \frac{V}{M_t N} = c^{-1}$ is a volume per monomer. Here, $\Omega_i = c\phi_i N f_D(q^2 N b^2/6)$ is the intramolecular correlation function and $f_D(x) = 2(e^{-x} - 1 + x)/x^2$ is the Debye function.

To calculate $g(N)$ and $h(N)$, we need the first and second derivatives of f^* with respect to $\chi_e N$. The first derivative yields

$$\frac{\partial f^*}{\partial(\chi_e N)} = -v^2\int^* \frac{d\mathbf{q}}{(2\pi)^3}\frac{\Omega_1\Omega_2}{(\Omega_1 + \Omega_2 - 2\chi_e v\Omega_1\Omega_2)} \qquad . \qquad (5.54)$$

Setting $\chi_e = 0$ and isolating the UV convergent part of this UV divergent integral yields the result found in Chapter 4:

$$\left.\frac{\partial f^*}{\partial(\chi_e N)}\right|_{\chi_e N=0} = \frac{\beta_1}{\bar{N}^{1/2}}\phi_1\phi_2 \qquad (5.55)$$

where $\beta_1 \equiv (6/\pi)^{3/2}$. Another derivative yields a UV convergent integral

$$\frac{\partial^2 f^*}{\partial(\chi_e N)^2} = \frac{-2v^3}{N}\int^* \frac{d\mathbf{q}}{(2\pi)^3}\frac{\Omega_1^2\Omega_2^2}{(\Omega_1 + \Omega_2 - 2\chi_e v\Omega_1\Omega_2)^2} \qquad (5.56)$$

and

$$\begin{aligned}
\left.\frac{\partial^2 f^*}{\partial(\chi_e N)^2}\right|_{\chi_e N=0} &= -2v\phi_1^2\phi_2^2 \int \frac{d\mathbf{q}}{(2\pi)^3} N f_D^2(q^2 N b^2/6) \\
&= -\frac{\phi_1^2\phi_2^2}{\bar{N}^{1/2}}\frac{6^{3/2}}{\pi^2}\int_0^\infty dx\, x^2 f_D^2(x^2) \\
&= -\beta_2 \phi_1^2\phi_2^2 \frac{1}{\bar{N}^{1/2}} \quad ,
\end{aligned} \tag{5.57}$$

where

$$\beta_2 = \frac{16}{15}\left(\frac{6}{\pi}\right)^{3/2}(7-4\sqrt{2}) \simeq 3.7814 \tag{5.58}$$

By substituting these results into Eq. (5.48), we obtain an expression of the form given in Eq. (5.6), with

$$g(N) \simeq (z^\infty)^2 \beta_2 \frac{N}{\bar{N}^{1/2}} + g_{\text{int}} \tag{5.59}$$

$$h(N) \simeq h_{\text{int}} \tag{5.60}$$

We thus obtain a dominant contribution to $g(N)$ that diverges as $g(N) \propto N^{1/2}$, but a dominant contribution to $h(N)$ that is independent of N. We show in what follows that while the above expression for the prefactor of the $N^{1/2}$ contribution is correct, the N-independent contributions to $g(N)$ and $h(N)$ given above are incomplete, because N-independent contributions can also arise from a two-loop contribution to the free energy.

5.3.2   Beyond one-loop

The one loop theory contains only the first term in an infinite expansion of f^* in powers of $\bar{N}^{-1/2}$. Using the full loop expansion produces expansions of $g(N)$ and $h(N)$ in powers of $\bar{N}^{-1/2}$, in which the dominant contribution to $g(N)$ is the $N^{1/2}$ divergence found in Eq. (5.59).

Because second and higher-order contributions to the loop expansion have not yet been calculated explicitly, we can only rely on very general arguments about their dependence on ϕ_1 and $\chi_e N$. To say anything about the composition dependence of $\partial f_{\text{ex}}/\partial\alpha$ and $\partial^2 f_{\text{ex}}/\partial\alpha^2$, we require expressions for the composition dependence of the first and second derivatives of the coefficients $\hat{f}^*_n(\phi_1, \chi_e N)$ with respect to $\chi_e N$. Both

our analysis of second order perturbation theory, and the explicit results obtained for the one-loop contribution, suggest that these derivatives be expressed as low order polynomials in $\phi_1 \phi_2$. We postulate that

$$\frac{\partial \hat{f}_n^*(\phi_1, \chi_e N)}{\partial(\chi_e N)}\bigg|_{\chi_e N = 0} = \hat{z}_n^* \phi_1 \phi_2 \tag{5.61}$$

$$\frac{\partial^2 \hat{f}_n^*(\phi_1, \chi_e N)}{\partial(\chi_e N)^2}\bigg|_{\chi_e N = 0} = -[\hat{g}_n^* \phi_1^2 \phi_2^2 + \hat{h}_n^* \phi_1 \phi_2] \quad . \tag{5.62}$$

For $n = 1$, we obtained $\hat{z}_1^* = \beta_1$, $\hat{g}_1^* = \beta_2$, and $\hat{h}_1^* = 0$. It is straightforward to confirm that substitution of these expressions into Eqs. (5.47) and (5.48), while using Eq. (5.50) for the derivatives of χ_e, yields expressions for $\partial f / \partial \alpha$ and $\partial^2 f / \partial \alpha^2$ with the required composition dependence. Furthermore, it can be shown that addition of terms of higher order in $\phi_1 \phi_2$ to either Eq. (5.61) or (5.62) would produce contributions to $\partial f_{\text{ex}} / \partial \alpha$ and $\partial^2 f_{\text{ex}} / \partial \alpha^2$ that are not consistent with the form required by the perturbation theory. Eqs. (5.61) and (5.62) thus seem to represent the most general possible composition dependence for these derivatives.

Using the above results to expand $z(N)$ to $\mathcal{O}(1/N)$ yields an expansion of the form that was used in Chapter 4 to fit simulation results for $z(N)$. We find

$$z(N) \simeq z^{\infty}\left[1 + \frac{\beta_1}{\sqrt{\bar{N}}}\right] + \frac{\gamma'}{N} + \mathcal{O}\left(\frac{1}{N^{3/2}}\right) \quad . \tag{5.63}$$

where

$$\gamma' = z_{\text{end}} + \frac{z^{\infty} \hat{z}_2^*}{c^2 b^6} \quad , \tag{5.64}$$

where $c^2 b^6 = \bar{N}/N$. The value of the constants z^{∞} and γ' can, of course, be determined by fitting simulation data to the above form. We find, however, that γ' contains both a model-specific end-group contribution and a universal two-loop contribution. A value for the end-group coefficient z_{end} could be obtained only if we had an analytic result for the $\hat{z}_2^*$ of the two-loop contribution, which we (thus far) do not.

Expanding the coefficients $g(N)$ and $h(N)$ to $\mathcal{O}(N^0)$

$$g(N) \approx (z^{\infty})^2 \beta_2 \frac{N}{\bar{N}^{1/2}} + A + \mathcal{O}\left(\frac{1}{\sqrt{N}}\right) \tag{5.65}$$

$$h(N) \approx B + \mathcal{O}\left(\frac{1}{\sqrt{N}}\right) \quad , \tag{5.66}$$

where

$$A \equiv g_{\text{int}} + \frac{(z^\infty)^2 \hat{g}_2^*}{c^2 b^6} \tag{5.67}$$

$$B \equiv h_{\text{int}} + \frac{(z^\infty)^2 \hat{h}_2^*}{c^2 b^6} \quad . \tag{5.68}$$

The constants A and B can be estimated by fitting simulation data to a power series in $\bar{N}^{1/2}$. An example of this procedure is given in the next section. Unambiguous estimates for the SCF parameters g_{int} and h_{int} could be obtained from this fitting procedure, however, only if we had analytic results for the coefficients $\hat{g}_2^*$ and $\hat{h}_2^*$ of the two-loop free energy.

5.4   Comparison to simulations

Hybrid Monte Carlo / Molecular Dynamics simulations of the bead-spring model (Section 3.1.1) at $\alpha = 0$ were performed to evaluate $g(N)$ and $h(N)$ for several chain lengths. These simulations allow us to test predictions of the loop expansion regarding the asymptotic dependence of these quantities on N for large N. In addition, simulations of blends with $\alpha > 0$ were conducted in semi-grand canonical ensemble to obtain data for the variance of the overall composition, in order to test the range of validity of a second order perturbation theory for the inverse structure factor $S^{-1}(\mathbf{q} \to 0)$.

All simulations used a $L \times L \times L$ cubic box with periodic boundary conditions. Simulations were conducted at $\alpha = 0$ for chains of lengths $N = 16, 32, 64, 128, 170$, and 256 (Table 5.1). Blend simulations, with $\alpha > 0$, were conducted only for chain lengths $N = 16, \ldots, 128$. As in the simulations reported in Chapter 4, the overall monomer number concentration was kept at $c = 0.7\sigma^{-3}$ and the parameters $\epsilon = k_{\text{B}}T$, $l = \sigma$, and $\kappa = 400 k_{\text{B}}T\sigma^{-2}$ were used. Thus, $z^\infty \approx 0.2965$ and $b \approx 1.404\sigma$, as previously determined. All simulation used hybrid MC/MD, reptation, single rebridging, and double rebridging MC moves as described in Chapter 3. Semi-grand canonical simulations of blends also used a move that can change the type of a randomly chosen chain.

5.4.1   Analysis of melt simulations ($\alpha = 0$)

In simulations of a one-component melt ($\alpha = 0$), we evaluate the properties $\langle I^2 \rangle$, $\sum_a \langle I_a^2 \rangle$, $\sum'_{a,b} \langle I_{ab}^2 \rangle$, and $\langle I \rangle$, from which we calculate $g(N)$ and $h(N)$.

In order to determine the box size needed to avoid significant finite size effects, we first obtained data for several box sizes for chains of length $N = 32$. Figs. 5.1 and 5.2 show the resulting values of g and h as functions of the ratio R_g/L, where R_g is the polymer radius of gyration. Much larger boxes are required to obtain accurate results for the second order coefficients $g(N)$ and $h(N)$ than those required to obtain accurate values of the first order coefficient $z(N)$. Based on the results of this study, and the assumption that the magnitude of deviation from the limit $L \to \infty$ is a function of the ratio R_g/L, for all chain lengths, we chose box dimensions $L \approx 10R_g$ for further study of all chain lengths of interest.

Figures 5.3 and 5.4 show our results for $g(N)$ and $h(N)$ for $N = 16, \ldots, 256$. Recall that the loop expansion predicts an asymptotic behavior in which $g(N) \sim C\sqrt{N}$, with a predicted prefactor C, and $h(N)$ approaches a constant in the limit $N \to \infty$. Our data appears to be consistent with both of these predictions, though the convergence towards the asymptotic behavior with increasing N appears to be quite slow.

The dotted line in Fig. 5.3 is an estimate of the asymptote for $g(N)$, of the form $C\sqrt{N} + A$, in which the slope C is given by the theoretical predicted value $C = (z^\infty)^2 \beta_2 (cb^3)^{-1} = 0.1716$. The apparent slope of the last few points appears to be close to the predicted value. A value of $A = -1.53$ for the constant in this asymptote was estimated somewhat crudely by fitting values of $g(N)$ for the three longest chains to an asymptotic form $C\sqrt{N} + A + D/\sqrt{N}$.

In Fig. 5.4, the values obtained for $h(N)$ vary from 0.49 to 0.52, consistent with the theoretical prediction of a constant value in the limit $N \to \infty$. The dotted line is a simple estimate of the asymptote that was obtained fitting values for the longest three

Table 5.1: Simulated models of melts and blends

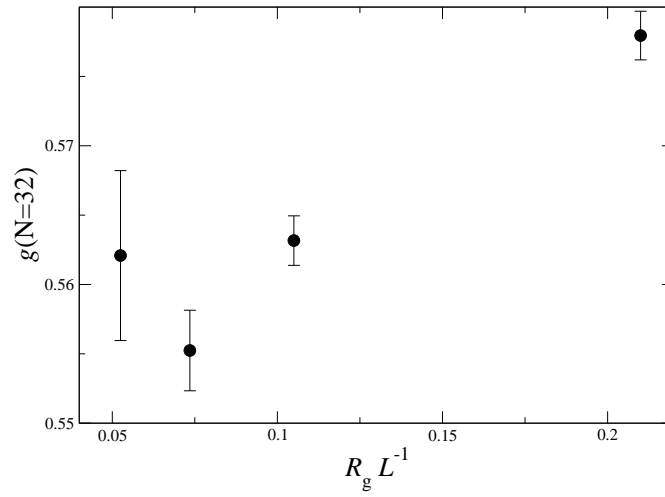| N	M_t	L	R_g/L
16	1176	29.955490	0.0883
32	588	29.955490	0.108
64	912	43.687674	0.105
128	1280	61.627417	0.105
170	1474	71.003996	0.105
256	1812	87.183314	0.105

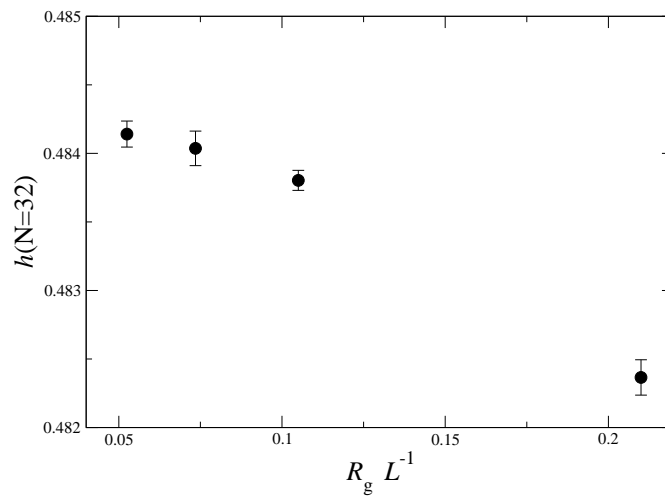Figure 5.1: Plot of $g(N = 32)$ vs. $\frac{R_g}{L}$.

Figure 5.2: Plot of $h(N = 32)$ vs. $\frac{R_g}{L}$.

chains to $B + E/\sqrt{N}$, which yields $B = 0.61$.

Though our data for $g(N)$ and $h(N)$ appears to be consistent with an approach towards the theoretically predicted asymptotic behavior, the data for our longest chains remains somewhat far from our estimates of the asymptotes. It appears that even longer chains would be needed to definitively test these predictions or (if they are confirmed) to obtain very accurate estimates of the constants A and B.

5.4.2 Composition fluctuations in critical blends ($\alpha > 0$)

The second order perturbation theory can also be used to calculate an inverse structure factor in the limit of long wave length using the identity

$$S^{-1}(0) \equiv \lim_{\mathbf{q} \to 0} S^{-1}(\mathbf{q}) = \frac{v}{k_{\mathrm{B}}T} \frac{\partial^2 \Delta f}{\partial \phi_1^2} \quad , \tag{5.69}$$

in which $v = c^{-1}$ is a volume per monomer. For a critical blend ($\phi_1 = 0.5$), Eq. (5.69) together with Eq. (5.2) yields

$$
\begin{aligned}
\frac{cNS^{-1}(0)}{2} &= 2 - \chi_a(\phi_1 = 0.5)N \\
&= 2 - N\frac{z(N)\alpha}{k_{\mathrm{B}}T} + \frac{N}{2}\left[\frac{1}{2}g(N) + h(N)\right]\left(\frac{\alpha}{k_{\mathrm{B}}T}\right)^2 \quad , \tag{5.70}
\end{aligned}
$$

where $\chi_a(\phi_1, \alpha)$ is given by Eq. (5.37). The coefficient of α^2, $\frac{1}{2}g(N) + h(N)$, as a function of N is plotted in Fig. 5.5.

The loop expansion prediction for the quantity can be obtained via Eqs. (5.65) and (5.66), giving

$$\frac{1}{2}g(N) + h(N) \approx \frac{(z^\infty)^2 \beta_2}{2cb^3}\sqrt{N} + \left(\frac{1}{2}A + B\right) + \mathcal{O}(\frac{1}{\sqrt{N}}) \quad . \tag{5.71}$$

As with $g(N)$ and $h(N)$, the simulation data seem to be consistent with the N scaling predicted by the loop expansion, approaching the asymptote $0.0858\sqrt{N} - 0.153$ as N increases. The convergence towards asymptote seems slow as is expected because $g(N)$ and $h(N)$ themselves showed slow convergence.

Semi-grand canonical simulations of critical blends with $\alpha \neq 0$ were performed in addition to measure

$$S(0) = \frac{N^2}{V}\langle \delta M_1^2 \rangle \quad , \tag{5.72}$$
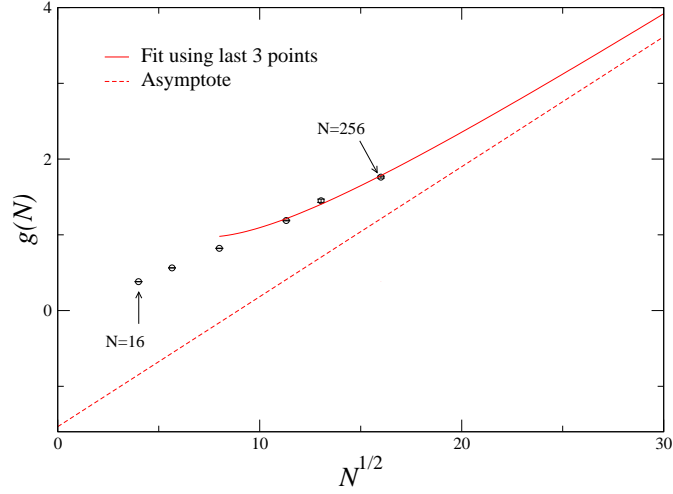
Figure 5.3: Plot of $g(N)$ vs. $\sqrt{N}$. The equation of the line of best fit is $0.1716\sqrt{N} - 1.5326 + 9.10968/\sqrt{N}$. For the coefficient of $\sqrt{N}$ term, the value predicted by loop expansion $(z^\infty)^2\beta_2(cb^3)^{-1}$ was used. The equation for the asymptotes is just $0.1716\sqrt{N} - 1.5326$

Figure 5.4: Plot of $h(N)$ vs. N. The equation of the line of best fit for the last three data points is $0.608287 - 1.36763/\sqrt{N}$.
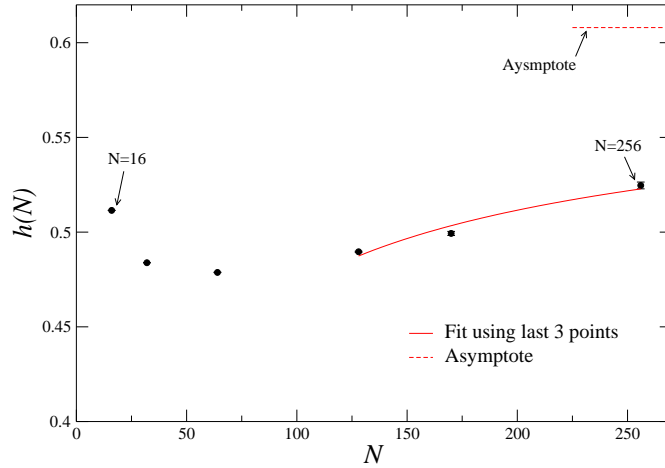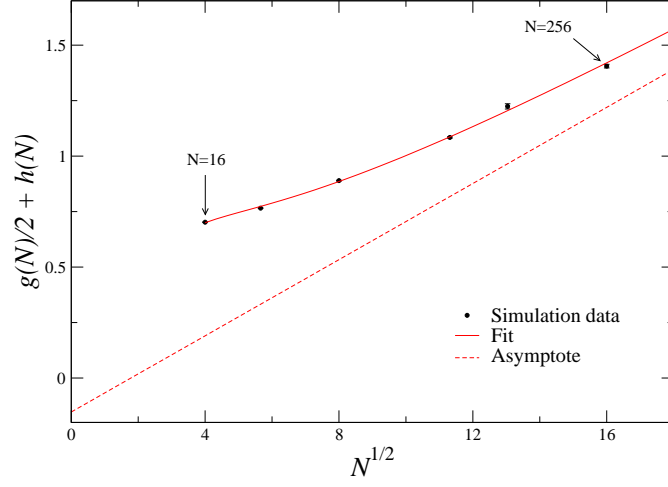
Figure 5.5: Plot of $\frac{1}{2}g(N) + h(N)$ vs. $\sqrt{N}$. The equation of the line of best fit is $0.0858\sqrt{N} - 0.153 + 3.59/\sqrt{N} + 6.22/N$. For the coefficient of $\sqrt{N}$ term, the value predicted by loop expansion $(z^\infty)^2 \beta_2 (2cb^3)^{-1}$ was used. The equation for the asymptote is just $0.0858\sqrt{N} - 0.153$.

where V is a volume of the system and $\delta M_1 \equiv M_1 - \langle M_1 \rangle$. The obtained data can be directly compared against the predictions of the perturbation theory as functions of α (Eq. (5.70)). The plots in Figure 5.6 show the accuracy of the second order perturbation theory predictions. For $N=64$ and $N=128$, the agreement is good up to about 50% of critical value of α (Appendix F). The agreement shown in the data for $N=32$ system should be taken as an accident based on the observed trend of the predictions by the perturbation theory, i.e. it deviates upward from the data for the shortest chain length and downward for the longest chain.

5.5 Conclusions

In this chapter, a second order perturbation theory of polymer blends was developed in an attempt to obtain the second order correction to the FH parameter χ_e. First, we obtained microscopic expressions for the first and second derivatives of free energy with respect to a small parameter α in canonical ensemble. This allowed us to obtain a perturbative expansion of free energy of mixing Δf up to second order in α.

Predictions for the N-dependence of the coefficients $g(N)$ and $h(N)$ of order α^2
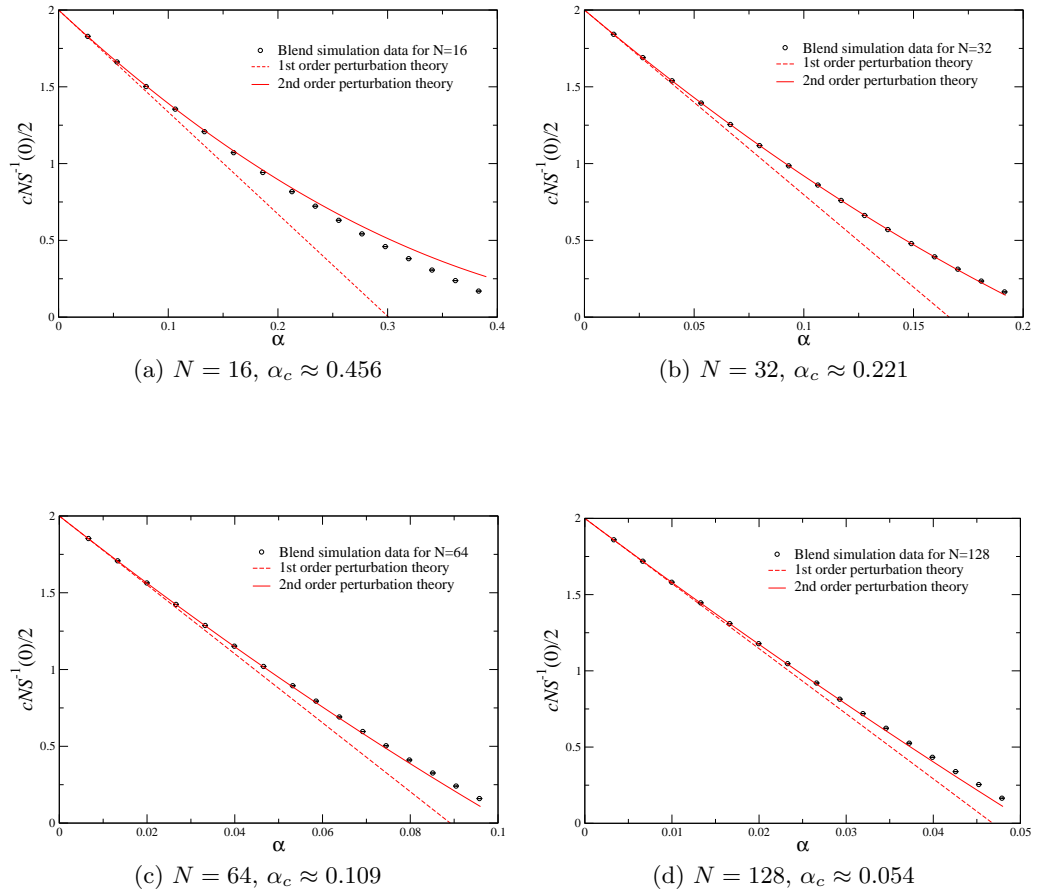
Figure 5.6: Comparison of blend simulation data with the predictions of the first and second order perturbation theories (Eq.(5.70)). Error bars for the data are shown but smaller than the size of a symbol.

were obtained by calculating these coefficients within the framework of the general loop expansion of free energy. This theory predicts that the coefficient $g(N)$ should diverge as $\sqrt{N}$ in the limit of long chains, with a known coefficient, but that $h(N)$ should approach a constant as $N \to \infty$. The data obtained from continuum Monte Carlo simulations were found to be consistent with this asymptotic behavior, although the longest chain length ($N = 256$) appeared to remain somewhat far from the estimated asymptote.

Our study of second order perturbation theory was originally motivated by the hope that, by examining the N dependence of the coefficients $g(N)$ and $h(N)$ in the expansion of the total free energy, we could extract values for the coefficients g_{int} and h_{int} in the corresponding expansion of the SCF interaction free energy. We found, however, that it was impossible by this method to distinguish between the desired terms in an expansion of the SCF free energy and contributions of a universal two-loop contribution to the free energy that has not yet been calculated. To obtain precise results for the SCF parameters g_{int} and h_{int}, it appears that we will need to first complete a theoretical analysis of the two-loop free energy, and perhaps also obtain data for longer chains.

We also examined the range of values of α over which a perturbation theory remains accurate, by comparing simulation data for $S^{-1}(0)$ at $\alpha > 0$ to predictions obtained from a second order perturbation theory in which the coefficients were measured in simulations at $\alpha = 0$. The expansion to second order in α was found to fit the data rather well most of the way to the critical point.

Chapter 6

Simulation of composition fluctuations in polymer blends

6.1 Introduction

The self consistent field theory (SCFT) for inhomogeneous polymer liquids, or the Flory-Huggins (FH) theory which is the homogeneous limit of SCFT, is the standard theoretical framework for understanding the thermodynamics of polymeric liquids [11, 12]. It has been believed that these type of phenomenological theories become exact in the limit of very long polymers [61, 62, 22]. The random phase approximation (RPA) for composition fluctuations obtained by using SCFT to calculate the susceptibility of a polymeric liquid is also supposed to become increasingly accurate in the limit $N \to \infty$ where N denotes a degree of polymerization.

This belief is based mainly on two kinds of evidence, the first of which is the success of FH theory and RPA theories in describing experimental data [8,63,64,65]. The other basis of the belief comes from coarse grained theories of fluctuations that attempt to correct SCFT [21,18,19,22] . In those theories, the fluctuation correction to SCFT free energy is found to be of order $1/\sqrt{N}$ smaller than entropy of mixing, implying that SCFT becomes exact in the hypothetical limit of infinitely long chain systems.

A natural question is then how one can identify deviations from the RPA for systems of chains of finite lengths and how well the theories of fluctuations describe the deviations, which are supposed to be rather small. This is different from previously

raised questions regarding the validity of the assumption of the RPA, i.e. the radius of gyration remains unperturbed and one can use the unperturbed single chain structure factor in the RPA [14, 66]. To quantify small deviations, however, one needs an accurate estimate of the FH interaction parameter χ. Unfortunately, fitting experimental or simulation data to the RPA expression to estimate χ makes this quantification difficult. That is because in the procedure, the RPA is used to fit the outcome of experiments, as opposed to predicting them and comparing with actual measurements. In Chapter 4, we proposed a way of estimating FH interaction parameter χ for a class of models of symmetric polymer blends. The idea was to apply a thermodynamic perturbation theory to the models and extrapolate the resulting free energy to the limit $N \to \infty$. The resulting free energy is then used to obtain the FH interaction parameter χ. The perturbation theory was also shown to justify the reason why some modified FH theories [52, 53, 54], where the original lattice coordination number is replaced by an effective coordination number, are more accurate than the original FH theory.

In this chapter, the results of extensive Monte Carlo (MC) simulations will be presented to test the predictions of a renormalized one-loop theory of blends [22, 23]. In addition, two related problems will be investigated in some detail, the first of which is the issue of how to find a correction to the estimation of the FH χ parameter proposed in Chapter 4. There, we obtained an estimation of χ to first order in α which controlled the incompatibility of two monomer species in blends. This problem was the main focus of Chapter 5 and there, we found it was not possible without an analytic result of a two-loop contribution to free energy. The approach to obtain a correction to second order in α here is to utilize composition fluctuations data of model blends and try to fit the data to the predictions of a general loop expansion [26, 22], of which the one-loop contribution is the first term. The other problem concerns the universality of coarse grained models of polymer [27, 28] and a numerical test of the feasibility of the premise will be attempted.

6.2   Background

We consider a system of volume V that contains M_1 homopolymer chains of type 1 and M_2 chains of type 2 at temperature T. In the simulations presented here, the two

types of polymer are structurally identical, and contain the same number of monomers per chain, $N = N_1 = N_2$. Let $v = \frac{V}{N M_t}$ be the average volume per monomer, and $\phi_i = M_i/M_t$ be the fraction of monomers (or chains) of type i, where $M_t = M_1 + M_2$ is the total number of chains.

Correlations in polymer mixtures can be characterized by the structure factor

$$S_{ij}(\mathbf{q}) \equiv \int d\mathbf{r} \, \langle \delta c_i(\mathbf{r}) \delta c_j(0) \rangle e^{i\mathbf{q} \cdot \mathbf{r}} \quad , \tag{6.1}$$

where $\delta c_i(\mathbf{r}) \equiv c_i(\mathbf{r}) - \langle c_i(\mathbf{r}) \rangle$ is a deviation in the concentration of monomers of type i from its ensemble average at point $\mathbf{r}$. In the idealized limit of effectively incompressible mixture, the matrix $S_{ij}(\mathbf{q})$ may be characterized by a scalar function $S(\mathbf{q}) = S_{11}(\mathbf{q}) = S_{22}(\mathbf{q}) = -S_{12}(\mathbf{q})$ In the same limit, the low-wavenumber limit of the scalar $S(\mathbf{q})$, $S(0) \equiv \lim_{\mathbf{q} \to 0} S(\mathbf{q})$, is related to the free energy of mixing per monomer Δf by the identity

$$S^{-1}(0) = \frac{v}{k_{\mathrm{B}} T} \frac{\partial^2 \Delta f}{\partial \phi_1^2} \quad , \tag{6.2}$$

where the derivative with respect to ϕ_1 is evaluated at fixed volume, fixed M_t, and fixed temperature.

In the simulations presented here, we extract a value for $S^{-1}(0)$ from the fluctuations in the overall number of chains of each type in semi-grand canonical ensemble, in which $M_t = M_1 + M_2$ is held constant, but M_1 and M_2 can be changed by moves that can change one type of chain into the other. In this ensemble, we may calculate $S_{ij}(0) = V^{-1} \int d\mathbf{r} \int d\mathbf{r}' \langle \delta c_i(\mathbf{r}) \delta c_j(\mathbf{r}') \rangle$ by noting that $\int d\mathbf{r} c_i(\mathbf{r}) = M_i N$. This yields a correlation function $S(0) = S_{11}(0) = S_{22}(0) = -S_{12}(0)$, for which

$$S(0) = \frac{N^2}{V} \langle \delta M_1^2 \rangle \quad , \tag{6.3}$$

where $\delta M_1 \equiv M_1 - \langle M_1 \rangle$. In this ensemble, this operational definition of $S(0)$ actually satisfies Eq. (6.2) exactly in the thermodynamic limit, notwithstanding the slight compressibility of any real liquid.

It is convenient to express the free energy of mixing per monomer Δf as a sum

$$\Delta f = k_{\mathrm{B}} T \sum_i \frac{\phi_i}{N} \ln \phi_i + f_{\mathrm{ex}} \quad , \tag{6.4}$$

where $i = 1$ or 2 is a species index, and f_{ex} is an excess free energy per monomer. Using this expression for Δf in Eq. (6.2), we obtain

$$S^{-1}(0) = v \left[\frac{1}{N\phi_1\phi_2} - 2\chi_a \right] \tag{6.5}$$

where χ_a is an "apparent" interaction parameter defined as

$$\chi_a \equiv -\frac{1}{2k_BT} \frac{\partial^2 f_{ex}}{\partial \phi_1^2} \quad . \tag{6.6}$$

The simplest approximation for Δf that we consider here is a generalized form of FH theory [7]. This approximation assumes that f_{ex} for a given potential is equal to some function

$$f_{ex} \simeq f_{int}(\phi_1, T) \tag{6.7}$$

of composition and temperature alone, but that f_{ex} is independent of chain length N. We refer to the postulated function $f_{int}(\phi_1, T)$ in what follows as a self-consistent field (SCF) interaction free energy. In this FH approximation, χ_a is approximated by an "effective" interaction parameter

$$\chi_e \equiv -\frac{1}{2k_BT} \frac{\partial^2 f_{int}}{\partial \phi_1^2} \tag{6.8}$$

that is also independent of chain length by assumption, but that can depend upon the interaction potential, temperature, and composition.

6.2.1 Perturbation theory

In all simulations presented here, the two species of chain are structurally identical chains of the same length, $N_1 = N_2$. A nonzero excess free energy exists only because the non-bonded pair interaction between unlike monomers (1-2 pairs) differs from the interaction between like monomers (1-1 and 2-2 pairs) by an amount proportional to a small parameter α. The model that we use here is thus of exactly the type considered in Chapters 4 and 5, in which we developed a perturbation theory for such models and the excess free energy was expanded in powers of α at constant temperature. Here, as in the perturbation theory, we use α as a control parameter, and simulate systems over a range of values of α at a constant temperature. We then compare results obtained for several chain lengths, and for two different polymer models.

The first order perturbation theory developed in Chapter 4 yields an expansion of f_{ex} to first order in α of the form

$$f_{\mathrm{ex}} \simeq \alpha z(N)\phi_1\phi_2 + \mathcal{O}(\alpha^2) \quad . \tag{6.9}$$

The quantity $z(N)$ is a measure of the number of inter-molecular contacts per monomer in a one-component reference liquid, with $\alpha = 0$. This "effective coordination number" depends slightly on chain length N, but approaches a model-dependent limiting value z^∞ in the limit $N \to \infty$. We have predicted and confirmed by simulation that $z(N)$ varies with chain length as

$$z(N) \simeq z^\infty \left(1 + \frac{\beta_1}{\sqrt{\bar{N}}}\right) + \frac{\gamma'}{N} \quad , \tag{6.10}$$

where $\beta_1 = (6/\pi)^{\frac{3}{2}}$ is a universal constant, while z^∞ and γ' are model-dependent constants, and $\bar{N} = Nb^6/v^2$ is an invariant degree of polymerization.

An expansion of $\chi_a(\phi_1, \alpha)$ at fixed temperature to first order in α, using Eqs. (6.6) and (6.9), is given by $\chi_a \simeq z(N)\alpha/k_{\mathrm{B}}T + \mathcal{O}(\alpha^2)$. We argued in Chapter 4 that, when comparing results of simulations of such symmetric models to a generalized FH theory, a corresponding first order approximation for the underlying SCF parameter $\chi_e(\phi_1, \alpha)$ could be obtained by simply taking the $N \to \infty$ limit of this approximation for χ_a. That is, we assume that $\chi_e(\phi_1, \alpha)$ can also be approximated by an expansion in powers of α, in which the first term is simply $\chi_e \simeq z^\infty \alpha/k_{\mathrm{B}}T$ In what follows, we will use the notation

$$\chi_{e1} \equiv \frac{z^\infty \alpha}{k_{\mathrm{B}}T} \tag{6.11}$$

to refer to this simple first-order approximation for χ_e.

6.2.2 Renormalized loop expansion

The renormalized one-loop theory (ROLT) [22,23] is a coarse grained theory of polymeric liquids that predicts small corrections to FH theory. It is based on an analysis of a coarse-grained model with pairwise additive pair interactions. As in the perturbation theory discussed above, the 1-2 pair interaction is assumed to differ from the 1-1 or 2-2 interaction by an amount that is controlled by a small parameter. In our presentation of the coarse-grained model, this parameter was referred to as a "bare" interaction

parameter, denoted by χ_0. Unlike the perturbation theory, the validity of the one-loop theory is not restricted to very small values of the control parameter χ_0 or α.

Straightforward power counting arguments given in Refs. [26] and [22] strongly suggest that the one-loop theory is only the first term within a systematic loop expansion of corrections to SCFT, in which the magnitude of these corrections is controlled by a small parameter $\bar{N}^{-1/2}$. The structure of the theory strongly suggests that the constant temperature excess free energy per monomer $f_{\mathrm{ex}}(\phi_1, \alpha, N)$ of symmetric blends of the type considered here may be well approximated as a sum of the following form:

$$f_{\mathrm{ex}} = f_{\mathrm{int}}(\phi_1, \alpha) + \frac{1}{N} f_{\mathrm{end}}(\phi_1, \alpha) + \frac{k_{\mathrm{B}}T}{N} f^*(\phi_1, \chi_e N, \bar{N}) \quad . \tag{6.12}$$

Here, f_{int} is a model-dependent SCF free energy energy of the sort postulated in Eq. (6.7), which is assumed to be independent of N, and f_{end} is a model-dependent free energy per chain arising from end-group contributions. f^* is a universal correction to SCF free energy per chain that can, in principle, be predicted order by order in a loop expansion as

$$f^*(\phi_1, \chi_e N, \bar{N}) = \sum_{n=1}^{\infty} \frac{1}{\bar{N}^{n/2}} \hat{f}_n^*(\phi_1, \chi_e N) \tag{6.13}$$

in which n is an index for the number of loops. Here, χ_e is a function of ϕ_1 and α alone that is related to f_{int} by Eq. (6.8).

From our simulations, we can obtain a value for the apparent interaction parameter χ_a defined in Eq. (6.6). The expression postulated above for the excess free energy yields a corresponding expression for χ_a in symmetric blends at constant T of the form:

$$\chi_a(\phi_1, \alpha, N) = \chi_e(\phi_1, \alpha) + \frac{\delta(\phi_1, \alpha)}{N} + \frac{1}{N} \chi^*(\phi_1, \chi_e N, \bar{N}) \quad , \tag{6.14}$$

where

$$\delta \equiv -\frac{1}{2k_{\mathrm{B}}T} \frac{\partial^2 f_{\mathrm{end}}}{\partial \phi_1^2} \tag{6.15}$$

$$\chi^* \equiv -\frac{1}{2} \frac{\partial^2 f^*}{\partial \phi_1^2} \quad . \tag{6.16}$$

Our analysis of the loop expansion suggests the existence of an expansion of χ^* of the form

$$\chi^*(\phi_1, \chi_e N, \bar{N}) = \sum_{n=1}^{\infty} \frac{1}{\bar{N}^{n/2}} \hat{\chi}_n^*(\phi_1, \chi_e N) \quad , \tag{6.17}$$

where we have defined

$$\hat{\chi}_n^*(\phi_1, \chi_e N) \equiv -\frac{1}{2 k_{\mathrm{B}} T} \frac{\partial^2 \hat{f}_n^*}{\partial \phi_1^2} \quad . \tag{6.18}$$

Only the one-loop ($n = 1$) contribution to χ^* has thus far been calculated [23].

In the remainder of this chapter, we attempt to test the extent to which the values of $S^{-1}(0)$ and χ_a measured in simulations of symmetric models of polymer mixtures at $\phi_1 = 1/2$ are consistent with the functional form postulated in Eq. (6.14).

6.2.3 Ordering in powers of $N^{-1/2}$

As the first step in the analysis of our simulation results, we plot and compare results for $\frac{c N S^{-1}(0)}{2}$ or $\chi_a N$ at $\phi_1 = 1/2$ as functions of $\chi_{e1} N$, where $\chi_{e1} = z^\infty \alpha / k_{\mathrm{B}} T$. A simple RPA theory with $\chi_e = \chi_{e1}$ predicts that results from different chain lengths should collapse in this representation. To understand the sources of the slight dependence on N, it is useful to expand contributions to $\chi_a N$, expressed as a function of $\chi_{e1} N$, as a series in powers of $N^{-1/2}$.

Here, we construct an expansion that retains all contributions to $\chi_a N$ of order N^{-1} or larger, or contributions to χ_a of order N^{-2} or larger. The starting point for this analysis is an expansion of Eq. (6.14) in which we approximate χ_e and δ/N by Taylor series in α, and approximate χ^* by a loop expansion. To truncate the expansions of χ_e and δ at the required order, we note that $\alpha \sim 1/N$ at $\chi_e N \sim 1$, and that δ appears multiplied by an explicit factor of $1/N$ in Eq. (6.14). To retain only contributions to χ_e and δ/N of order N^{-2} or larger, we must thus approximate

$$\chi_e(\alpha) \simeq z^\infty \alpha + z_2 \alpha^2 \tag{6.19}$$

$$\delta(\alpha) \simeq w\alpha \quad . \tag{6.20}$$

The approximation for χ_e to second order in α will be referred to as χ_{e2}. Here and hereafter, because we are interested only in analyzing data taken a fixed composition $\phi_1 = 1/2$, we suppress the dependence of quantities such as $z_2(\phi_1)$ and $w(\phi_2)$ upon ϕ_1, and treat them for this purpose as constants. Also we set $k_{\mathrm{B}} T = 1$ for notational convenience. Note that an accurate value of the coefficient z^∞ can be obtained for any model of interest by the procedure discussed in Chapter 4, but that the coefficients z_2 and w are unknown. To approximate f^* to $\mathcal{O}(N^{-1})$, we must retain the one and

two-loop contributions to f^*, giving an approximation

$$\chi^* \simeq \frac{1}{\bar{N}^{1/2}} \hat{\chi}_1^*(\chi_e N) + \frac{1}{\bar{N}} \hat{\chi}_2^*(\chi_e N) \quad , \tag{6.21}$$

in which χ_e is approximated by Eq. (6.19). Here, we have again suppressed all dependence on ϕ_1.

Using these approximations for χ_e, δ, and f^*, we can now order contributions to $\chi_a N$, for α of $\mathcal{O}(1/N)$, in powers of $N^{-1/2}$. The dominant $\mathcal{O}(1)$ contribution to $\chi_a N$ is given by $\chi_{e1} N$. The one-loop contribution to f^* yields a contribution to $\chi_a N$ of $\mathcal{O}(N^{-1/2})$. The quadratic contribution $z_2 \alpha^2$ to χ_e, the linear contribution $w\alpha$ to δ, and the two loop contribution to f^* yield contributions to $\chi_a N$ of order N^{-1}.

The predicted ordering can be made more explicit by rewriting or approximating each term in the expansion of $\chi_a N$ as an explicit function of $\chi_{e1} N = z^\infty \alpha N$. Expanding the difference

$$N\delta\chi_1 \equiv \chi_a N - \chi_{e1} N \tag{6.22}$$

as a function of χ_{e1} to $\mathcal{O}(N^{-1})$ yields

$$\begin{aligned}
N\delta\chi_1 \simeq{} & \frac{1}{\sqrt{\bar{N}}} \hat{\chi}_1^*(\chi_{e1} N) \\
& + \frac{1}{N} \left[\frac{w}{z^\infty} \chi_{e1} N + \frac{z_2}{(z^\infty)^2} (\chi_{e1} N)^2 \right] \\
& + \frac{1}{\bar{N}} \hat{\chi}_2^*(\chi_{e1} N) \quad .
\end{aligned} \tag{6.23}$$

The terms on the right hand side of the second line were obtained by rewriting α as χ_{e1}/z_1 in the expansions of $\chi_e(\alpha)$ and $\delta(\alpha)$. Further corrections that arise from our replacement of $\chi_e(\alpha)$ by χ_{e1} in $\hat{\chi}_1^*$ and $\hat{\chi}_2^*$ are of $\mathcal{O}(N^{-3/2})$ or smaller, and so can be neglected to this order.

The above analysis suggests the following graphical construction. After collecting data $\chi_a(\alpha, N)$ for each model, for several different chain lengths, we plot values of the quantity $\bar{N}^{1/2} N\delta\chi_1$ for all N together as a function of $\chi_{e1} N$. If the above theory is correct, values of this quantity for different chain lengths should almost collapse in this representation, and should approach the known function $\hat{\chi}_1^*(\chi_{e1} N)$ in the limit $N \to \infty$, with systematic differences that scale as $N^{-1/2}$ for sufficiently long chains.

6.2.4 Overview of analysis

In the remainder of this chapter, we test the consistency of our data with the above analysis in three steps, which are presented in Secs. 6.4, 6.5, and 6.6, respectively.

The first step, which is presented in Sec. 6.4 is simply to plot results for $\bar{N}^{1/2} N \delta \chi_1$ vs. $\chi_{e1} N$ for all chain lengths of both models, as described in Sec. 6.2.3.

The second step, presented in section 6.5, is an attempt to explicitly fit our results for the bead-spring model for four different chain lengths to the model given in Eq. (6.12). More precisely, we will use Eqs. (6.19) and (6.20) as approximations for $\chi_e(\alpha)$ and $\delta(\alpha)$ while χ^* will be approximated by Eq. (6.21). In this fit, we use the known value z^∞ and the theoretically predicted form of the one-loop correction $\hat{\chi}_1^*(\chi_e N)$, but allow the coefficients z_2, w and (notably) the entire function $\hat{\chi}_2^*(\chi_e N)$ to vary so as to minimize the error of a simultaneous fit to data from several chain lengths.

In the final step of our analysis, we attempt to test directly whether our data for two different models is consistent with any model of the form given in Eq. (6.12), which postulates that the difference $\chi_a N - \chi_e N - \delta$ is a universal function of $\chi_e N$ and $\bar{N}$. The procedure we have devised to test this, and the results, are discussed in Sec. 6.6.

6.3   Models and simulation methods

Monte Carlo simulations of both a continuum bead-spring model (BSM) and the bond fluctuation lattice model (BFM) of polymer blends have been conducted. Both these two models and the methods used to simulate them were described in Chapter 3 in detail.

Four different chain lengths were studied for each model. All simulations for each model were conducted at a single temperature over a range of values of a perturbation theory parameter α. All simulations presented in this chapter were conducted in a constant volume cubic unit cell with periodic boundary conditions, using a semi-grand canonical ensemble with equal chemical potentials for both species, so that $\langle \phi_1 \rangle = 1/2$ on average. Also, Eq. (6.3) was used to calculate values of $S^{-1}(0)$.

The main quantity of interest for the purpose of testing the ROLT is $S^{-1}(0)$. Therefore, its system size dependence was first investigated taking $N = 32$ as a representative system. It was found that for the BSM, the finite size effect was negligible up to

$\chi_{e1}N \simeq 1.8$ when $L \approx 10R_g$ where R_g is a radius of gyration. For the BFM, it was found that $L \approx 10R_g$ was large enough for $\chi_{e1}N \lesssim 1.7$.

6.3.1 BSM

All of our simulations of the bead-spring model, we use the same potential energy parameters ($\epsilon = k_BT$, $l = \sigma$, and $\kappa = 400\epsilon/\sigma^2$) and the same total number concentration ($c = 0.7\sigma^{-3}$) as those used in our previous studies of the first and second order perturbation theory for this model. We have simulated blends containing chains of lengths $N = 16, 32, 64$, and 128. An effective coordination number of $z^\infty = 0.2965$ and an infinite chain statistical segment length $b = 1.404\sigma$ were reported in Chapter 4.

For chain conformation sampling, we used a hybrid Monte Carlo/molecular dynamics move, reptation, and a variant of configurational bias double rebridging move, as in our previous simulations of melts with $\alpha = 0$. To simulate blends, we introduced a semi-grand canonical move that attempts to change the type of all of the monomers of a randomly chosen chain.

The relative weight of the moves was such that 2 out of 5 attempted moves were semi-grand moves, and the runs were designed so as to spend comparable amounts of computer time on each of the other types of move.

6.3.2 BFM

For the BFM, the volume fraction of monomers of type i is given by $\phi_i = 8NM_i/L^3$, where L is measured in units of the unit cell length in the underlying simple cubic lattice. The factor 8 is a result of the fact that in this model, each monomer occupies 8 corners of an elementary cube of this cubic lattice. We set the volume fraction of empty sites ϕ_v at 0.5, which previous workers have argued corresponds to a dense melt [67]. The chain lengths chosen for simulations are N=10, 20, 39, and 78. continuum model. For this model, we obtained the parameters z^∞ and b from Refs. [34] and [68], giving $z^\infty \approx 4.2$ and $b \approx 3.244$.

We used a combination of random monomer displacements and reptation moves to sample chain conformations, in addition to a move that can change the type of an entire chain. Each MC sweep consisted of: 1 random displacement per monomer, 3

reptation moves per chain, and 0.25 semi grand moves per chain. The code that we used for simulations of the BFM was graciously provided by Dr. Marcus Müller at the University of Göttingen.

6.4 Results

In this section, we present the results of measurements of $S^{-1}(0)$ using both models. Here, all results are plotted vs. $\chi_{e1}N$, where $\chi_{e1} = z^\infty \alpha$ is a first order approximation for $\chi_e(\alpha)$.

6.4.1 BSM

Fig. 6.1 shows the normalized inverse scattering intensity $S^{-1}(0)$ as a function of $\chi_{e1}N$ for $N = 16, 32, 64,$ and 128. As can be seen, the data gradually approaches the prediction of the RPA with $\chi_a = \chi_e$ as N increases. The predictions of a self-consistent renormalized one-loop theory prediction is shown for $N = 32$ as a representative example of the agreement between theory and simulation.

Fig. 6.1 also shows the extrapolated critical behavior of $S(0)$ in an infinite system near the critical point, as a series of dashed lines. Each of these lines represents an approximation of the form $S^{-1}(0) = A[(\chi_{e1}N)_c - (\chi_{e1}N)]^\gamma$, with $\gamma = 1.24$. The critical parameter value $(\chi_{e1}N)_c$ was obtained by a standard finite size scaling analysis [69] similar to that of Deutsch and Binder [41], which is discussed in Appendix F. The critical amplitude A for each chain length was estimated by adjusting it such that the line goes through the data point closest to the critical point.

Figure 6.2 shows the corresponding results for the plot of $\sqrt{\bar{N}}N(\chi_a - \chi_{e1})$ vs. $\chi_{e1}N$ for the BSM. The solid line is the prediction of the one-loop theory. The fact that data from different chain lengths nearly collapse in this representation confirms that the dominant contribution to $N(\chi_a - \chi_{e1})$ is indeed proportional to $1/\sqrt{\bar{N}}$. We see that the one-loop theory also provides a reasonable approximation for $\chi_a - \chi_{e1}$ for this model. The agreement is particularly good small values of $\chi_{e1}N$, but a systematic deviations from the one-loop theory are apparent at intermediate values of $\chi_{e1}N > 1$, where the data for the longest chain lengths falls above the one-loop theory.

As explained in Ref. [23], the fact that χ_a is slightly larger χ_{e1} for relatively low
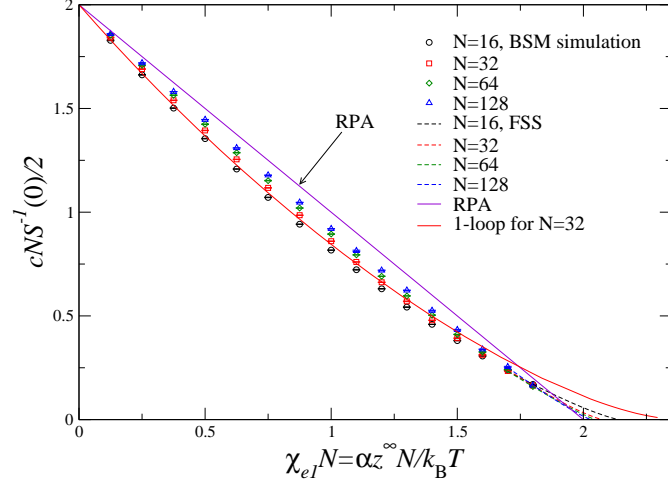
Figure 6.1: Plot of $\frac{cNS^{-1}(0)}{2}$ vs. $\chi_{e1}N$ for the BSM for four different chain lengths. The line labelled RPA is $2 - \chi_{e1}N$, which is the RPA prediction for a system with $\chi_e = \chi_{e1}$. In addition to simulation data, asymptotic critical behavior for each chain length, extrapolated to an infinite system, is shown by a dotted line.
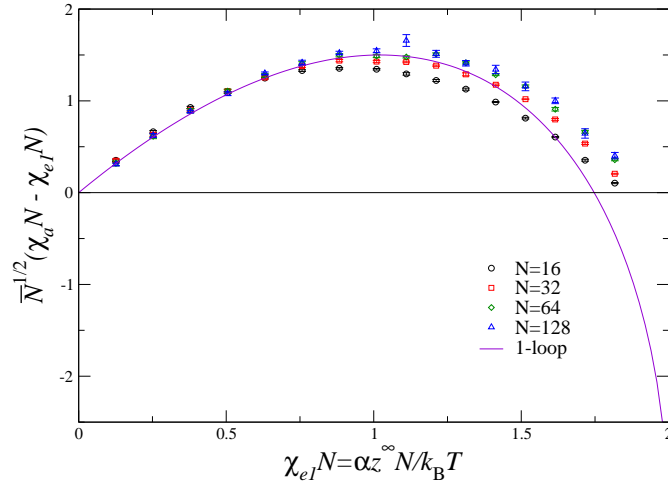

Figure 6.2: Reduced plot of the deviation $\delta\chi_1$ from the RPA prediction, for the BSM data that is also shown in Fig. 6.1

values of $\chi_{e1}N$ is the result of a subtle dependence of the depth of the correlation hole upon chain length. That is, for a system of finite chain, $z(N)$ is larger than z^∞ because a monomer of a finite chain is more exposed to monomers from other chains than a monomer of an infinitely long chain. Near the critical point, however, this correlation hole effect gets cancelled by the effects of long-wavelength composition fluctuations, which tend to reduce χ_a.

6.4.2 BFM

Figs. 6.3 and 6.4 shows corresponding data for $\frac{cNS^{-1}(0)}{2}$ and $\sqrt{\overline{N}}N\delta\chi_1$, respectively, for the bond fluctuation lattice model. In Fig. 6.4, data for four different chain lengths collapse almost perfectly, indicating that $N\delta\chi_1$ is almost exactly proportional to $\bar{N}^{-1/2}$. As also found for the BSM, agreement with the one-loop theory is excellent for small values of $\chi_{e1}N$, and less so when $\chi_{e1}N > 1$. In this representation, results of the BFM are noticeably different from from those obtained with the BSM, and lie much further from the one-loop prediction.

6.5 Testing the loop expansion

To test the loop expansion more quantitatively, we have fitted our data for the bead-spring model simulations to the truncated expansion described in Sec. 6.2.3. We have constructed a simultaneous fit of the data for four chain length N =16,32, 64, and 128 to the Eq. (6.14), while using Eqs. (6.19) and (6.20) for $\chi_e(\alpha)$ and $\delta(\alpha)$ and expansion (6.21) for $\chi^*(\chi_e(\alpha)N)$. That is, we model the simulation data with the following equation:

$$\chi_a N \simeq \chi_{e2}N + w\alpha + \frac{1}{\overline{N}^{1/2}}\hat{\chi}_1^*(\chi_{e2}N) + \frac{1}{\overline{N}}\hat{\chi}_2^*(\chi_{e2}N) \tag{6.24}$$

where $\chi_{e2} = z^\infty\alpha + z_2\alpha^2$. In this fit, we use the known value of z^∞, but treat the coefficients z_2 and w as fitting coefficients. We also use the theoretical prediction for the one-loop function $\hat{\chi}_1^*(\chi_e N)$, since this is known, but allow the unknown two-loop contribution $\hat{\chi}_2^*(\chi_e N)$ to vary to fit the data. Specifically, we approximate $\hat{\chi}_2^*(\chi_e N)$ at
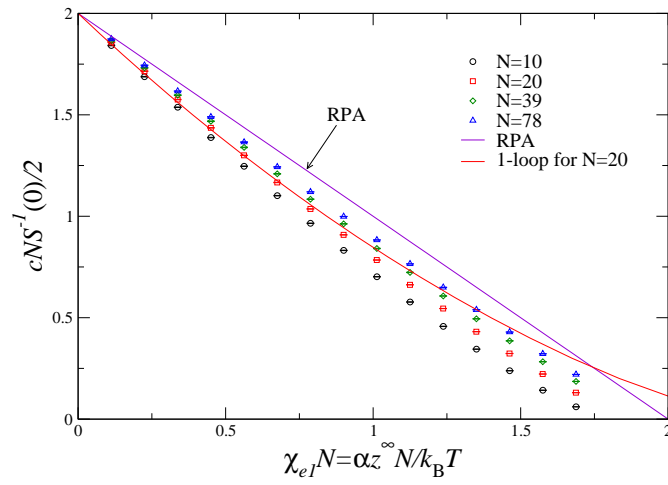
Figure 6.3: Plot of $\frac{cNS^{-1}(0)}{2}$ vs. $\chi_{e1}N$ for BFM for chain lengths $N =$10, 20, 39, and 78.
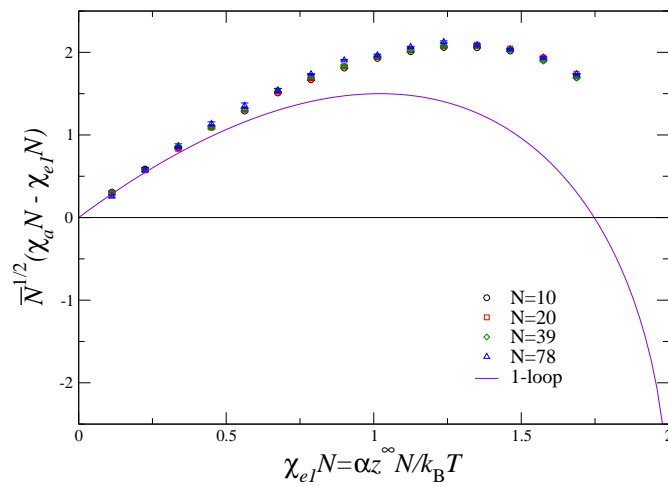

Figure 6.4: N scaling of deviations from the RPA for the BFM.

$\phi_1 = 1/2$ by a power series

$$\hat{\chi}_2^*(\chi_e N) = \sum_{k=1}^{k_{\max}} a_k (\chi_e N)^k. \tag{6.25}$$

in which the coefficients $a_1, \ldots, a_{k_{\max}}$ are treated as fitting coefficients. We have used $k_{\max} = 7$ because this was found to yield an adequate representation of the required function. Despite the fact that we allow the entire function $\hat{\chi}_2^*(\chi_e N)$ to vary so as to optimize the fit, the model still strongly constrains the data because: (1) we test the ability of the theory to simultaneously fit data for several chain lengths while using the same values for all parameters and, (2) the theory predicts both the dominant one-loop correction to the simplest RPA and the $\bar{N}$-dependence of the smaller two-loop correction.

Some information from our analyses of first and second order perturbation theory has also been used to constrain the fit. We showed in Chapter 5 that the loop expansion predicts first and second derivatives of $\chi_a(\alpha)$ of the form (Eqs. (5.63) and (5.71))

$$
\begin{aligned}
\left. \frac{\partial \chi_a}{\partial \alpha} \right|_{\alpha=0} &= z^\infty \left(1 + \frac{(6/\pi)^{3/2}}{\sqrt{\bar{N}}} \right) + \frac{\gamma'}{N} + \mathcal{O}(N^{-3/2}) \\
- \left. \frac{\partial^2 \chi_a}{\partial \alpha^2} \right|_{\alpha=0} &= \frac{3.7814 (z^\infty)^2}{2} \frac{N}{\sqrt{\bar{N}}} + \tau + \mathcal{O}(N^{-1/2}) \quad .
\end{aligned}
\tag{6.26}
$$

In the model we consider here, γ' and τ are given by

$$\gamma' = w + \frac{z^\infty}{c^2 b^6} a_1 \tag{6.27}$$

$$\tau = -2 \left(z_2 + \frac{(z^\infty)^2}{c^2 b^6} a_2 \right) \tag{6.28}$$

where a_1 and a_2 are coefficients in expansion (6.25). In the previous two chapters, we have fit data for the first and second derivatives of the free energy of this model to corresponding functions of N, and thereby obtained values $\gamma' \approx 0.3004$ and $\tau \approx -0.153$. We have fitted the data for blends subject to constraints imposed by Eqs. (6.27) and (6.28). By this procedure, we constrain our fit to data for χ_a at $\alpha > 0$ to be consistent with our earlier analysis of first and second order perturbation theory coefficients for this model.

We have implemented a simple procedure (based on a random walk in parameter space) to minimize the quantity

$$M \equiv \sum_N \sum_\alpha \left([\chi_a N](\alpha, N) - y(\alpha, N; z_2, w, \{a_k\})\right)^2 \quad , \tag{6.29}$$

subject to constraints (6.27) and (6.28), where

$$[\chi_a N](\alpha, N) \equiv 2 - \frac{cNS^{-1}(0)}{2} \tag{6.30}$$

is value $\chi_a N$ measured in a simulation for a particular value of α and N, and where $y(\alpha, N; z_2, w, \{a_k\})$ is the corresponding value predicted by the renormalized loop theory (Eq. (6.24)). The double summation in Eq. (6.29) is over all $N = 16, \ldots, 128$ and all values of α at which $S^{-1}(0)$ was measured.

Interestingly, we found that it is possible to obtain a rather good fit of this model to the BSM data, but that the parameters required to obtain a good fit are not unique: It is possible to obtain almost equally good fits over a range of values of the parameter z_2 and w within which the optimized function $\hat{\chi}_2^*(\chi_e N)$ changes substantially. Figure 6.5 shows several different fits, each of which was obtained by constraining the value of z_2 and minimizing the figure of merit with respect to the other parameters. Table 6.1 shows the resulting values of the figure of merit M obtained by this procedure. Though M does have a minimum, it varies rather little over a significant range of different values of z_2. Fig. (6.6) shows plots of the function $\hat{\chi}_2^*(\chi_e N)$ that were obtained by this optimization procedure for different values of z_2. Here, we see that the function $\hat{\chi}_2^*$ changes substantially over the same range of values of z_2.

The fact that this fit is not unique means that it cannot be used to determine precise values for the constants z_2 and w. We believe that this is closely related to

Table 6.1: z_2 vs. figure of merit (Eq.(6.29)) and true χ^2

z_2	Figure of merit	true χ^2
0.1974	0.245	1696
0.085	0.200	1217
0.05	0.189	1094
-0.439	0.239	2177
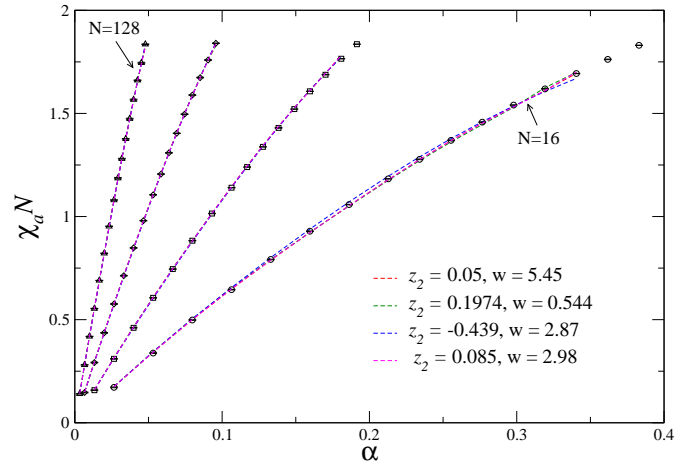
Figure 6.5: $\chi_a N$ vs. α for the BSM. Symbols represent the BSM simulation data for N=16, 32, 64, and 128. Each data point has an error bar smaller than the size of a symbol. The fit lines for N=16 and 32 do not go through all the data points because the last few points were excluded in the optimization.

Figure 6.6: Numerically determined $\hat{\chi}_2^*(\chi_e N)$ vs. $\chi_e N$. The line tagged with $z_2 = 0.05$ correspond to the smallest figure of merit.

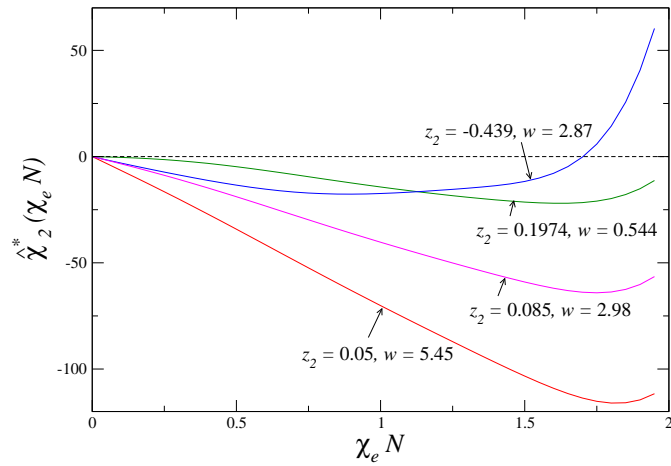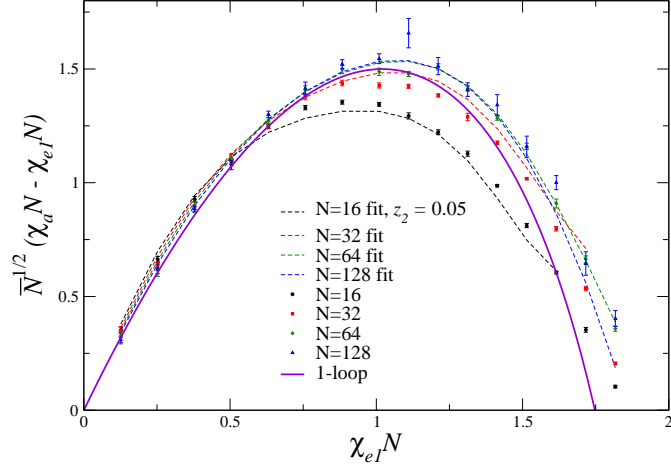Figure 6.7: $\sqrt{\bar{N}}(\chi_a N - \chi_{e1} N)$ vs. χ_{e1} for the BSM. This representation of data and fit shows the difference more clearly.

our conclusion in Chapter 5 that it will be impossible to determine values for these quantities by examining the N dependence of data for the first and second derivatives of the free energy with respect to α at $\alpha = 0$ until we have an analytic prediction for the two-loop correction. We suspect that the problem is that the fit is sensitive to the values of the constants γ' and τ that appear in Eqs. (6.27) and (6.28), but rather insensitive to changes in w and a_1 or z_2 and a_2 that leave γ' and τ unchanged. As in our analysis of second order perturbation theory, we conclude that we would need analytic prediction of $\hat{\chi}_2^*(\chi_e N)$ to determine precise values of z_2 and w.

Figs. 6.7 and 6.8 show two slightly different representations of the fit obtained using $z_2 = 0.05$. Both of these representations show differences between the fit and the data more clearly than in Fig. (6.5). In Fig. (6.8), $\chi_{e2} = z^\infty \alpha + z_2 \alpha^2$ denotes the quadratic approximation for $\chi_e(\alpha)$ given in Eq. (6.19), using the chosen value of z_2.

A similar fit of the data for the BFM model (not shown here) led to similar conclusions. Because we have not analyzed second derivatives of the free energy for the BFM, we did not impose constraint (6.28) in this fit.

We conclude that our simulation data are consistent with the proposed model, but that a fit to this model does not yet allow us to determine accurate values for all of the parameters in the model.
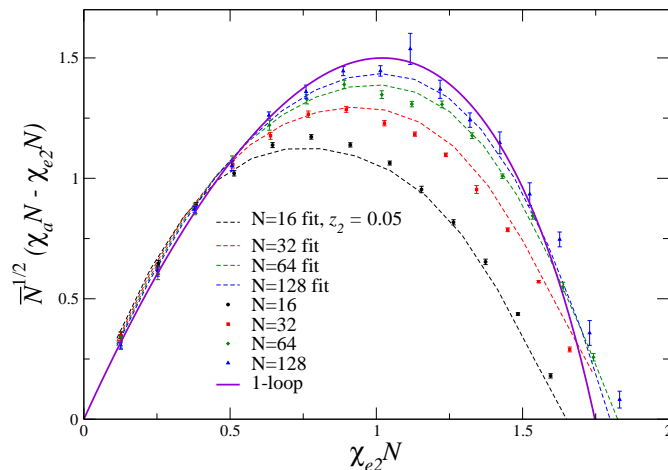
Figure 6.8: using $\chi_{e2}N$ instead of $\chi_{e1}N$

6.6   Testing universality

An implicit assumption behind the use of any coarse grained model of a polymer liquid can be stated as follows: the behavior at length scales much larger than a monomer scale is assumed to be universal, independent of many microscopic details.

Eq. (6.14) suggests that $\chi_a N$ can be expressed, for any model of a symmetric polymer blend with $\phi_1 = 1/2$, as the sum of a universal function of $\chi_e N$ and $\bar{N}$ plus a non-universal end-group contribution δ that is different for different models. To simplify the discussion, consider an idealized situation in which this end-group contribution can be ignored, either because it is negligible, or because we find a way to approximately correct for it. To further simplify matters, we restrict ourselves to the case of structurally symmetric polymer blends with $\phi_1 = 1/2$. In this case, the loop expansion suggests we could express $\chi_a N$ as a function

$$\chi_a N = h(\chi_e N, \bar{N}) \tag{6.31}$$

where

$$h(\chi_e N, \bar{N}) \equiv \chi_e N + \chi^*(\chi_e N, \bar{N}) \quad . \tag{6.32}$$

is a function that is believed to be the same for all such models, though the relationship between the parameter χ_e and microscopic parameters is different in each model.

When comparing values of χ_e in different models, we must remember that the definition of χ_e is somewhat arbitrary, because one can always redefine a "monomer" by grouping together two or more primary repeat units, while also redefining χ_e so as to leave the product $\chi_e N$ unchanged. Furthermore, after a definition of a "monomer" is chosen for each model, chains with the same value of $\bar{N}$ generally have different values of N in different models, because the ratio $\bar{N}/N = c^2 b^6$ differs in different models. To avoid having to keep track of a dependence on both $\bar{N}$ and N, it is useful to define a quantity

$$\bar{\chi}_e \equiv \chi_e N/\bar{N} \quad , \tag{6.33}$$

such that $\bar{\chi}_e \bar{N} = \chi_e N$.

Consider a comparison of results from two models a and b, such as the BSM and BFM, in which the free energy of mixing in model a is controlled by a microscopic parameter X_a and in model b by a parameter X_b. Let $\bar{\chi}_e$ be given for models a and b by functions $F_a(X_a)$ and $F_b(X_b)$, respectively, such that

$$\bar{\chi}_e = F_a(X_a) = F_b(X_b) \quad . \tag{6.34}$$

For simplicity, we assume that $F_a(F_a)$ and $F_b(X_b)$ are monotonic functions, and denote the inverse mappings by F_a^{-1} and F_b^{-1}, defined such that $X_a = F_a^{-1} \circ F_a(X_a)$ and $X_b = F_b^{-1} \circ F_b(X_b)$. Here and hereafter, we use the symbol $\circ$ to denote functional composition, so that $F_a \circ F_b(X_b) \equiv F_a(F_b(X_b))$. We also define a mapping

$$Q(X_b) \equiv F_a^{-1} \circ F_b(X_b) \tag{6.35}$$

that maps each value of the microscopic parameter X_b for model b onto a corresponding value of microscopic parameter X_a for model a, such that X_a and X_b yield the same value of $\bar{\chi}_e$.

Imagine that we had data for $\chi_a N$ vs. X_a or X_b from simulations of both models for several matched pairs of systems, such that each pair contains two systems simulated with models a and b at the same value of $\bar{N}$, using different values of N. Eq. (6.31) implies that the data from each such pair of systems would overlap in a plot of $\chi_a N$ vs. $\chi_e N$. Unfortunately, we cannot construct this plot unless we know the functions $F_a(X_a)$ and $F_b(X_b)$ for both models, which we do not. Eq. (6.31) also implies, however, that the data for $\chi_a N$ from a pair of simulations of models a and b with matched values

of $\bar{N}$ should overlap if both sets of data are plotted versus any variable $M(\bar{\chi}_e)N$, where $M(\bar{\chi}_e)$ is any mapping (i.e., function) of $\bar{\chi}_e$. Consider, specifically, the plots obtained by plotting both sets of data for $\chi_a N$ vs. the variable $X_a N$. For model a, this simply yields a plot of $\chi_a N$ vs. $X_a N$. For model B, this yields a plot of $\chi_a N$ vs. $Q(X_b)N$, where Q is the mapping defined in Eq. (6.35).

This argument implies that, if $\chi_a N$ is indeed given by a universal function $h(\chi_e N, \bar{N})$, in the sense discussed above, then it should be possible to construct a mapping $X_a = Q(X_b)$ such that, given data from pairs of systems with matched values of $\bar{N}$, each plot of $\chi_a N$ vs. $Q(X_b)N$ constructed using data from model b should overlap with a corresponding plot of $\chi_a N$ vs. $X_a N$ using data from model a at the same value of $\bar{N}$. This statement is not trivial because it requires that the same mapping $Q(X_b)$ collapse the data for all values of $\bar{N}$. One could thus imagine choosing $Q(X_b)$ so as to perfectly overlap data obtained from one pair of systems with matched values of $\bar{N}$, and then test the consistency with Eq. (6.31) by determining how well the resulting mapping collapses the data obtained from several other matched pairs with other values of $\bar{N}$. Note that this test cannot, by itself, tell us anything about how the postulated function $h(\chi_e N, \bar{N})$ depends upon $\chi_e N$ and $\bar{N}$. It simply tests whether data from two different models is compatible or incompatible with the hypothesized existence of such a function.

As already noted, Eq. (6.31) ignores end-group contributions to $\chi_a N$, which are given by model-dependent function $\delta(\alpha)$. If we allow for such contributions, Eq. (6.14) predicts only that the difference

$$\chi_a N - \delta(\alpha) = h(\chi_e N, \bar{N}) \tag{6.36}$$

is given by a universal function h. Ideally, we would thus like to be able to construct approximations for $\delta(\alpha)$ for two models of interest, and then apply the analysis described above to the difference $\chi_a N - \delta$. If we assume that δ can be approximated to the required accuracy by Eq. (6.20), then we only need a value for the coefficient w for each model. We showed in Chapters 4 and 5 that one can estimate the related coefficient γ', given in Eq. (6.27), by fitting the N-dependence of $z(N)$, but that it is impossible to infer a value for w from this fit without a theoretical prediction for the coefficient $a_1 \equiv \partial \hat{\chi}_2^* / \partial(\chi_e N)|_{\chi_e N=0}$.

In order to compensate for non-universal end-group effects as much as possible,

however, we have chosen to consider a quantity

$$U \equiv \chi_a N - \gamma' \alpha \quad . \tag{6.37}$$

To evaluate this quantity, a value of γ' must be determined from a fit of the N-dependence of $z(N)$ for each model of interest. By using the expansion of $\chi_a N$ to $\mathcal{O}(N^{-1})$, and Eq. (6.27) for γ', it is straightforward to show that U may be approximated to the same order by a sum

$$
\begin{aligned}
U \quad \simeq \quad & \chi_e N + \frac{\hat{\chi}_1^*(\chi_e N)}{\sqrt{\bar{N}}} \\
+ \quad & \frac{1}{\bar{N}} \left[\hat{\chi}_2^*(\chi_e N) - \chi_e N \left. \frac{\partial \hat{\chi}_2^*}{\partial (\chi_e N)} \right|_{\chi_e N = 0} \right] + \cdots \quad .
\end{aligned} \tag{6.38}
$$

In this the expansion, the subtraction of $\gamma' \alpha$ has removed all dependence on the model-dependent coefficient w. To this order, the only difference between the expansions of U and $\chi_a N - \delta$ is the second term in the last line of Eq. (6.38). Unlike w, this new term is universal function of $\chi_e N$ and $\bar{N}$. We thus conclude that U can be approximated to this order by a universal function

$$U \simeq h(\chi_e N, \bar{N}) - \frac{\chi_e N}{\bar{N}} \left. \frac{\partial \hat{\chi}_2^*}{\partial (\chi_e N)} \right|_{\chi_e N = 0} \tag{6.39}$$

of $\chi_e N$ and $\bar{N}$, albeit a slightly different one than the function $h(\chi_e N, \bar{N}) = \chi_a N - \delta$ in which we were originally interested. Finally, we note that the above test of the universality of the data obtained from two models can be applied to any quantity that we expect to be a universal function of $\chi_e N$ and $\bar{N}$, and so can just as well be applied to U as to $\chi_a N - \delta$.

We apply the above ideas to our data as follows. We take U as the universal quantity of interest, take the BSM as model a and BFM as model b and attempt to find a mapping Q that, as nearly as possible, collapses data for U from both models at equal values of $\bar{N}$. For this purpose, we use control parameters X_a and X_b given by the linear approximations for χ_e in these two models, so that $X_a \equiv \chi_{e1}^{\mathrm{BSM}}$ and $X_b \equiv \chi_{e1}^{\mathrm{BFM}}$. We approximate mapping $X_a = Q(X_b)$ by a low order polynomial

$$Q(X_b) = \frac{N_b}{N_a} \sum_{k=1}^{k_{\max}} C_k X_b^k \tag{6.40}$$

with $C_1 = 1$, using $k_{\max} = 2$ or 3. The coefficients C_2 and (sometimes) C_3 are treated as fitting parameters. The prefactor of N_b/N_a is the ratio of the degrees of polymerization for chains of model b (BFM) and a (BSM) with the same value of $\bar{N}$. We include this prefactor and set $C_1 = 1$ as a matter of convention, to guarantee that $N_a Q(X_b) = N_b X_b$ at low values of α, so that corresponding states yield corresponding values of $\chi_{e1}N$. We determine optimal values C_k for $k > 1$ by minimizing the quantity

$$\sum_{\bar{N}} \sum_{X_b} \left[U_b(X_b, \bar{N}) - U_a(Q(X_b), \bar{N}) \right]^2 \quad , \tag{6.41}$$

where $U_b(X_b, \bar{N})$ represents a value of U evaluated with model b at specified values of X_b and $\bar{N}$, and similarly for $U_a(X_a, \bar{N})$. Because the values of $\bar{N}$ and X_a used in the BSM simulations do not match those used in the BFM simulations, we have used the fit to our BSM data that was developed in Sec. 6.5, with $z_2 = 0.05$, to interpolate values of $\chi_a N$ to chain lengths and values of X_a that corresponding to the values of $\bar{N}$ and F_b for which data was taken in the BFM simulations (these correspond to interpolated chain lengths $N = 12.13$, 24.26, 47.30, and 94.61 in the BSM). The sum over values of $\bar{N}$ and X_b is thus a sum over values for which we took data for the BFM.

As with plots of $\chi_a N$, differences between the models can be seen most easily by plotting values of the difference $U - \chi_{e1}N$ rather than U. Figure 6.9 shows values for $U - \chi_{e1}N$ for both models, in which the discrete data points are results obtained for the BFM (model b) and the lines are a fit to the data for the BSM (model a), where the data for the BSM is plotted at the same set of values of $\bar{N}$ as those for which data was taken for the BFM. Figs. 6.10 and 6.11 show the results of our attempt to collapse the results for the BFM (model b) and BSM (model a) plotted vs. the variable $X_a N$ used for BSM in Fig. 6.9. Fig. 6.10 was obtained using a quadratic fit to $Q(X_b)$ ($k_{\max} = 2$), for which we obtain an optimal value $C_2 = 1.895$. Fig. 6.11 was obtained using a cubic fit ($k_{\max} = 2$), for which we obtain $C_2 = 1.479$ and $C_3 = 5.399$. Both plots show values of $U - X_a N_a$ vs. $X_a N_a$, in which we have used values of $X_a = Q(X_b)$ to plot the BFM data on this scale.

The cubic polynomial approximation for $Q(X_b)$ yields an extremely good data collapse. This analysis thus confirms that it is possible to describe the data for U from both models in terms of a single universal function of two variables $\chi_e N$ and $\bar{N}$.
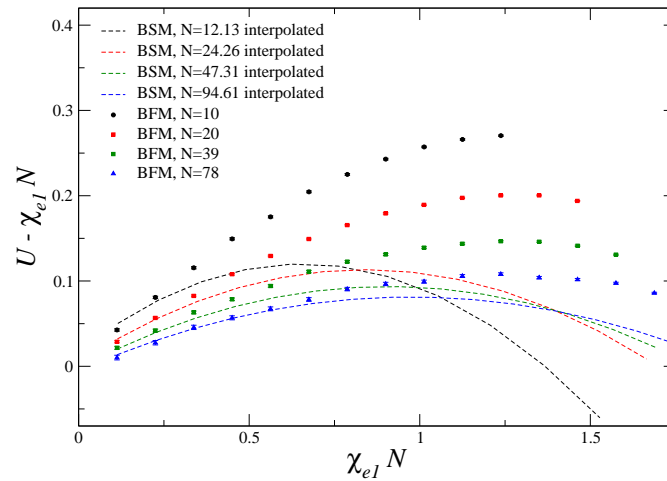
Figure 6.9: Plots of $U - \chi_{e1}N$ vs. $\chi_{e1}N$ for both models, before any attempt to collapse the data. Lines represent the results of the fit to the data for the BSM interpolated to values of N that correspond to the values of $\bar{N}$ at which data was taken for the BFM.

Figure 6.10: Values of $U - X_aN_a$ vs. X_aN_a for both models, in which values of X_a for the BFM (discrete points) are given by the mapping $X_a = Q(X_b)$, using a quadratic approximation for $Q(X_b)$ ($k_{\max} = 2$).

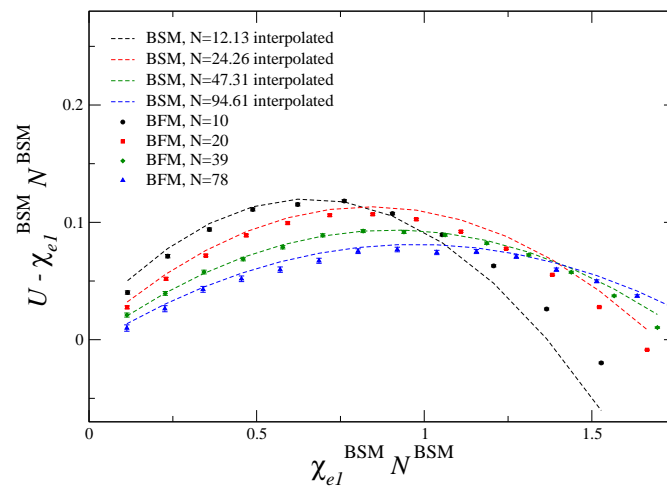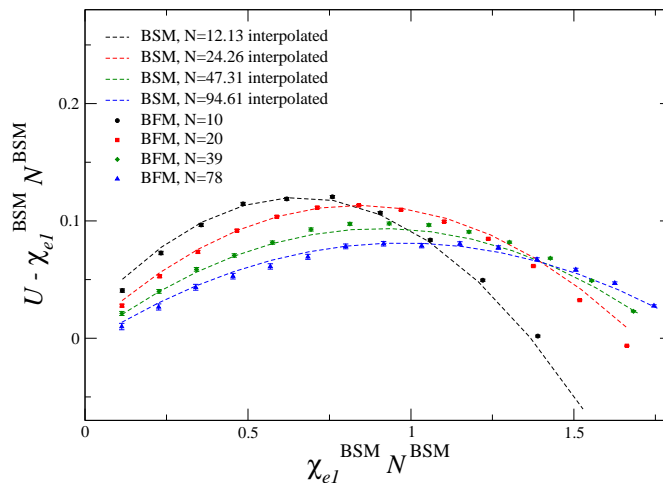Figure 6.11: Values of $U - X_a N_a$ vs. $X_a N_a$ for both models, in which values of X_a for the BFM (discrete points) are given by the mapping $X_a = Q(X_b)$, using a cubic polynomial approximation for $Q(X_b)$ ($k_{\max} = 3$).

6.7 Conclusions

In this chapter, there were three main goals we attempted to achieve. The first was a quantitative test of the prediction of the renormalized one-loop theory (ROLT) for blends. To reduce ambiguity in comparison, an accurate FH interaction parameter χ (denoted by χ_e) was needed and obtained by taking the limit $N \to \infty$ of a perturbative expansion of free energy of blends. This allowed χ_e to be expressed as a series in powers of small parameter α proportional to the incompatibility between two monomer species.

For the comparison between the theory and simulations, first we used the leading order term only, defined as $\chi_{e1} = z^\infty \alpha$. By measuring collective composition fluctuations characterized by $S^{-1}(\mathbf{q} \to 0)$ using two coarse grained models of polymers, it was found that the ROLT of blends accurately describes the correlation effects for relatively small values of $\chi_{e1} N$. For larger $\chi_{e1} N$, it was shown that a non-universal end effect and non-linear terms in the expansion of χ_e start to affect the data as well as higher order loop contributions.

Next, knowing the importance of the non-linear terms in χ_e for large values of α, we sought to obtain the next order correction $z_2 \alpha^2$ to χ_e. In Chapter 5, we found that it was not possible without knowing both first and second derivative of two-loop

contribution to free energy, $\hat{f}_2^*(\chi_e N)$, at $\chi_e N = 0$. Instead, composition fluctuation data were utilized and a simple data fitting was tried to match them with a prediction involving z_2, an end-group contribution, and the two-loop contribution $\hat{\chi}_2^*$, all of which were unknown and treated as fitting parameters. We found that the posed optimization problem had multiple solutions that fit the data almost equally well. We were thus able to confirm that the data for the BSM appears to consistent with the known predictions of the loop expansion, but unable to refine the first-order perturbation theory estimates of the SCF free energy and interaction parameter that we gave in Chapter 4.

Finally, we conducted a test on the universality of the two coarse grained models of polymer chosen for the study. We showed that for a quantity which is a function of $\chi_e N$ and $\bar{N}$ (in other words, a physical property of the blend at the length scale similar or lager than a polymer), it should be possible that data of one model can be put on top of those of the other by an appropriate transformation of a microscopic parameter of the former. We tested this idea taking BSM as a reference model and attempted to bring BFM data onto BSM data, taking U (Eq. (6.37)) as a target universal function. A single mapping was able to collapse data for four different chain lengths. We were thereby able to show the data for these two models are at least compatible with the existence of a universal theory for corrections to the RPA of the form postulated here.

All the analyses conducted suggest that the renormalized loop theory of correlation is consistent with simulation data of coarse grained models. Also, the two models used in this study did exhibit consistency in their collective composition fluctuation, supporting the universality assumption of coarse grained models in scales similar or larger than chain dimension.

Chapter 7

Summary

The main findings in this thesis were presented in Chapters 4, 5, and 6.

In Chapter 4, we developed a perturbation theory of symmetric blends to first order in a small parameter α that controls the incompatibility between two monomer species. We considered a class of lattice and continuum models and for both, we found the free energy of mixing can be written in the original Flory-Huggins (FH) form except that a lattice coordination number was replaced by an effective coordination number $z(N)$, which properly accounts for local liquid structure. A simple random walk model for an effective incompressible melt predicted that for a finite N, $z(N)$ is larger than $z(N \rightarrow \infty)$ by a fractional amount of order $\mathcal{O}(N^{-1/2})$. This model was found to fit simulation data very well. Lastly, we proposed a way to obtain the FH parameter χ by extrapolating the perturbation theory to the limit $N \rightarrow \infty$.

In Chapter 5, the perturbation theory of previous chapter was extended to second order in α. The main motivation was to obtain an accurate estimation of the FH parameter χ to second order in α. Microscopic expression for the second derivative of free energy per monomer was derived, providing a way to measure the quantity in a simulation. Next a general loop expansion was used to predict the chain length dependence of the second derivative. It allowed us to identify the parameters that are required to obtain the second order correction to the FH parameter χ. The results of a bead-spring model simulation agreed with the prediction of the loop expansion for N dependence. However, it was not possible to obtain the parameters due to lack of an analytical prediction for a two loop contribution to free energy.

There were three goals in Chapter 6. First, using the prescription to obtain the FH parameter χ proposed in Chapter 4, we compared the predictions of a renormalized one loop theory to simulations of two coarse grained models of symmetric blends at the critical composition. We found the theory accurately describe collective composition fluctuations and quantitative agreement between theory and simulations was good for relatively small values of χN. Second, we attempted to obtain the second order correction to the FH parameter χ by utilizing the composition fluctuation data. We tried to fit the data using the prediction of the loop expansion and found that they are consistent with the theory. However, this method was unable to find a unique solution to the problem. Lastly, we conducted a simple test on the universality assumption of coarse grained models. Properties of polymer liquids at length scale much larger than a size of monomer should not be so sensitive to the microscopic details of a given model. We showed that for such quantities, one can bring data from two different models together by a mapping procedure. The mapping was attempted using a lattice model and a continuum model and we obtained results which supported the hypothesis.

References

[1] M. L. Huggins. *J. Chem. Phys.*, 9:440, 1941.

[2] P. J. Flory. *J. Chem. Phys.*, 9:660, 1941.

[3] T. Kawakatsu. *Statistical Physics of Polymers*. Springer, 2004.

[4] P. G. de Gennes. *Scaling Concepts in Polymer Physics*. Cornell University Press, 1979.

[5] M. Doi. *Introduction to Polymer Physics*. Oxford Science Publication, 1996.

[6] P. C. Hiemenz and T. Lodge. *Polymer Chemistry*. CRC Press, 2007.

[7] I. C. Sanchez. *Polymer*, 30:471, 1989.

[8] M. Shibayama, S. Yang, and R. S. Stein. *Macromolecules*, 18(11):2179–2187, 1985.

[9] R. S. Stein, C.T. Murry, H. Yang, V. Soni, and R.J. Lo. *Physica B & C*, 137:194, 1986.

[10] C. Han, B. Bauer, J. Clark, Y. Muroga, Y. Matsushita, Q. T.-C. M. Okada, T. Chang, and I. Sanchez. *Polymer*, 29:2002, 1988.

[11] F. Schmid. *J. Phys.:Condens. Matter*, 10:8105, 1998.

[12] M. W. Matsen. *J. Phys.:Condens. Matter*, 14:R21, 2001.

[13] A. Sariban and K. Binder. *J. Chem. Phys.*, 86(10):5859–5873, 1987.

[14] A. Sariban and K. Binder. *Macromolecules*, 21:711–726, 1988.

[15] O. N. Vassiliev and M. W. Matsen. *J. Chem. Phys.*, 118(16):7700–7713, 2003.

[16] M. W. Matsen, G. H. Griffiths, R. A. Wickham, and O. N. Vassiliev. *J. Chem. Phys.*, 124:024904, 2006.

[17] M. Olvera de la Cruz, S. F. Edwards, and I. C. Sanchez. *J. Chem. Phys.*, 89(3):1704–1708, 1988.

[18] R. Holyst and A. Vilgis. *J. Chem. Phys.*, 99(6):4835–4844, 1993.

[19] R. Holyst and A. Vilgis. *Phys. Rev. E*, 50(3):2087–2092, 1994.

[20] G. H. Fredrickson, A. J. Liu, and F. S. Bates. *Macromolecules*, 27(9):2503–2511, 1994.

[21] Z.-G. Wang. *J. Chem. Phys.*, 117:481, 2002.

[22] P. Grzywacz, J. Qin, and D. C. Morse. *Phys. Rev. E*, 76:061802, 2007.

[23] J. Qin and D. C. Morse. *J. Chem. Phys*, 130:224902, 2009.

[24] D. C. Morse and J. K. Chung. *J. Chem. Phys.*, 130:224901, 2009.

[25] P. G. de Gennes. *J. Phys.(Paris)*, 31:235, 1970.

[26] D. C. Morse. *Ann. Phys.*, 321:2318, 2006.

[27] K. Binder, editor. *Monte Carlo and Molecular Dynamics Simulations in Polymer Science*. Oxford University Press, 1995.

[28] V. Galiatsatos, editor. *Molecular Simulation Methods for Predicting Polymer Properties*. John Wiley & Sons, 2004.

[29] S. Yip, editor. *Handbook of Materials Modeling*. Springer, 2005.

[30] R. B. Bird, R. C. Armstrong, and D. Hassager. *Dynamics of Polymeric Liquids*. J. Wiley, 1971.

[31] K. Kremer and G. S. Grest. *J. Chem. Phys.*, 92:5057, 1990.

[32] I. Carmesin and K. Kremer. *Macromolecules*, 21:2819, 1988.

[33] H.-P. Deutsch and K. Binder. *Macromolecules*, 25:6214–6230, 1992.

[34] M. Müller and K. Binder. *Comput. Phys. Commun*, 84:173, 1994.

[35] D. Frenkel and B. Smit. *Understanding Molecular Simulation*. Academic Press, 2002.

[36] M. P. Allen and D. J. Tildesley. *Computer Simulation of Liquids*. Oxford Science Publications, 1987.

[37] W. H. Press, S. A. Teukolsky, W. T. Vetterling, and B. P. Plannery. *Numerical Recipes in C: The Art of Scientific Computing*. Cambridge University Press, 1992.

[38] D. P. Landau and K. Binder. *A Guide to Monte Carlo Simulations in Statistical Physics*. Cambridge University Press, 2000.

[39] M. E. J. Newman and G. T. Barkema. *Monte Carlo Methods in Statistical Physics*. Oxford University Press, 1999.

[40] B. Mehlig, D. Heermann, and B. Forrest. *Phys. Rev. B*, 45:679, 1992.

[41] H.-P. Deutsch. *J. Stat. Phys*, 67:1039–1082, 1992.

[42] B. Forrest and U. W. Suter. *J. Chem. Phys*, 102:7256, 1995.

[43] M. N. Rosenbluth and A. W. Rosenbluth. *J. Chem. Phys*, 23:356, 1954.

[44] J. J. de Pablo, M. Laso, and U. W. Suter. *J. Chem. Phys*, 96:2395, 1992.

[45] F. A. Escobedo and J. J. de Pablo. *J. Chem. Phys*, 102:2636, 1994.

[46] Z. Chen and F. A. Escobedo. *J. Chem .Phys*, 24:11382, 113.

[47] N. C. Karayiannis, V. G. Mavrantzas, and D. N. Theodorou. *Phys. Rev. Lett*, 88:105503, 2002.

[48] N. C. Karayiannis, V. G. Mavrantzas, and D. N. Theodorou. *J. Chem. Phys*, 117:5465, 2002.

[49] B. Banaszak and J. J. de Pablo. *J. Chem .Phys*, 119:2456, 2003.

[50] P. H. Verdier and W. H. Stockmayer. *J. Chem. Phys*, 36:227, 1962.

[51] J. Qin. PhD thesis, University of Minnesota, 2009.

[52] M. Müller and K. Binder. *Macromolecules*, 28:1825–1834, 1995.

[53] G. S. Grest and M.-D. Lacasse. *J. Chem. Phys.*, 105:10583–10594, 1996.

[54] F. A. Escobedo and J. J. de Pablo. *Macromolecules*, 32:900–910, 1999.

[55] H. P. Deutsch and K. Binder. *J. Phys. II France*, 3:1049–1073, 1993.

[56] H. Fried and K. Binder. *J. Chem. Phys.*, 94(12):8349–8366, 1991.

[57] H. Fried and K. Binder. *Europhysics Letters*, 16(3):237–242, 1991.

[58] T. Pakula, K. Karatasos, S. Anastasiadis, and G. Fytas. *Macromolecules*, 30:8463, 1997.

[59] M. Murat, G.S. Grest, and K. Kremer. *Macromolecules*, 32:595, 1999.

[60] B. Banaszak and J. J. de Pablo. *Macromolecules*, 32:900–910, 1999.

[61] P. G. de Gennes. *J. Phys. (France) Lett.*, 38:441, 1977.

[62] J. F. Joanny. *J. Phys. A*, 11:L117, 1978.

[63] R. Krishnamoorti, W. W. Graessley, N. P. Balsara, and D. J. Lohse. *J. Chem. Phys*, 100:3894, 1994.

[64] H. S. Jeon, J. H. Lee, and N. P. Balsara. *Macromolecules*, 31:3328, 1998.

[65] H. S. Jeon, J. H. Lee, N. P. Balsara, and M. C. Newstein. *Macromolecules*, 31:3340, 1998.

[66] T. A. Vilgis and M. Benmouna. *Makromol. Chem., Theory Simul.*, 1:25, 1992.

[67] W. Paul, K. Binder, D. Heermann, and W. Kremer. *J. Phys. II*, 1:37, 1991.

[68] J. P. Wittmer, P. Beckrich, H. Meyer, A. Cavallo, A. Johner, and J. Baschagel. *Phys. Rev. E.*, 76:011803, 2007.

[69] V. Privman, editor. *Finite Size Scaling and Numerical Simulation of Statistical Systems.* World Scientific, 1990.

[70] P. Young. Monte Carlo simulations in statistical physics. Personal lecture note, Jan 2006.

[71] H. Müller-Krumbhaar and K. Binder. *J. Stat. Phys.*, 8:1, 1973.

[72] P. M. Chaikin and T. C. Lubensky. *Principles of Condensed Matter Physics.* Cambridge University Press, 1995.

[73] A. M. Ferrenberg and R. H. Swendsen. *Phys. Rev. Lett*, 61:2635, 1988.

[74] A. M. Ferrenberg and R. H. Swendsen. *Phys. Rev. Lett*, 63:1195, 1989.

[75] C. H. Bennett. *J. Comput. Phys*, 22:245, 1976.

Appendix A

One loop approximation for correlation free energy

There are at least two ways to derive the one loop free energy [22, 26]. The first one is the Edwards auxiliary field formalism where the partition function of the system is transformed into a functional integral over complex chemical potential field and its fluctuation around the saddle point value is approximated by a Gaussian distribution. The other is through a fictitious charging process where the interaction between polymer chains are turned on gradually, which will be described in this section.

We start with the interaction energy of the same form as Eq. (2.7), but introduce a charging parameter η that takes a value between 0 and 1, i.e.

$$U_{\text{int}} = \frac{\eta}{2} \sum_{i,j} \int d\mathbf{r} \int d\mathbf{r}' \ U_{ij}(\mathbf{r} - \mathbf{r}') c_i(\mathbf{r}) c_j(\mathbf{r}') \quad . \tag{A.1}$$

With some intra chain potential energy U_{chain}, the configurational part of the partition function is given by

$$Z = \int d\Gamma \ e^{-\beta(U_{\text{chain}} + U_{\text{int}})} \quad , \tag{A.2}$$

where $\int d\Gamma$ is an integral over distinct micro-states and the Helmholtz free energy of

the system is $\beta F = -\ln Z$. Taking a derivative of F with respect to η, one gets

$$
\begin{aligned}
\frac{\partial F}{\partial \eta} &= -\beta^{-1}\frac{1}{Z}\frac{\partial Z}{\partial \eta} \\
&= \frac{1}{Z}\int d\Gamma\, e^{-\beta(U_{\text{chain}}+U_{\text{int}})}\frac{\partial U_{\text{int}}}{\partial \eta} \\
&= \left\langle \frac{\partial U_{\text{int}}}{\partial \eta}\right\rangle \\
&= \frac{1}{2}\sum_{i,j}\int d\mathbf{r}\int d\mathbf{r}'\, U_{ij}(\mathbf{r}-\mathbf{r}')\langle c_i(\mathbf{r})c_j(\mathbf{r}')\rangle.
\end{aligned}
\tag{A.3}
$$

For a homogeneous liquid, the number density can be written as $c_i(\mathbf{r}) = c_i + \delta c_i(\mathbf{r})$. Therefore,

$$
\begin{aligned}
\frac{\partial F}{\partial \eta} &= \frac{1}{2}\sum_{i,j}\int d\mathbf{r}\int d\mathbf{r}'\, U_{ij}(\mathbf{r}-\mathbf{r}')\big[c_i c_j + \langle \delta c_i(\mathbf{r})\delta c_j(\mathbf{r}')\rangle\big] \\
&= \frac{V}{2}\sum_{i,j}\bar{U}_{ij}c_i c_j + \frac{1}{2}\sum_{i,j}\int d\mathbf{r}\int d\mathbf{r}'\, U_{ij}(\mathbf{r}-\mathbf{r}')S_{ij}(\mathbf{r}-\mathbf{r}') \quad,
\end{aligned}
\tag{A.4}
$$

where we defined $\bar{U}_{ij} \equiv \int d\mathbf{r} U_{ij}(\mathbf{r})$. Using the inverse Fourier transforms of $U_{ij}(\mathbf{r}) = \int \frac{d\mathbf{q}}{(2\pi)^3}\, e^{-i\mathbf{q}\cdot\mathbf{r}}\, \tilde{U}_{ij}(\mathbf{q})$ and $S_{ij}(\mathbf{r}) = \int \frac{d\mathbf{q}}{(2\pi)^3}\, e^{-i\mathbf{q}\cdot\mathbf{r}}\, \tilde{S}_{ij}(\mathbf{q})$, the second term of Eq. (A.4) can be rewritten

$$
\begin{aligned}
\frac{V}{2}&\sum_{i,j}\int d\mathbf{r}\, U_{ij}(\mathbf{r})S_{ij}(\mathbf{r}) \\
&= \frac{V}{2}\sum_{i,j}\int \frac{d\mathbf{q}}{(2\pi)^3}\, \tilde{U}_{ij}(\mathbf{q})\int \frac{d\mathbf{q}'}{(2\pi)^3}\, \tilde{S}_{ij}(\mathbf{q}')\int d\mathbf{r}\, e^{-i(\mathbf{q}+\mathbf{q}')\cdot\mathbf{r}} \\
&= \frac{V}{2}\sum_{i,j}\int \frac{d\mathbf{q}}{(2\pi)^3}\, \tilde{U}_{ij}(\mathbf{q})\int d\mathbf{q}'\, \tilde{S}_{ij}(\mathbf{q}')\delta(\mathbf{q}+\mathbf{q}') \\
&= \frac{V}{2}\sum_{i,j}\int_{\mathbf{q}} \tilde{U}_{ij}(\mathbf{q})\tilde{S}_{ij}(\mathbf{q};\eta).
\end{aligned}
\tag{A.5}
$$

The first line of the above equation results from the translational invariance of the system and in the last line, η was used as an extra argument for $\tilde{S}_{ij}(\mathbf{q};\eta)$ to indicate the quantity depends on it. Also $\int_{\mathbf{q}}$ was introduced as a short hand notation for $\int \frac{d\mathbf{q}}{(2\pi)^3}$.

Integrating both sides of Eq. (A.4) with respect to η from 0 to 1 yields

$$
\begin{aligned}
F(\eta &= 1) - F(\eta = 0) \\
&= \frac{V}{2}\sum_{i,j}\bar{U}_{ij}c_i c_j + \frac{V}{2}\int_{\mathbf{q}}\int_0^1 d\eta\, \text{Tr}\left[\tilde{\mathbf{U}}(\mathbf{q})\tilde{\mathbf{S}}(\mathbf{q};\eta)\right] \quad,
\end{aligned}
\tag{A.6}
$$

where $F(\eta = 1)$ is the free energy of the fully interacting chains and $F(\eta = 0)$ is the free energy of the corresponding non interacting chains. One loop approximation for correlation free energy (Eq. (2.37)) is obtained by using the RPA for the structure factor (Eq. (2.26)) with the Gaussian random walk model for the single chain statistics. Then, $\tilde{\mathbf{S}}^{(0)} = \tilde{\boldsymbol{\Omega}}$ where $\tilde{\boldsymbol{\Omega}}$ was defined by its matrix elements Eq. (2.38) and the integration over η can be carried out as follows.

$$
\begin{aligned}
\int_0^1 d\eta \ \mathrm{Tr}\ \left[\tilde{\mathbf{U}}(\mathbf{q})\tilde{\mathbf{S}}(\mathbf{q};\eta)\right] &= \int_0^1 d\eta \ \mathrm{Tr}\ \left[\tilde{\mathbf{U}}(\tilde{\boldsymbol{\Omega}}^{-1} + \eta\tilde{\mathbf{U}})^{-1}\right] \\
&= \int_0^1 d\eta \ \mathrm{Tr}\ \left[\tilde{\mathbf{U}}(\mathbf{I} + \eta\tilde{\boldsymbol{\Omega}}\tilde{\mathbf{U}})^{-1}\tilde{\boldsymbol{\Omega}}\right] \\
&= \int_0^1 d\eta \ \mathrm{Tr}\ \left[(\mathbf{I} + \eta\tilde{\boldsymbol{\Omega}}\tilde{\mathbf{U}})^{-1}\tilde{\boldsymbol{\Omega}}\tilde{\mathbf{U}}\right] \qquad \text{(A.7)} \\
&= \int_0^1 d\eta \frac{\partial}{\partial\eta} \ln\left[\det\left|\mathbf{I} + \eta\tilde{\boldsymbol{\Omega}}\tilde{\mathbf{U}}\right|\right] \\
&= \ln\left[\det\left|\mathbf{I} + \tilde{\boldsymbol{\Omega}}\tilde{\mathbf{U}}\right|\right]
\end{aligned}
$$

In the above derivation, a property of matrix valued functions was used, i.e. if $\mathbf{Y} = \mathbf{Y}(\eta)$ is a square matrix valued function,

$$
\frac{\partial}{\partial\eta} \ln\left[\det|\mathbf{Y}|\right] = \mathrm{Tr}\left[\mathbf{Y}^{-1}\frac{\partial\mathbf{Y}}{\partial\eta}\right] \qquad \text{(A.8)}
$$

Substituting Eq. (A.7) in Eq.(A.6), the free energy per volume $f = F/V$ becomes

$$
f = \frac{F}{V} \quad = \quad \frac{1}{2}\sum_{i,j}\bar{U}_{ij}c_i c_j + \frac{1}{2}\int_{\mathbf{q}} \ln\left[\det\left|\mathbf{I} + \tilde{\boldsymbol{\Omega}}\tilde{\mathbf{U}}\right|\right] \qquad \text{(A.9)}
$$

besides the trivial Flory-Huggins ideal entropy of mixing term f_{id} (Eq. (2.35)) and free energy density of non interacting chains. The first and the second term are identified with Eq. (2.36) and Eq. (2.37), respectively.

Appendix B

Detailed balance and convergence toward equilibrium

Here, we establish the fact that the detailed balance condition will drive $P_l(t = 0)$ to P_l^{eq}. The discussion presented is based on the work by Young [70]. As a measure of convergence, let us define a quantity $G(t)$

$$
\begin{aligned}
G(t) & \equiv \sum_l \frac{1}{P_l^{eq}} (P_l(t) - P_l^{eq})^2 \\
& = \sum_l \frac{1}{P_l^{eq}} [P_l^2(t) - 2P_l(t)P_l^{eq} + (P_l^{eq})^2] \\
& = \sum_l \frac{P_l^2(t)}{P_l^{eq}} - 1 > 0
\end{aligned}
\tag{B.1}
$$

The difference between $G(t+1)$ and $G(t)$ can be written as,

$$
\begin{aligned}
\Delta G & \equiv G(t+1) - G(t) \\
& = \sum_l \frac{P_l^2(t+1)}{P_l^{eq}} - \sum_l \frac{P_l^2(t)}{P_l^{eq}} \\
& = \sum_{l,m,n} \left[w_{m \to l} w_{n \to l} \frac{P_m P_n}{P_l^{eq}} \right] - \sum_l \frac{P_l^2}{P_l^{eq}}.
\end{aligned}
\tag{B.2}
$$

In the last line, the time argument has been suppressed and Eq. (3.11) was used for $P_l(t+1)$. Furthermore, using detailed balance condition Eq. (3.13),

$$
\sum_{l,m,n} \left[w_{m \to l} w_{n \to l} \frac{P_m P_n}{P_l^{eq}} \right] = \sum_{l,m,n} \left[w_{l \to m} w_{l \to n} P_l^{eq} \frac{P_m P_n}{P_m^{eq} P_n^{eq}} \right]
\tag{B.3}
$$

$$\sum_m \frac{P_m^2}{P_m^{eq}} = \sum_{l,m} w_{m\to l} \frac{P_m^2}{P_m^{eq}}$$

$$= \sum_{l,m} w_{l\to m} P_l^{eq} \left(\frac{P_m}{P_m^{eq}}\right)^2$$

$$= \sum_{l,m,n} w_{l\to m} w_{l\to n} P_l^{eq} \left(\frac{P_m}{P_m^{eq}}\right)^2$$

$$= \frac{1}{2} \sum_{l,m,n} w_{l\to m} w_{l\to n} P_l^{eq} \left(\frac{P_m}{P_m^{eq}}\right)^2 + \frac{1}{2} \sum_{l,m,n} w_{l\to m} w_{l\to n} P_l^{eq} \left(\frac{P_n}{P_n^{eq}}\right)^2$$

$$\text{(B.4)}$$

Combining Eq. (B.3) and Eq. (B.4) to write ΔG gives us

$$\Delta G = -\frac{1}{2} \sum_{l,m,n} w_{l\to m} w_{l\to n} P_l^{eq} \left(\frac{P_m}{P_m^{eq}} - \frac{P_n}{P_n^{eq}}\right)^2 < 0. \qquad \text{(B.5)}$$

This demonstrates that $P_l(t)$ will approach P_l^{eq} arbitrarily close as time progresses. One necessary condition which is usually not addressed explicitly is ergodicity assumption that the system at hand should be able to visit all the states given sufficient amount of time.

Appendix C

Calculation of error in observable

In the course of a simulation, instantaneous values of a system property such as energy per monomer or an order parameter are recorded at a fixed interval. At the end of the simulation, the data are used to estimate the true mean value of the observable by forming an arithmetic average. To be precise, assume we record values of a quantity y at some interval to form a sequence $\{y(1), y(2), \cdots, y(N_s)\}$ (N_s observations in total). The unbiased estimator of true mean $\langle y \rangle$ is the sample mean

$$\bar{y} \equiv \frac{1}{N_s} \sum_{i=1}^{N_s} y(i). \tag{C.1}$$

One would be interested in knowing the uncertainty or error in this estimated value. As a measure of the error, we will take $\langle (\delta \bar{y})^2 \rangle$ where $\delta \bar{y} \equiv \bar{y} - \langle y \rangle$. Then,

$$
\begin{aligned}
\langle (\delta \bar{y})^2 \rangle &= \langle \bar{y}^2 \rangle - \langle y \rangle^2 \\
&= \frac{1}{N_s^2} \sum_{i,j=1}^{N_s} \langle y(i) y(j) \rangle - \langle y \rangle^2 \\
&= \frac{1}{N_s^2} \sum_{i,j=1}^{N_s} [\langle y(i) y(j) \rangle - \langle y \rangle^2]
\end{aligned} \tag{C.2}
$$

If y is a stationary process, $\langle y(i)y(j)\rangle = \langle y(i-j)y(0)\rangle$ and

$$\langle(\delta\bar{y})^2\rangle = \frac{1}{N_s^2}\sum_{i,j=1}^{N_s}[\langle y(i-j)y(0)\rangle - \langle y\rangle^2]$$

$$= \frac{1}{N_s^2}\sum_{i,j=1}^{N_s}F(i-j), \tag{C.3}$$

in which we defined $F(\tau) \equiv \langle y(\tau)y(0)\rangle - \langle y\rangle^2$, which is an even function of τ. The double sum of $F(i-j)$ can be expressed as

$$\sum_{i,j=1}^{N_s}F(i-j) = \sum_{\tau=-N_s+1}^{N_s-1}F(\tau)n(\tau)$$

$$= N_sF(0) + 2\sum_{\tau=1}^{N_s-1}F(\tau)n(\tau), \tag{C.4}$$

where $n(\tau) = N_s - \tau$ is the multiplicity of $F(\tau)$. Now we make an assumption that $F(\tau)$ goes to 0 fast such that we can set

$$\sum_{\tau=1}^{N_s-1}F(\tau)(N_s-\tau) \approx N_s\sum_{\tau=1}^{N_s-1}F(\tau) \tag{C.5}$$

Combining Eqs (C.3), (C.4) and (C.5), we obtain

$$\langle(\delta\bar{y})^2\rangle \approx \frac{1}{N_s^2}\left[N_sF(0) + 2N_s\sum_{\tau=1}^{N_s-1}F(\tau)\right]$$

$$= \frac{F(0)}{N_s}\left[1 + 2\sum_{\tau=1}^{N_s-1}\frac{F(\tau)}{F(0)}\right]. \tag{C.6}$$

$F(0)$ is the true variance $\langle y^2\rangle - \langle y\rangle^2$ and its unbiased estimator is known to be $\frac{N_s}{N_s-1}\sigma_y^2$ where $\sigma_y^2 = \overline{y^2} - \bar{y}^2$ is the sample variance. The final expression for the error becomes

$$\langle(\delta\bar{y})^2\rangle \approx \frac{\sigma_y^2}{N_s-1}\left[1 + 2\sum_{\tau=1}^{N_s-1}\frac{F(\tau)}{F(0)}\right] \tag{C.7}$$

In practice, $\frac{F(\tau)}{F(0)}$ is also replaced by a normalized autocorrelation function measured during a simulation. Eq. (C.7) reduces to the well known expression $\sigma_y^2/(N_s-1)$ in case all measured y's are statistically independent. The reported error or uncertainty is $\pm\sqrt{\langle(\delta\bar{y})^2\rangle}$. The derived expressions are also consistent with the result obtained by Müller-Krumbhaar and Binder [71].

Appendix D

Second order perturbation theory in other ensembles

In this appendix, we present an alternative derivation of the second order perturbation theory. Here we construct a second order perturbation theory in a semi-grand ensemble, and then recover results for a canonical ensemble. The advantage of considering a semigrand ensemble is that probability arguments are particularly simple in a semigrand ensemble with $\alpha = 0$, since each molecule can be either type 1 or 2 at random. The disadvantage is that the second derivative with respect to α turns out to be different in semi-grand and canonical ensembles, forcing us to go through a second step to obtain the desired result for canonical ensemble.

Let Z_s and Z_c represent the semi-grand and canonical partition functions, respectively, for a system with a total of M_t molecules. They are related by the following relation (Eq. (3.26) of Section 3.3)

$$Z_s(\mu, \alpha) = \sum_{M_1=0}^{M_t} e^{\mu M_1} Z_c(M_1, \alpha) \quad , \tag{D.1}$$

where μ is the chemical potential difference between a chain of type 1 and a chain of type 2.

Our immediate goal is to develop expressions for the first and second derivatives of free energy $F = -\ln Z$ with respect to α in the limit $\alpha = 0$ in both ensembles. Eqs. (5.11) and (5.12) hold in either ensemble, if Z is interpreted as the appropriate partition

function, where derivatives of Z_s and expectation values are evaluated at constant μ in semi-grand ensemble, while derivatives of Z_c and expectation values are evaluated at constant M_1 in canonical ensemble.

D.1 Semi grand canonical ensemble

When working in semi-grand ensemble at $\alpha = 0$, we can take advantage of the fact in this case that each molecule may be chosen to be of type 1 or 2 at random, independently of choices made for others. The quantity Θ may be expressed in this ensemble as a sum

$$
\begin{aligned}
\Theta &= \frac{1}{2} \sideset{}{'}\sum_{a,b} I_{ab}(f_{a1}f_{b2} + f_{a2}f_{b1}) \\
&= \frac{1}{2} \sideset{}{'}\sum_{a,b} I_{ab}\bar{f}_{12}(a,b) \quad ,
\end{aligned}
\tag{D.2}
$$

where we have defined

$$
\bar{f}_{12}(a,b) \equiv f_{a1}f_{b2} + f_{a2}f_{b1}
\tag{D.3}
$$

for $a \neq b$, and where f_{ai} is a boolean variable that is 1 if molecule a is of type i and zero otherwise. The prime on the top of a summation symbol means that the sum is taken over all the molecules whose indices are distinct, e.g. over all $a \neq b$, including both $a > b$ and $a < b$. To evaluate averages in semi-grand ensemble at $\alpha = 0$, we simply assume that variable f_{ai} for molecule a is chosen to be 1 with probability ϕ_i and 0 with probability $1 - \phi_i$. That is, we substitute ϕ_i for either f_{ai} or f_{bi} at the end of any calculation. Note also that the boolean variable satisfies $f_{ai}f_{aj} = \delta_{ij}f_{ai}$. In the limit $\alpha \to 0$ of interest, we therefore obtain

$$
\begin{aligned}
\langle \Theta \rangle &= \frac{1}{2} \sideset{}{'}\sum_{a,b} \langle I_{ab}(f_{a1}f_{b2} + f_{a2}f_{b1}) \rangle \\
&= \sideset{}{'}\sum_{a,b} \langle I_{ab} \rangle \phi_1 \phi_2 \quad .
\end{aligned}
\tag{D.4}
$$

For $\langle \Theta^2 \rangle$, we have

$$
\langle \Theta^2 \rangle = \frac{1}{4} \sideset{}{'}\sum_{a,b} \sideset{}{'}\sum_{c,d} \langle I_{ab}I_{cd} \rangle \bar{f}_{12}(a,b)\bar{f}_{12}(c,d)
\tag{D.5}
$$

The terms in Eq. (D.5) can be divided into three categories, i.e. terms with all the indices distinct, terms with three out of four distinct and the rest. The result is

$$
\begin{aligned}
\langle \Theta^2 \rangle \;=\;& \frac{1}{4} \sideset{}{'}\sum_{a,b,c,d} \langle I_{ab} I_{cd} \rangle \bar{f}_{12}(a,b) f_{12}(c,d) \\
+\;& 4 \times \frac{1}{4} \sideset{}{'}\sum_{a,b,d} \langle I_{ab} I_{ad} \rangle f_{12}(a,b) f_{12}(a,d) \\
+\;& 2 \times \frac{1}{4} \sideset{}{'}\sum_{a,b} \langle I_{ab}^2 \rangle \, [f_{12}(a,b)]^2
\end{aligned}
\tag{D.6}
$$

The factor 4 in the second line is because there are four possibilities for choosing three distinctive indices, i.e. $a = c$ which is shown and $a = d, b = c$, and $b = d$. The factor 2 in the third line comes from two possibilities, i.e. $a = c, b = d$ which is shown and $a = d, b = c$. Using $f_{ai} f_{aj} = \delta_{ij} f_{ai}$ and setting $f_{ai} = f_{bi} = \phi_i$ for random labelling yields,

$$
\begin{aligned}
\langle \Theta^2 \rangle = \sideset{}{'}\sum_{a,b,c,d} \langle I_{ab} I_{cd} \rangle (\phi_1 \phi_2)^2 \\
+ \left(\sideset{}{'}\sum_{a,b,d} \langle I_{ab} I_{ad} \rangle + \sideset{}{'}\sum_{a,b} \langle I_{ab}^2 \rangle \right) \phi_1 \phi_2 \quad .
\end{aligned}
\tag{D.7}
$$

The term multiplied by $\phi_1 \phi_2$ in Eq. (D.7) can be written as,

$$
\begin{aligned}
\sideset{}{'}\sum_{a,b,d} \langle I_{ab} I_{ad} \rangle + \sideset{}{'}\sum_{a,b} \langle I_{ab}^2 \rangle &= \sum_a \sum_{b \neq a} \sum_{d \neq a} \langle I_{ab} I_{ad} \rangle \\
&= \sum_a \langle I_a^2 \rangle \quad ,
\end{aligned}
\tag{D.8}
$$

where we defined

$$
I_a \equiv \sum_{b \neq a} I_{ab} \quad .
\tag{D.9}
$$

Using the following identity,

$$
\begin{aligned}
\langle I^2 \rangle &= \sideset{}{'}\sum_{a,b} \sideset{}{'}\sum_{c,d} \langle I_{ab} I_{cd} \rangle \\
&= \sideset{}{'}\sum_{a,b,c,d} \langle I_{ab} I_{cd} \rangle + 4 \sideset{}{'}\sum_{a,b,d} \langle I_{ab} I_{ad} \rangle + 2 \sideset{}{'}\sum_{a,b} \langle I_{ab}^2 \rangle
\end{aligned}
\tag{D.10}
$$

$\sum'_{a,b,c,d}\langle I_{ab}I_{cd}\rangle$ can be written as,

$$\sum_{a,b,c,d}^{'} \langle I_{ab}I_{cd}\rangle$$

$$= \langle I^2 \rangle - 4\sum_{a,b,d}^{'}\langle I_{ab}I_{ad}\rangle - 2\sum_{a,b}^{'}\langle I_{ab}^2 \rangle$$

$$= \langle I^2 \rangle - 4\left(\sum_{a,b,d}^{'}\langle I_{ab}I_{ad}\rangle + \sum_{a,b}^{'}\langle I_{ab}^2 \rangle\right) + 2\sum_{a,b}^{'}\langle I_{ab}^2 \rangle$$

$$= \langle I^2 \rangle - 4\sum_{a}\langle I_a^2 \rangle + 2\sum_{a,b}^{'}\langle I_{ab}^2 \rangle. \tag{D.11}$$

Substituting Eq. (D.8) and Eq. (D.11) into Eq. (D.7) yields the desired expression for $\langle \Theta^2 \rangle$. Combining all the results, the variance in Θ can be written as

$$\langle \Theta^2 \rangle - \langle \Theta \rangle^2 = G_s \phi_1^2 \phi_2^2 + H_s \phi_1 \phi_2 \quad , \tag{D.12}$$

where we have defined

$$G_s \equiv \langle I^2 \rangle - 4\sum_{a}\langle I_a^2 \rangle + 2\sum_{a,b}^{'}\langle I_{ab}^2 \rangle - \langle I \rangle^2 \tag{D.13}$$

$$H_s \equiv \sum_{a}\langle I_a^2 \rangle \tag{D.14}$$

$$I \equiv \sum_{a} I_a = \sum_{a,b}^{'} I_{ab}. \tag{D.15}$$

The subscript of s is used to denote semi-grand ensemble, because we find that the variance of Θ has the same form, but with different coefficients, in semi-grand and canonical ensemble.

D.2   Canonical ensemble via Legendre transformation

The simplest way to obtain corresponding results for the derivatives of the canonical free energy $-\ln Z_c$ is to calculate $\ln Z_c$ from $\ln Z_s$ by Legendre transformation [72]. For a sufficiently large system

$$\ln Z_c(M_1, \alpha) = \ln Z_s(\mu, \alpha) - \mu M_1 \tag{D.16}$$

where (in semi-grand ensemble) M_1 denotes $\langle M_1 \rangle$. These quantities obey the usual identities

$$
\begin{aligned}
M_1 &= \frac{\partial \ln Z_s(\mu, \alpha)}{\partial \mu} \\
\mu &= -\frac{\partial \ln Z_c(M_1, \alpha)}{\partial M_1} \quad .
\end{aligned}
$$
(D.17)

Taking a derivative of both sides of Eq. (D.16) with respect to α yields

$$
\begin{aligned}
\left. \frac{\partial \ln Z_c}{\partial \alpha} \right|_{M_1} &= \left. \frac{\partial [\ln Z_s(\mu, \alpha) - \mu M_1]}{\partial \alpha} \right|_{M_1} \\
&= \left. \frac{\partial \ln Z_s}{\partial \alpha} \right|_\mu + \left. \frac{\partial \ln Z_s}{\partial \mu} \right|_\alpha \left. \frac{\partial \mu}{\partial \alpha} \right|_{M_1} - \left. \frac{\partial \mu}{\partial \alpha} \right|_{M_1} M_1 \\
&= \left. \frac{\partial \ln Z_s}{\partial \alpha} \right|_\mu \quad .
\end{aligned}
$$
(D.18)

Thus, the same result for first derivatives is obtained in either ensemble. Taking a derivative with respect to α again yields

$$
\begin{aligned}
\left. \frac{\partial^2 \ln Z_c}{\partial \alpha^2} \right|_{M_1} &= \left. \frac{\partial^2 \ln Z_s}{\partial \alpha^2} \right|_\mu + \frac{\partial^2 \ln Z_s(\mu, \alpha)}{\partial \alpha \partial \mu} \left. \frac{\partial \mu}{\partial \alpha} \right|_{M_1} \\
&= \left. \frac{\partial^2 \ln Z_s}{\partial \alpha^2} \right|_\mu + \left. \frac{\partial M_1}{\partial \alpha} \right|_\mu \left. \frac{\partial \mu}{\partial \alpha} \right|_{M_1}
\end{aligned}
$$
(D.19)

The first term on the right hand side of Eq. (D.19) calculated at $\alpha = 0$ is the quantity that we evaluated in semi-grand ensemble. To evaluate the additional terms, we may use the 1st order perturbative expansion of the canonical free energy:

$$
-\ln Z_c = M_t \sum_i \phi_i \ln \phi_i + \alpha M_t N z(N) \phi_1 \phi_2 + \mathcal{O}(\alpha^2)
$$
(D.20)

, where

$$
z(N) \equiv \langle I \rangle / (M_t N)
$$
(D.21)

is the effective coordination number. Taking a derivative with respect to M_1 at fixed M_t yields the equation of state

$$
\mu = \ln(\phi_1/\phi_2) + \alpha N z(N)(\phi_2 - \phi_1) + \mathcal{O}(\alpha^2) \quad .
$$
(D.22)

Differentiating with respect to α at fixed M_1 (or fixed ϕ_1) yields

$$
\left. \frac{\partial \mu}{\partial \alpha} \right|_{M_1} = N z(N)(\phi_2 - \phi_1) \quad .
$$
(D.23)

Implicit differentiation of Eq. (D.22) with respect to α at fixed μ yields

$$0 = \left[\frac{1}{\phi_1} + \frac{1}{\phi_2}\right] \left.\frac{\partial \phi_1}{\partial \alpha}\right|_\mu + N z(N)(\phi_2 - \phi_1) \quad, \tag{D.24}$$

or

$$\begin{aligned}
\left.\frac{\partial M_1}{\partial \alpha}\right|_\mu &= M_t \left.\frac{\partial \phi_1}{\partial \alpha}\right|_\mu \\
&= -M_t N z(N)(\phi_2 - \phi_1)\phi_1\phi_2 \quad,
\end{aligned} \tag{D.25}$$

where $\left.\frac{\partial M_1}{\partial \alpha}\right|_\mu$ is understood to be the value of the derivative calculated at $\alpha = 0$. Combining results, using an identity $(\phi_1 - \phi_2)^2 = 1 - 4\phi_1\phi_2$, yields

$$\begin{aligned}
\left.\frac{1}{M_t N} \frac{\partial^2 \ln Z_c}{\partial \alpha^2}\right|_{M_1} &= \left.\frac{1}{M_t N} \frac{\partial^2 \ln Z_s}{\partial \alpha^2}\right|_\mu \\
&+ N z^2(N)\phi_1\phi_2(4\phi_1\phi_2 - 1)
\end{aligned} \tag{D.26}$$

for the corresponding intensive property. It is worth noting that the correction term qualitatively changes the result, since the correction increases linearly with N for $N \gg 1$, while the quantity on the left hand side increases as $\sqrt{N}$ for large N, which will be shown in Sec. 5.3

The final result for second order perturbation theory in canonical ensemble is thus

$$\left.\frac{\partial^2 \ln Z_c}{\partial \alpha^2}\right|_{M_1} = G_c \phi_1^2 \phi_2^2 + H_c \phi_1 \phi_2 \tag{D.27}$$

where

$$\begin{aligned}
G_c &\equiv \langle I^2 \rangle - 4 \sum_a \langle I_a^2 \rangle + 2 \sum_{a,b}' \langle I_{ab}^2 \rangle - \langle I \rangle^2 \\
&+ 4\langle I \rangle^2 / M_t \tag{D.28} \\
H_c &\equiv \sum_a \langle I_a^2 \rangle - \langle I \rangle^2 / M_t \quad. \tag{D.29}
\end{aligned}$$

These results agree with those obtained in Chapter 5 by working directly in canonical ensemble.

Figure D.1 shows how differently the second derivative of free energy behaves as a function of composition of species 1 in the two ensembles. The curve for canonical ensemble (red line) was obtained by using Eqs. (D.28) and (D.29) in Eq. (D.27). On
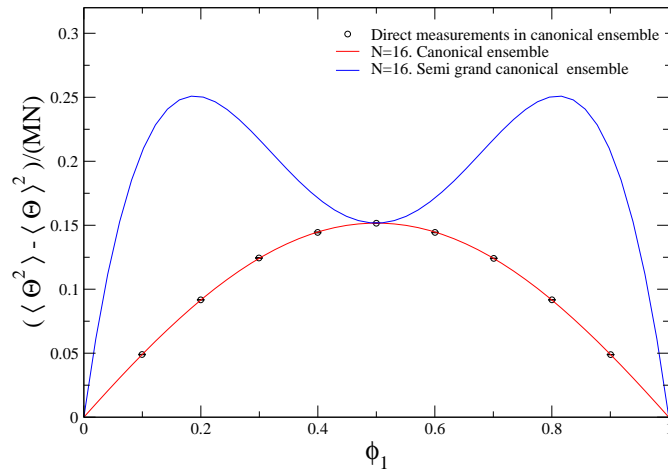
Figure D.1: Plot of $\frac{\langle\Theta^2\rangle - \langle\Theta\rangle^2}{MN}$ vs. ϕ_1.

the other hand, Eqs. (D.13) and (D.14) together with Eq. (D.12) yield the curve for semi grand canonical ensemble (blue line). To check the validity of the derivations given for $G(N)$ and $H(N)$, additional direct measurements in canonical ensemble were done, which are shown as circles with error bars smaller than the size of a symbol.

Appendix E

Histogram reweighting method

Histogram reweighting method [73, 74, 41] allows one to extrapolate the simulation results obtained at a specific value of parameter such as temperature to nearby parameter values. The basic idea is to construct an approximate density of states of the model from raw simulation data. If a simulation done at only one parameter is used, the method is called single histogram method. On the other hand, in multi histogram reweighting method, multiple simulations done at different parameters are combined to give more accurate estimation of the density of states of model.

E.1 Single histogram reweighting method

In the semi grand canonical ensemble discussed in Sec. 3.3, the partition function was defined as (Eq. (3.22)),

$$\mathcal{L}_{SG}(\beta, \Delta\mu) \equiv \int_{-M_t}^{M_t} dM \int dE e^{\beta \frac{NM\Delta\mu}{2}} e^{-\beta E} \tilde{\Gamma}(M, E).$$

The probability density of the system having energy E and order parameter M is given by

$$P_{\beta, \Delta\mu}(E, M) = \mathcal{L}_{SG}^{-1} e^{\beta \frac{NM\Delta\mu}{2}} e^{-\beta E} \tilde{\Gamma}(M, E) \tag{E.1}$$

It is possible, however, to obtain an estimate of the probability during a simulation by making a histogram $H_{\beta, \Delta\mu}(E, M)$. Let $\mathcal{N}$ be the total number of pairs E, M observed. Then, we can approximate Eq. (E.1) with $H_{\beta, \Delta\mu}(E, M)/\mathcal{N}$, or

$$\tilde{\Gamma}(M, E) \approx \mathcal{N}^{-1} H_{\beta, \Delta\mu}(E, M) \mathcal{L}_{SG}(\beta, \Delta\mu) e^{-\beta \frac{NM\Delta\mu}{2}} e^{\beta E} \tag{E.2}$$

135

A density of states is a quantity independent of simulation parameters β and $\Delta\mu$. Therefore, estimated $\tilde{\Gamma}(M, E)$ can be used to approximate a partition function and a probability distribution at some parameters other than the ones at which the simulation was done.

To apply the method to a problem where a chemical mismatch parameter ξ is in the pair potential energy as in the model we study, it needs to be modified slightly from its original form [53]. The total potential energy of the model polymer blend can be written as

$$
\begin{aligned}
E &= U_{bond} + U_{nonbond} \\
&= U_{bond} + \sum_{i<j}^{AA} v_{AA}(r_{ij}) + \sum_{i<j}^{BB} v_{BB}(r_{ij}) + \sum_{i<j}^{AB} v_{AB}(r_{ij}) \\
&= U_{bond} + \sum_{i<j}^{AA,BB} \epsilon F(r_{ij}) + \sum_{i<j}^{AB} \epsilon(1+\xi)F(r_{ij}) \\
&= E_0 + \xi\Theta
\end{aligned}
\tag{E.3}
$$

where $\sum_{i<j}^{AA}$, for example, is a sum over all A monomer pairs without double counting. Also two quantities were defined in the last line as

$$
E_0 \equiv U_{bond} + \epsilon \sum_{i<j}^{AA,AB,BB} F(r_{ij}),
\tag{E.4}
$$

$$
\Theta \equiv \epsilon \sum_{i<j}^{AB} F(r_{ij}).
\tag{E.5}
$$

The semi grand partition function can be written as

$$
\mathcal{L}_{SG}(\beta, \Delta\mu, \xi) \equiv \int_{-M_t}^{M_t} dM \int dE_0 \int d\Theta \; e^{\beta \frac{NM\Delta\mu}{2}} e^{-\beta(E_0+\xi\Theta)} \tilde{\Gamma}(M, E_0, \Theta)
\tag{E.6}
$$

To extrapolate to nearby $(\beta', \Delta\mu', \xi')$, a histogram $H_{\beta,\Delta\mu,\xi}(M, E_0, \Theta)$ has to be constructed during a simulation. The approximate density of states is given by

$$
\tilde{\Gamma}(M, E_0, \Theta) \approx \mathcal{N}^{-1} H_{\beta,\Delta\mu,\xi}(M, E_0, \Theta) \mathcal{L}_{SG}(\beta, \Delta\mu, \xi) e^{-\beta \frac{NM\Delta\mu}{2}} e^{\beta(E_0+\xi\Theta)},
\tag{E.7}
$$

where $\mathcal{N}$ is again the total number of observed triplets (M, E_0, Θ). In the following, subscript $(\beta, \Delta\mu, \xi)$ will be omitted and prime will be used to imply quantities at parameters $(\beta', \Delta\mu', \xi')$ for notational simplicity. With Eq. (E.7), the semi grand canonical

partition function at $(\beta', \Delta\mu', \xi')$ can be expressed as

$$
\begin{aligned}
\mathcal{L}'_{SG} &\approx \mathcal{N}^{-1}\mathcal{L}_{SG} \int dM \int dE_0 \int d\Theta \; H(M, E_0, \Theta) \\
&\times \; e^{(\beta'\Delta\mu' - \beta\Delta\mu)\frac{NM}{2} - (\beta - \beta')E_0 - (\beta'\xi' - \beta\xi)\Theta}.
\end{aligned}
\tag{E.8}
$$

The probability density of (M, E_0, Θ) with the new parameters is

$$
P'(M, E_0, \Theta) \approx \frac{H(M, E_0, \Theta)e^{(\beta'\Delta\mu' - \beta\Delta\mu)\frac{NM}{2} - (\beta - \beta')E_0 - (\beta'\xi' - \beta\xi)\Theta}}{\int dM \int dE_0 \int d\Theta \; H(M, E_0, \Theta)e^{(\beta'\Delta\mu' - \beta\Delta\mu)\frac{NM}{2} - (\beta - \beta')E_0 - (\beta'\xi' - \beta\xi)\Theta}}.
\tag{E.9}
$$

Note that the unknown $\mathcal{L}_{SG}$ was canceled out because it was present both on the numerator and the denominator.

For the study conducted in this thesis where models of symmetric blend are simulated at a fixed temperature, we can further simplify the results because $\Delta\mu = 0$ and $\beta = \beta'$. That is,

$$
P'(M, E_0, \Theta) \approx \frac{H(M, E_0, \Theta)e^{-\beta(\xi' - \xi)\Theta}}{\int dM \int dE_0 \int d\Theta \; H(M, E_0, \Theta)e^{-\beta(\xi' - \xi)\Theta}}.
\tag{E.10}
$$

Defining $H(M, \Theta) \equiv \int dE_0 \; H(M, E_0, \Theta)$, we finally obtain

$$
\begin{aligned}
P'(M, \Theta) &= \int dE_0 P'(M, E_0, \Theta) \\
&\approx \frac{H(M, \Theta)e^{-\beta(\xi' - \xi)\Theta}}{\int dM \int d\Theta \; H(M, \Theta)e^{-\beta(\xi' - \xi)\Theta}}.
\end{aligned}
\tag{E.11}
$$

The main use of this method is to obtain the ensemble average of the order parameter M as a smooth function of ξ, especially near the critical point. Because ξ is coupled to the quantity Θ, however, it is necessary to keep complete two dimensional histogram of (M, Θ).

E.2   Multiple histogram reweighting method

The basic idea in using multiple histograms is to get the best estimate of the density of states by combining them with proper weights. Since E_0 of the reference state with

$\xi = 0$ is irrelevant in formulating the method, we can rewrite Eq. (E.6) as

$$\mathcal{L}_{SG}(\beta, \Delta\mu, \xi) \equiv \int dM \int dE_0 \int d\Theta \; e^{\beta \frac{NM\Delta\mu}{2}} e^{-\beta(E_0 + \xi\Theta)} \tilde{\Gamma}(M, E_0, \Theta)$$

$$= \int dM \int d\Theta \; e^{\beta \frac{NM\Delta\mu}{2}} e^{-\beta\xi\Theta} \tilde{\Gamma}(M, \Theta), \qquad (E.12)$$

with $\tilde{\Gamma}(M, \Theta) \equiv \int dE_0 \tilde{\Gamma}(M, E_0, \Theta)$. The density of states as a function of M and Θ can be related to the histogram $H(M, \Theta)$ using the approximation

$$\mathcal{N}^{-1} H(M, \Theta) \approx \mathcal{L}_{SG}^{-1} \; e^{\beta \frac{NM\Delta\mu}{2}} e^{-\beta\xi\Theta} \tilde{\Gamma}(M, \Theta)$$

or,

$$\tilde{\Gamma}(M, \Theta) \approx \mathcal{N}^{-1} \mathcal{L}_{SG} \; e^{-\beta \frac{NM\Delta\mu}{2}} e^{\beta\xi\Theta} H(M, \Theta) \qquad (E.13)$$

Now imagine multiple simulations are done at s different sets of parameters $(\beta_i, \Delta\mu_i, \xi_i)$ with $i = 1, 2, \cdots, s$. Each simulation will yield its own approximate density of states

$$\tilde{\Gamma}_i(M, \Theta) = \mathcal{N}_i^{-1} \mathcal{L}_i \; e^{-\beta_i \frac{NM\Delta\mu_i}{2}} e^{\beta_i \xi_i \Theta} H_i(M, \Theta). \qquad (E.14)$$

The natural next step would be to combine all of the estimates to form the best estimate of the density of states as

$$\tilde{\Gamma}(M, \Theta) \approx \sum_{i=1}^{s} w_i(M, \Theta) \tilde{\Gamma}_i(M, \Theta) \qquad (E.15)$$

It turns out that one can find out $w_i(M, \Theta)$ by minimizing an error in $\tilde{\Gamma}(M, \Theta)$ caused by errors in $H_i(M, \Theta)$ [75, 41] to get

$$w_i(M, \Theta) = \frac{(1 + 2\tau_i)^{-1} H_i(M, \Theta) \tilde{\Gamma}_i^{-1}(M, \Theta)}{\sum_{i=1}^{s} (1 + 2\tau_i)^{-1} H_i(M, \Theta) \tilde{\Gamma}_i^{-1}(M, \Theta)}, \qquad (E.16)$$

where τ_i is the autocorrelation time of both M and Θ during a simulation with ith set of parameters. In practice, the results do not depend severely on them [41]. Substituting the optimal weights $w_i(M, \Theta)$ into Eq. (E.15) yields the best estimate of the density of states

$$\tilde{\Gamma}(M, \Theta) \approx \frac{\sum_{i=1}^{s} (1 + 2\tau_i)^{-1} H_i(M, \Theta)}{\sum_{i=1}^{s} (1 + 2\tau_i)^{-1} H_i(M, \Theta) \tilde{\Gamma}_i^{-1}(M, \Theta)}$$

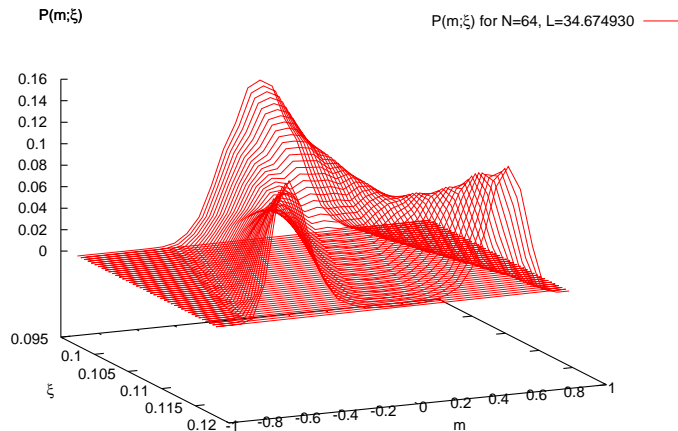$$= \frac{X(M, \Theta)}{Y(M, \Theta)} \qquad (E.17)$$

Figure E.1: The probability density of the normalized order parameter $m = \frac{M}{M_t}$ at various values of ξ. The simulated blend was a system with $M_t = 456$ and $N = 64$ at $\langle \frac{M_A}{M_t} \rangle = 0.5$. Four histograms were generated at $\xi = 0.107, 0.108, 0.109,$ and 0.110 while $\xi_c \approx 0.109$

With this, the partition function (Eq. (E.12)) and the probability density $P(M, \Theta)$ with any set of parameter $(\beta, \Delta\mu, \xi)$ can be obtained. Figure E.1 shows an example of such a plot where four histograms at $\xi = 0.107, 0.108, 0.109$ and 0.110 were combined to estimate the density of states while $\beta = 1$ and $\Delta\mu = 0$. However, one last step before using Eq. (E.17) is to determine $\mathcal{L}_i$'s self consistently because they are needed in the calculation of $Y(M, \Theta) = \sum_{i=1}^{s}(1 + 2\tau_i)^{-1}H_i(M, \Theta)\tilde{\Gamma}_i^{-1}(M, \Theta)$. This can be done iteratively by first assigning an initial guess value for each $\mathcal{L}_i^{(0)}$ to construct $\tilde{\Gamma}^{(0)}(M, \Theta)$. Then we can compute partition functions using Eq. (E.12), yielding $\mathcal{L}_i^{(1)}$, which will be different from $\mathcal{L}_i^{(0)}$ in general. This step is repeated until all $\mathcal{L}_i$ for $i = 1, 2, \cdots, s$ are converged. The initial values are taken to be $\mathcal{N}_i$ for each i and the rate of convergence is high , usually within a hundred iterations.

Appendix F

Critical point of model polymer blend

To estimate the critical points of model blends in the thermodynamic limit (infinitely large system) from simulations done in finite systems, the finite size scaling (FSS) analysis techniques [69] were used together with the multiple histogram reweighting method described in Appendix E.2. The development of the multi-histogram reweighting method made the FSS technique very reliable in characterizing critical behavior of models of polymers and other statistical systems. Here, a brief description of the FSS analysis relevant to the work in this thesis is presented based on the extensive review by Deutsch [41]. Then, the results of the FSS analysis to determine the critical points of the continuum bead-spring model used in this thesis will be presented.

F.1 Finite size scaling theory

Let $t \equiv \frac{T-T_c}{T_c}$, $\mu \equiv \Delta\mu - \Delta\mu_c$ and $m \equiv \frac{M_A - M_B}{M_A + M_B}$, which is a normalized order parameter. If L is the linear dimension of the simulation cell, FSS theory ansatz of the form of order parameter distribution is given by

$$P(t(L), \mu(L), m(L), L) = L^v \tilde{P}(L^u t, L^{d-v}\mu, L^v m) \quad . \tag{F.1}$$

Note that on the right hand side of Eq. (F.1), the system size dependence has been separated explicitly in the factor L^v and $\tilde{P}$ does not depend on L by itself, but through

combinations of L and other parameters. The exponents u and v are defined by the following relations.

$$u \equiv \frac{d}{\gamma + 2\beta} \tag{F.2}$$

$$v \equiv \frac{\beta d}{\gamma + 2\beta} \quad, \tag{F.3}$$

where d is a dimensionality, β is the critical exponent for the order parameter, and γ is the critical exponent for its susceptibility in the scaling region, i.e.

$$m = \hat{B}|t|^{\beta} \tag{F.4}$$

$$\chi = \hat{C}_{\pm}|t|^{-\gamma} \quad, \tag{F.5}$$

with critical amplitudes $\hat{B}$ and $\hat{C}_{\pm}$. Conventional critical exponents such as α (exponent for specific heat) can be expressed in terms of u and v.

$$\alpha = 2 - \frac{d}{u}, \quad \beta = \frac{v}{u}, \quad \gamma = \frac{d - 2v}{u} \tag{F.6}$$

Because of the form of Eq. (F.1), moments of the order parameter m takes the following form:

$$\langle m^k \rangle_L = L^{-kv} \tilde{m}_k(L^u t, L^{d-v} \mu) \quad, \tag{F.7}$$

where m_k is given by

$$m_k(L^u t, L^{d-v} \mu) \equiv \int dx\, x^k \tilde{P}(L^u t, L^{d-v} \mu, x). \tag{F.8}$$

F.2 Determination of critical point

The form of Eq. (F.7) can be taken advantage of in the determination of critical temperature or in the case of study in this thesis, critical value of α. One can form a ratio of some powers of the moments of the order parameter such that system size L cancels out. That is, if one chooses two pairs of integers (i, j) and (l, k) that satisfy $ij = lk$, then

$$U_{ij}^{lk} \equiv \frac{\langle m^l \rangle_L^k}{\langle m^i \rangle_L^j} = \frac{[m_l(L^u t, L^{d-v} \mu)]^k}{[m_i(L^u t, L^{d-v} \mu)]^j} \tag{F.9}$$

If a system with a linear dimension L is at the critical point where $t = 0$ and $\mu = 0$, the value of the ratio would be independent of the system size, given by $\frac{[m_l(0,0)]^k}{[m_i(0,0)]^j}$. For the

case of symmetric blends, $\Delta\mu_c = 0$ because of AB symmetry, and all the simulations in this thesis were conducted at $\mu = 0$. Therefore, if there are multiple simulation systems with different sizes, one can determine the critical temperature or critical α by measuring the ratios for those systems as functions of α and identify a point where all data curves intersect with each other. In Figs. F.1a $\sim$ F.1d, $U_{12}^{21} = \frac{\langle m^2 \rangle}{\langle |m| \rangle^2}$ are plotted as functions of α for four different chain lengths of the BSM. The use of $\langle |m| \rangle$ instead of $\langle m \rangle$ is necessary to introduce spontaneous symmetry breaking [41], i.e. for a finite system, the odd moments of the order parameter remain at 0 after phase separation, in contrast to the behavior of a corresponding infinitely large system.
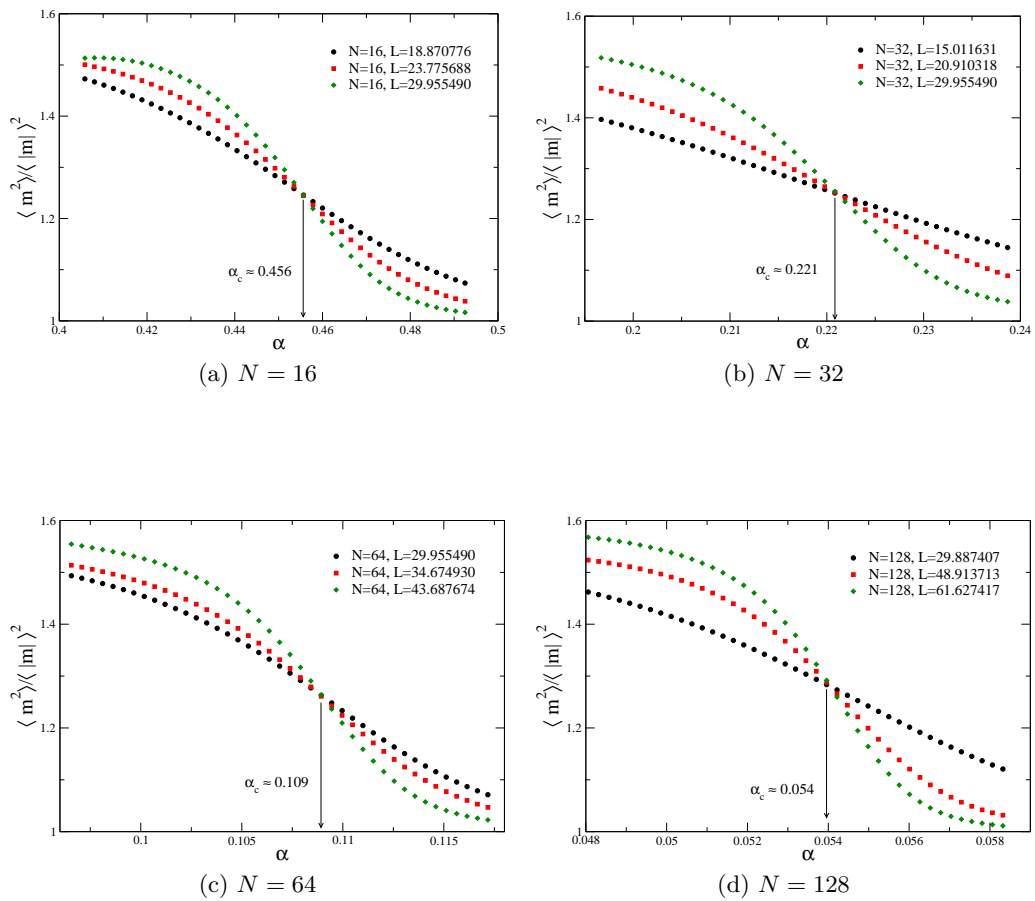
Figure F.1: Plot of U_{12}^{21} vs. α for N=16, 32, 64, and 128 of the BSM. The critical value α_c for each chain length was determined graphically by identifying a point where curves obtained from three different sizes of the system intersect.